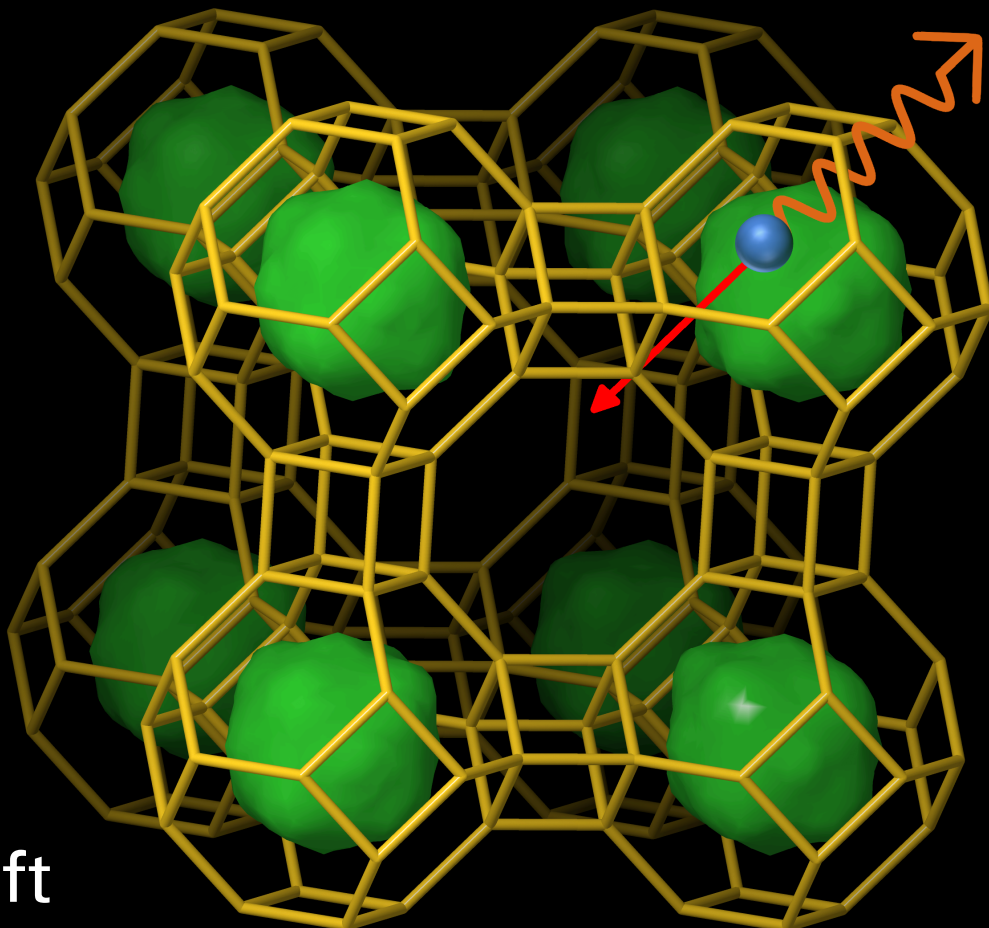


Increasing Specific Activity of ^{166}Ho through Szilard-Chalmers Effect in ^{165}Ho -loaded Zeolite A

Esther Spruit



Cover image adapted from [1].

Increasing Specific Activity of ^{166}Ho through Szilard-Chalmers Effect in ^{165}Ho -loaded Zeolite A

Esther Spruit

July 2023

A thesis submitted to the Delft University of Technology in
partial fulfilment of the requirements for the degree of
Master of Science in Applied Physics,
to be defended publicly on Friday July 21, 2023 at 14:00.

Esther Spruit: *Increasing Specific Activity of ^{166}Ho through Szilard-Chalmers Effect in ^{165}Ho -loaded Zeolite A (2023)*

The work in this thesis was carried out in the:

Applied Radiation and Isotopes
Delft University of Technology

Supervisors: Dr. ir. R.M. de Kruijff
Dr. K. Djanashvili
Thesis committee: Dr. ir. L.J. Bannenberg



Abstract

Holmium-166 is a promising radionuclide for therapeutic and imaging applications due to its advantageous decay characteristics. However, these applications require or would benefit from a higher specific activity of ^{166}Ho than that obtained via a $^{165}\text{Ho}(n,\gamma)^{166}\text{Ho}$ reaction by irradiating a pure ^{165}Ho target. The specific activity is limited, because only a minor fraction of the ^{165}Ho target nuclides is converted into ^{166}Ho during irradiation and these isotopes are inseparable using conventional chemical methods, since they are of the same element. The Szilard-Chalmers effect facilitates this separation by changing the chemical state of the produced radionuclide due to the recoil induced by neutron absorption. Nevertheless, currently applied target materials, mainly ligands, are unsuitable for commercial scale production with sufficient yield and specific activity, because of: radiolysis, isotopic interchange and recombination. It is proposed that these processes can be significantly reduced by exploiting zeolites, which are materials with interconnected cavities, to bind ^{165}Ho target nuclides in the closed cages prior to irradiation. The concept behind is, that upon recoil the ^{166}Ho nuclides relocate to the open cages, from which they are extracted after irradiation, while the ^{165}Ho target nuclides remain locked in the closed cages. This results in an increased specific activity. Therefore, the aim of this thesis is to examine the increase in the specific activity of ^{166}Ho produced via a (n,γ) reaction by applying the Szilard-Chalmers effect using zeolite A.

A procedure to achieve the optimal loading of holmium into the open cages (18.3 wt% Ho) and closed cages (93.3% of total holmium) of zeolite A was investigated, as well as the efficiency of its extraction from the open cages (between 39 and 55%). The obtained specific activity and yield were analysed upon irradiation of these zeolite A samples. Irradiating zeolite A with ^{165}Ho exclusively in the open cages resulted in only a slight increase of the specific activity (maximal 3.3 GBq/g), but a relatively good yield (maximal 53%). In contrast, irradiation of zeolite A with ^{165}Ho loaded in both the closed and the open cages, resulted in a considerably lower yield (maximal 14.4%), but a substantially increased specific activity (maximal 7.3 GBq/g), which is a factor 5.2 higher than without the Szilard-Chalmers effect. Nevertheless, further improvement should be considered as a higher specific activity is key to successful radionuclide therapy. This could potentially be achieved by increasing the extraction efficiency by exploring other types of zeolites, in search of more suitable functional characteristics.

Acknowledgements

First and foremost, I would like to sincerely express my gratitude to my supervisors Robin and Kristina. Our weekly meetings kept me on track; discussing my challenges and the results I achieved so far, provided valuable insights on how to proceed in the sequential weeks. You also reminded me, that it is impossible to investigate every aspect within the scope of a master's thesis, requiring me to make informed choices.

I want to voice my appreciation to Baukje for introducing me to the basics of the laboratory and answering my countless questions. This has helped me to grow as an experimental researcher. It is truly remarkable to look back and realise that, at the start, I had never even held a pipette, yet eventually, I found myself able to help other students. Additionally, I would like to express my gratitude to Delia van Rij for her support with the INAA measurements, as well as to Robert Dankelman and Stephen Eustace for conducting the XRD and NMR measurements.

To all the staff and fellow students at ARI, thanks for the fun coffee and lunch breaks. Especially thanks to Joran for the discussions during our 17:00 hot chocolate breaks or stair-running workouts. Finally, I can positively answer your frequently asked question, "How is the writing going?"

Furthermore, I would like to show my deep appreciation to my boyfriend, Alexander, for helping me improve the language and clarity of this thesis, despite not understand any of the underlining theory. Your support has been immeasurable throughout this journey.

Contents

List of Figures	xiii
List of Tables	xv
List of Acronyms	xvii
List of Symbols	xix
1. Introduction	1
2. Theoretical Background	5
2.1. Zeolites	5
2.1.1. General structure	5
2.1.2. Cation exchange	6
2.1.3. Calcination	7
2.1.4. Zeolite A	7
2.1.4.1. Structure of zeolite A	7
2.1.4.2. Cation sites in zeolite A	7
2.1.4.3. Selection of zeolite A	8
2.2. Holmium	9
2.2.1. Holmium-166	9
2.2.1.1. Production routes for ^{166}Ho	9
2.2.1.2. Medical applications of ^{166}Ho	10
2.3. Specific activity	11
2.3.1. Specific activity for production via a direct (n,γ) reaction	11
2.4. Szilard-Chalmers effect	12
2.4.1. Requirements for applying the Szilard-Chalmers method	13
2.4.2. Szilard-Chalmers effect in zeolites	14
2.4.2.1. Requirement 1: chemical state change of produced radionuclide upon recoil	14
2.4.2.2. Requirement 2: no recombination or interchange	14
2.4.2.3. Requirement 3: no release of target nuclides	15
2.4.2.4. Requirement 4: separation of produced and target nuclides	15
2.5. Measurement devices	15
2.5.1. ICP	15
2.5.1.1. ICP-OES	16
2.5.1.2. ICP-MS	16
2.5.2. Wallac gamma counter	16
2.5.3. HPGe detector	17
2.5.4. INAA	17
2.5.5. XRD	17
2.5.6. MAS-NMR	18
3. Experimental Method	19
3.1. Specifications of applied materials and devices	19

Contents

3.2. Characterising zeolite A	21
3.2.1. Loading	21
3.2.2. Calcination	22
3.2.3. Holmium extraction	22
3.2.3.1. Extraction with 1 ml ammonium chloride solution	23
3.2.3.2. Extraction with 15 ml ammonium chloride solution	23
3.2.4. Recombination and interchange of holmium ions	24
3.3. General applied steps	24
3.3.1. Mixing	24
3.3.2. Washing	25
3.3.3. Drying	25
3.3.3.1. Freeze dryer	25
3.3.3.2. Vacuum desiccator	25
3.4. Measuring holmium	25
3.4.1. ICP-OES	26
3.4.2. ICP-MS	26
3.4.3. INAA	27
3.4.4. Tracer of ^{166}Ho	28
3.4.4.1. Wallac gamma counter	28
3.4.4.2. Filling volume correction	29
3.5. Irradiating zeolite A containing holmium	29
3.5.1. Irradiation procedure	29
3.5.2. Extraction after irradiation	30
3.5.3. Activity measurements with the Wallac gamma counter	31
3.5.3.1. Detector efficiency	31
3.5.4. Activity measurements with the HPGe detector	32
3.5.4.1. Geometry effects	32
3.5.5. Radiolysis	33
3.5.5.1. XRD	33
3.5.5.2. MAS-NMR	33
3.6. Calculations with measured quantities	33
3.6.1. Holmium weight percentage	33
3.6.2. Decrease of water in zeolite during heating in furnace	34
3.6.3. Characterising holmium extraction	34
3.6.3.1. Characterising the 1 ml extraction	34
3.6.3.2. Characterising the 15 ml extraction	35
3.6.4. Specific activity	35
3.6.5. Relocation of ^{166}Ho between open and closed cages upon recoil	36
3.6.5.1. Recoil from open to open cages	36
3.6.5.2. Recoil from closed to open cages	36
4. Results and Discussion	39
4.1. Characterisation of applied methods	39
4.1.1. Triplicate experiments	39
4.1.2. Washing	39
4.1.3. Drying	39
4.1.3.1. Time in vacuum desiccator	40
4.1.4. Measuring holmium	42
4.1.4.1. ICP-OES	42
4.1.4.2. ICP-MS	43

4.1.4.3.	INAA	43
4.1.4.4.	Tracer study	43
4.1.5.	Wallac gamma counter	44
4.1.5.1.	Filling volume	44
4.1.5.2.	Detector efficiency	44
4.1.6.	HPGe detector	45
4.1.6.1.	Filling volume	46
4.2.	Characterising zeolite A	47
4.2.1.	Loading	48
4.2.1.1.	Loading time and temperature	48
4.2.1.2.	Holmium concentration	49
4.2.1.3.	pH	50
4.2.2.	Extraction	51
4.2.2.1.	Extraction time and temperature	51
4.2.2.2.	Different loading	53
4.2.2.3.	Extraction volume	54
4.2.3.	Calcination	56
4.2.3.1.	Dehydration	58
4.2.4.	Recombination and interchange of holmium ions	58
4.3.	Irradiating zeolite A containing holmium	59
4.3.1.	Extraction characteristics	59
4.3.1.1.	Extraction of ^{165}Ho	61
4.3.1.2.	Extraction of ^{166}Ho	63
4.3.2.	Specific activity of eluates	63
4.3.3.	Probability of relocation upon recoil	65
4.3.4.	Radiolysis	68
4.3.4.1.	XRD	68
4.3.4.2.	MAS-NMR	69
5.	Conclusion	71
6.	Recommendations	73
6.1.	Future research required for applying zeolite A	73
6.2.	Elaborate on current findings	74
	Bibliography	75
A.	Structure of zeolite X and L	81
B.	Further calculations	83
B.1.	Water extraction in furnace	83
B.2.	Determining O_i for probability of relocation upon recoil	83
B.3.	Error analysis for ^{166}Ho relocation upon recoil	84
C.	Extraction characteristics	85
C.1.	Extraction characteristics for non-irradiated zeolite	85
C.2.	Extraction characteristics for irradiated zeolite	91
D.	Supplementary information about the applied methods	95
D.1.	Tracer study	95
D.2.	LTA loss during experiments	95

Contents

D.3. Pipetting	95
D.4. Recommendations for similar research	96

List of Figures

1.1. Overview of medical applications of ^{166}Ho	2
2.1. Examples of some zeolite frameworks and the secondary building units they are composed of.	5
2.2. Structure of zeolite A, with cation sites.	8
2.3. Production and decay scheme of holmium-166.	10
4.1. Holmium concentration in washing solutions.	40
4.2. Percentage of water extracted for increasing time periods in the desiccator. . .	41
4.3. Influence of the filling volume on the measured count-rate with the Wallac gamma counter.	45
4.4. Influence of the filling volume on the measured count-rate with the HPGe detector.	47
4.5. Influence of the filling volume on the measured count-rate with the HPGe detector, zoomed in for a range of 0.2–1.4 ml.	48
4.6. The wt% Ho in zeolite A after loading with different loading times at 20°C and 80°C.	49
4.7. The wt% Ho for loading with different concentrations of holmium chloride solution.	50
4.8. The wt% Ho for loading with different pH.	51
4.9. Holmium extraction from the open cages for different extraction times and temperatures.	52
4.10. Holmium extraction from the open cages for different loading procedures. . .	54
4.11. Holmium concentration in the first eluate with different extraction times for a 15 ml extraction.	55
4.12. 15 ml extraction.	56
4.13. Total percentage of holmium extracted for an extraction volume of 10 and 15 ml. .	56
4.14. Influence of calcination on the percentage of extracted holmium.	57
4.15. ^{165}Ho and ^{166}Ho extraction of irradiated zeolite with a 1 ml ammonium chloride solution.	60
4.16. ^{165}Ho and ^{166}Ho extraction with a 1 ml ammonium chloride solution of irradiated zeolite loaded at 20°C for 1 d.	61
4.17. ^{165}Ho and ^{166}Ho extraction of irradiated zeolite with a 15 ml ammonium chloride solution.	62

LIST OF FIGURES

4.18. Specific activity of ^{166}Ho for a 1 ml and a 15 ml extraction.	65
4.19. Probability of ^{166}Ho relocating from an open cage to an open cage upon recoil.	67
4.20. Probability of ^{166}Ho relocating from a closed cage to an open cage upon recoil.	67
4.21. Diffractogram of Na-LTA before and after irradiation for 3 min.	69
4.22. ^{27}Al -MAS-NMR spectrum of Na-LTA before and after irradiation for 3 min.	70
4.23. ^{29}Si -MAS-NMR spectrum of Na-LTA before and after irradiation for 3 min.	70
A.1. Structure of zeolite X, with cation sites.	81
A.2. Structure of zeolite L.	82
C.1. Extraction characteristics for holmium extraction from the open cages with a 1 ml ammonium chloride solution for different extraction times and temperatures.	86
C.2. Extraction characteristics for holmium extraction from the open cages with a 1 ml ammonium chloride solution for different loading procedures.	87
C.3. Extraction characteristics for holmium extraction with a 15 ml ammonium chloride solution.	88
C.4. Influence of calcination on the extraction characteristics for a 1 ml extraction.	89
C.5. ^{165}Ho and ^{166}Ho extraction characteristics of irradiated zeolite with a 1 ml ammonium chloride solution.	91
C.6. ^{165}Ho and ^{166}Ho extraction characteristics of irradiated zeolite loaded at 20°C for 1 d with a 1 ml ammonium chloride solution.	92
C.7. ^{165}Ho and ^{166}Ho extraction characteristics of irradiated zeolite with a 15 ml ammonium chloride solution.	93

List of Tables

2.1. The distribution of cations over the different sites in dehydrated zeolite A.	8
3.1. Specification of the applied chemicals.	19
3.2. Specification of the applied devices.	20
3.3. Neutron fluxes in the BP3 pneumatic irradiation facility of the 2.3 MW nuclear research reactor (Hoger Onderwijs Reactor) of the Reactor Institute Delft.	29
3.4. Irradiated zeolite samples and subsequent performed extractions.	30
3.5. Parameters for MAS-NMR measurements	33
C.1. Decrease in wt% Ho for the 15 ml extractions.	85
C.2. Decrease in wt% Ho for the 1 ml extractions.	90

List of Acronyms

HPGe	high purity germanium	17
ICP	inductively coupled plasma	15
ICP-MS	Inductively coupled plasma mass spectrometry	16
ICP-OES	Inductively coupled plasma optical emission spectroscopy	16
INAA	Instrumental neutron activation analysis	17
IUPAC	International Union of Pure and Applied Chemistry	11
LTA	Linde type A	7
MAS-NMR	magic-angle-spinning nuclear magnetic resonance	18
Na-LTA	$\text{Na}_{12}(\text{SiO}_2)_{12}(\text{AlO}_2)_{12} \cdot 26.7 \text{H}_2\text{O}$	7
NMR	Nuclear magnetic resonance	18
XRD	X-ray diffraction	17

List of Symbols

Symbol	Unit	Description
$\#C_{HPGe}$		number of counts measured with the HPGe detector
$\%Ex$	%	percentage of ^{166}Ho extracted
θ	$^\circ$	angle of incoming X-ray compared to the lattice plane
λ	m	wavelength
σ	b	cross section
Φ	$\text{cm}^{-2} \text{s}^{-1}$	neutron flux
A	Bq	activity
$A_{^{166}\text{Ho}}$	Bq	^{166}Ho activity
$A_{background}$	CPM	background count-rate
A_{cor}	CPM	count-rate measured with the Wallac corrected for the background, time of measurement and filling volume
A_{HPGe}	CPM	count-rate measured with the HPGe detector corrected for the background and the time of measurement
A_{meas}	CPM	count-rate measured with the Wallac
A_{Wallac}	CPM	count-rate measured with the Wallac corrected for the background and the time of measurement
c	m/s	speed of light
$C_{^{165}\text{Ho}}$	M	^{165}Ho concentration
C_i		percentage of holmium in the closed cages before irradiation
$CFSA$	Bq/g	carrier free specific activity
d	m	distance between lattice planes
E_γ	J or MeV	energy of the γ -photon
$E_{\gamma,tot}$	MeV	sum of γ -photon energies
E_R	J or MeV	recoil energy
$\overline{E_{R,tot}}$	eV	mean total recoil energy
$F_{A/counts}$	Bq/CPM	factor correlating the count-rate measured with the Wallac to the activity of ^{166}Ho
$F_{cor,V}$	ml^{-1}	filling volume correction factor
$F_{N/A}$	mol/CPM	amount of holmium per measured count-rate
h		isotopic abundance
M	g/mol	molar mass
m	g	mass
m_a	kg or u	atomic mass of a nuclide

List of Symbols

Symbol	Unit	Description
m_{after}	g	mass after heating in the furnace
$m_{before,corr}$	g	corrected mass before heating in the furnace
m_{sample}	g	mass of the sample
N		number of water molecules per unit cell
N_{av}	mol ⁻¹	Avogadro's constant
N_{Ho}	mol	amount of holmium
O_f		percent of ¹⁶⁶ Ho nuclides present in the open cages after irradiation
O_i		percentage of holmium in the open cages before irradiation
$P(C_i \rightarrow O_f)$		probability of a ¹⁶⁶ Ho nuclide to relocate from a closed cage to an open cage upon recoil
$P(O_f \rightarrow Ex)$		probability that holmium was extracted from an open cage
$P(O_i \rightarrow O_f)$		probability of a ¹⁶⁶ Ho nuclide to remain in its open cage or to relocate to another open cage upon recoil
R_{H_2O}	%	water removed in the furnace as weight percentage of the initial mass
SA	Bq/g	specific activity
SA_{sat}	Bq/g	limit of specific activity produced by a direct (n,γ) reaction for long irradiation times
t_0		moment in time directly after irradiation
$t_{1/2}$	s	half-life
T_{cal}	°C	calcination temperature
t_{det}	s	measurement time
T_{ex}	°C	extraction temperature
t_{ex}	h	extraction time
t_{irr}	s	irradiation time
T_{load}	°C	loading temperature
t_{load}	h or d	loading time
t_{meas}	s	time between irradiation and measurement
t_{proc}	s	time required to process the zeolite after irradiation
V_{ex}	ml	extraction volume
V_{meas}	ml	volume of the measured sample
wt% Ho	%	weight percentage of holmium

1. Introduction

Holmium-166 is a promising radioactive nuclide for medical applications, for therapeutic as well as imaging implementations, due to its advantageous decay characteristics. First of all, it has a half-life of 26.79 hours [2]. A suitable range of the half-life for radionuclides for therapeutic applications is between 6 hours and 7 days [3]. This half-life is sufficiently long to process the holmium between production and administering it to the patient, while having a sufficiently short half-life to limit the time a patient needs to be hospitalised and isolated during treatment [4], since 95% of the radiation is deposited in less than 5 days.

Secondly, holmium-166 is a theranostic radionuclide. This is a nuclide that emits simultaneously a gamma ray, and an alpha or a beta particle, which possess diagnostic and therapeutic capabilities respectively [5]. Holmium-166 emits high-energy beta particles with a maximum energy of 1.84 MeV of which approximately 85% is emitted in the 1.76–1.84 MeV range [2]. The beta particles in this energy range have an average soft tissue penetration depth of 3.3 mm [2], although already 90% of the total radiation dose will be delivered within 2.1 mm [6]. These favourable characteristics of the emitted beta particles allow for successful application in internal radiotherapy. During the decay of holmium-166, a low energy gamma photon is also emitted, with an energy of 80.57 keV and a yield of 6.7%, facilitating nuclear imaging possibilities [6]. The emissions of higher energetic gamma rays have a low abundance (below 0.9%) and do not restrict medical application [2]. The simultaneous emission of both gamma rays for imaging and beta particles for therapy enables applying a scout dose with a smaller activity before applying a therapeutic dose. The emitted gamma radiation of this scout dose is used to accurately determine the total dose and the distribution of the dose during therapy, which is needed for personalised precision medicine. Moreover, there is no discrepancy in bio-distribution of the imaging and therapeutic radio-pharmaceutical with theranostic radionuclides. [6]

Holmium-166 is applied in a variety of medical fields, such as rheumatism, vasculopathy and oncology. Currently, several compounds containing holmium-166 are used in patients, see Figure 1.1, and the number of clinical applications and clinical trials is growing. For instance, rheumatoid arthritis could be treated by radiosynoviorthesis. During this treatment a ^{166}Ho labelled chitosan or FHMA-complex is injected into the affected joints. The radiation causes necrosis of the synovium. In order to treat vasculopathy diseases, intraluminal irradiation could be applied. In this case a ^{166}Ho coating is applied on the stent or the dilatation balloon, to prevent re-stenosis or to treat blood vessel wall abnormalities. In oncology ^{166}Ho compounds are for example used in many intratumoural treatments. One of these treatments uses ^{166}Ho labelled antibodies or tumour-seeking peptides for the treatment of melanomas. However, presently other radionuclides are used more often due to a higher specific activity. [5, 6]

The specific activity is defined as the amount of radioactivity per total mass of that element [7], in this case the mass of ^{165}Ho and ^{166}Ho combined. Hence, the specific activity will be larger with a relative high concentration of radioactive ^{166}Ho atoms compared to the concentration of stable non-radioactive ^{165}Ho atoms. The specific activity is maximal for a carrier free isotope, this is when only radioactive holmium-166 is present.

The specific activity of the radionuclide is an important quality criteria for medical applications [8]. If the radiopharmaceutical has higher specific activity, less foreign substance

1. Introduction

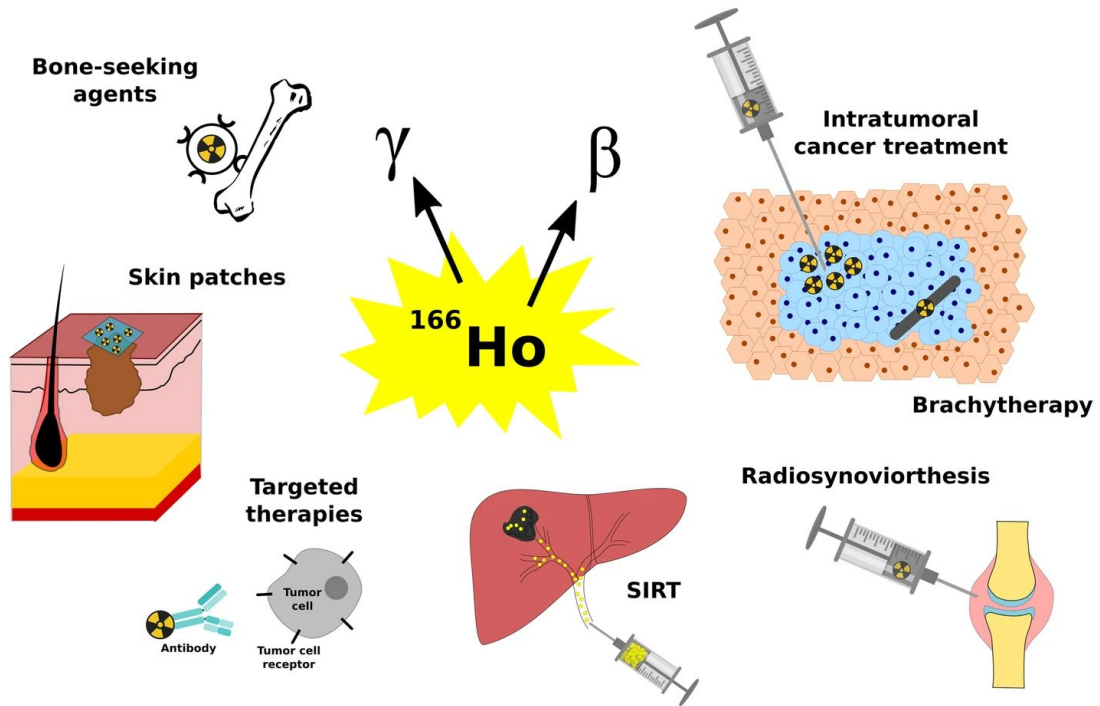


Figure 1.1: Overview of medical applications of ^{166}Ho . [6]

has to be administered. This limits side effects, such as chemical toxicity effects induced by the metals inserted into the body [9]. A high specific activity is especially important for targeted radionuclide therapy. The number of binding sites for the labelled antibody or peptide on a tumour is often limited [10]. Non-radioactive labelled antibodies or peptides occupy the binding sites, blocking this receptor for radioactive labelled targeting vectors, without giving a radiation dose. Hence, a high specific activity is required to obtain the required radio-therapeutic effect.

However, the specific activity of ^{166}Ho is insufficient, when produced by a (n, γ) reaction for irradiation of a pure ^{165}Ho target [10]. During irradiation only a small amount of the target ^{165}Ho nuclides will be converted into ^{166}Ho . As these isotopes are of the same element, they are nearly inseparable, resulting in a low specific activity. Holmium-166 is produced carrier free by irradiation of dysprosium-164. Nevertheless, this production route requires an extremely high neutron flux, as it entails a double neutron capture via dysprosium-165, which has a short half-life of only 2.3 h [10]. This method is not suitable to produce holmium-166 on a large scale [10]. Accelerator based production routes are also unable to produce larger quantities of carrier free holmium-166 [10].

The Szilard-Chalmers effect can be used to increase the specific activity of radionuclides produced via a (n, γ) reaction [2]. This effect facilitates the separation of the produced radioisotope from the irradiated target material by causing the produced radioisotope to change to a different chemical state than the non-reacted target material during irradiation. For this purpose, the target isotope is chemically bound. When a target nuclide absorbs a neutron and is transformed into the produced radioisotope, there is an increase in energy. This excess energy is released in a cascade of γ -rays, which results in a recoil of the produced

radionuclide. This recoil energy might be sufficiently large to break the chemical bond, which changes the chemical state of the produced radionuclide. Consequently, the produced radionuclide can be separated from the still chemically bound target nuclide, resulting in a higher specific activity. [9, 11] To achieve a high specific activity the following three processes should be minimised:

- Recombination, restoring the chemical bond between the produced radioactive nuclide with the target complex,
- Isotopic exchange, interchanging the bound target nuclides with the unbound radionuclides,
- Radiolysis, releasing stable target nuclides.

In literature a large variety of holmium complexes has been examined to increase the specific activity of ^{166}Ho using the Szilard-Chalmers method. The improvement of specific activity is described with the enrichment factor, which is the ratio of the obtained specific activity to the theoretical specific activity without the application of the Szilard-Chalmers effect. Braun and Rausch [12] have found there is a recoil of ^{166}Ho into fullerene cages, producing radio-metallofullerenes with an increased specific activity. However, the yield of this process is only 3.6% and no enrichment factor has been specified. In other researches many ligands with oxygen or nitrogen donor atoms are studied. For example, Safavi-Tehrani et al. [9] have analysed holmium oxalate, 4-aminobenzoate and 8-hydroxyquinolate, for which they have obtained an enrichment factor of 1.51. Zeisler and Weber [2] have examined the same three ligands, for which they have realised a better enrichment factor of 4–66. Nevertheless, there is no clear difference between these two studies that explains these varying results. Zeisler and Weber [2] have evaluated eight more oxygen and/or nitrogen containing ligands, resulting in an enrichment factor between 3 and 22. However, the yield in these two publications is low (<1%) for high enrichment factors and only samples with a lower enrichment factor obtained a higher yield (10–25%). Another ligand containing oxygen and nitrogen, Ho-DOTA, has been intensively investigated. Zhernosekov et al. [11] have obtained an enrichment factor that strongly decreased for longer irradiation periods. Irradiating for half hour resulted in an enrichment factor of 90, while irradiating for six hours decreased the enrichment factor to 7.3. Additionally, a previous master thesis by Wout Schenk [13] about Ho-DOTA has obtained an enrichment factor of 1.62 ± 0.03 . The main causes of this limited yield and specific activity obtained with these ligand complexes are radiolysis, isotopic exchange and recombination [2, 9, 11, 13]. Therefore, they require immediate post-production processing and hinder application for longer irradiations. Consequently, these ligand complexes are unsuitable for commercial scale production with sufficient yield and specific activity.

These three processes decreasing the specific activity are expected to be significantly reduced, when the holmium-165 target nuclides are bound to the closed cages of a zeolite. Zeolites have a crystal structure composed of tetrahedrally coordinated silicon and aluminium atoms with oxygen atoms in between, forming a rigid, 3-dimensional, honeycomb like structure with a network of interconnected cages. The negative charge of the AlO_4^- units is compensated by cations, which are exchangeable. The exchange characteristics are determined by the type of cation and its position within the framework. Cations in the large 'open' cages are readily exchanged, while cations in the smaller 'closed' cages are trapped. Irradiating zeolite with holmium-165 target nuclides in the closed cages, could cause the produced holmium-166 to recoil to an open cage. Extracting after the irradiation removes the holmium-166 from the open cages, while leaving the holmium-165 nuclides bound in the closed cages, resulting in an increased specific activity. Radiolysis is anticipated to be limited, since zeolite X maintains its crystallinity up to a received neutron fluence of

1. Introduction

10^{19} neutrons cm^{-2} , while typical fluences applied for commercial production of isotopes are in the order of 10^{14} neutrons cm^{-2} [14, 15]. Isotopic exchange and recombination are expected to have minimal impact, because the relocation of isotopes between the open and closed cages only commences at temperatures above 60°C [16].

In literature the Szilard-Chalmers effect has been utilised to map cation locations of zeolites X, Y, L and A [14, 17, 18]. These studies have provided evidence of a cation relocation between the open and closed cages of zeolites due to the recoil after absorption of a neutron. These studies have mainly analysed monovalent and divalent cations and some trivalent cations, such as lanthanum. However, there has been no mention of the specific activity in these studies. Nevertheless, a particularly noteworthy research by Campbell [19] has achieved promising results for increasing the specific activity of praseodymium-142 utilising zeolite X. This research has reported an enrichment factor in the range of 50–80, with a yield of approximately 55%. These findings suggest that the promising characteristics of zeolites could be applied to enhance the specific activity of holmium-166.

Therefore, the aim of this thesis is to examine the increase in the specific activity of ^{166}Ho produced by a (n,γ) reaction, applying the Szilard-Chalmers effect using zeolite A. To this end, first the process of loading holmium into the open cages has to be studied. Secondly, a suitable calcination procedure is required to relocate the holmium ions from the open to the closed cages. Thirdly, the extraction of holmium from the open cages needs to be examined. Then the zeolite with holmium is irradiated to determine: the obtained specific activity, the yield and the relocation of holmium-166 between the open and closed cages upon recoil.

In Chapter 2 some background information will be provided. Chapter 3 will explain the applied methods including the procedures for: loading, calcination, extraction and irradiation and the determination of: the wt% Ho in zeolite, the concentration of holmium in eluates, the specific activity and the probability of relocation upon recoil. The results of these experiments will be discussed in Chapter 4. The conclusion is given in Chapter 5. Chapter 6 recommends suggestions for further work.

2. Theoretical Background

In this chapter the theoretical background information required to understand the rest of the thesis is given. First the structure and characteristics of zeolites are discussed in Section 2.1. Then several properties of holmium are given in Section 2.2. The specific activity is discussed in Section 2.3. This could be increased using the Szilard-Chalmers effect, which is explained in Section 2.4. Finally, in Section 2.5 the apparatus used for this study are explained.

2.1. Zeolites

First zeolites in general will be discussed, then in specific zeolite A will be discussed, since this zeolite is used in this research.

2.1.1. General structure

Zeolites are composed of a framework of silicon, aluminium and oxygen atoms. The framework is build up of tetrahedrally coordinated silicon atoms with oxygen atoms in between. These tetrahedra are linked to form secondary building units, such as simple polyhedra (cubes, hexagonal prisms, cubo-octahedra and truncated-octahedra). These secondary building units are repeated to form a crystalline, rigid, 3-dimensional structure. Some examples of zeolite structures and their secondary building units are depicted in Figure 2.1. These structures contain a network of interconnected channels and cavities, with molecular dimensions. These cavities are referred to as cages. [20, 21]

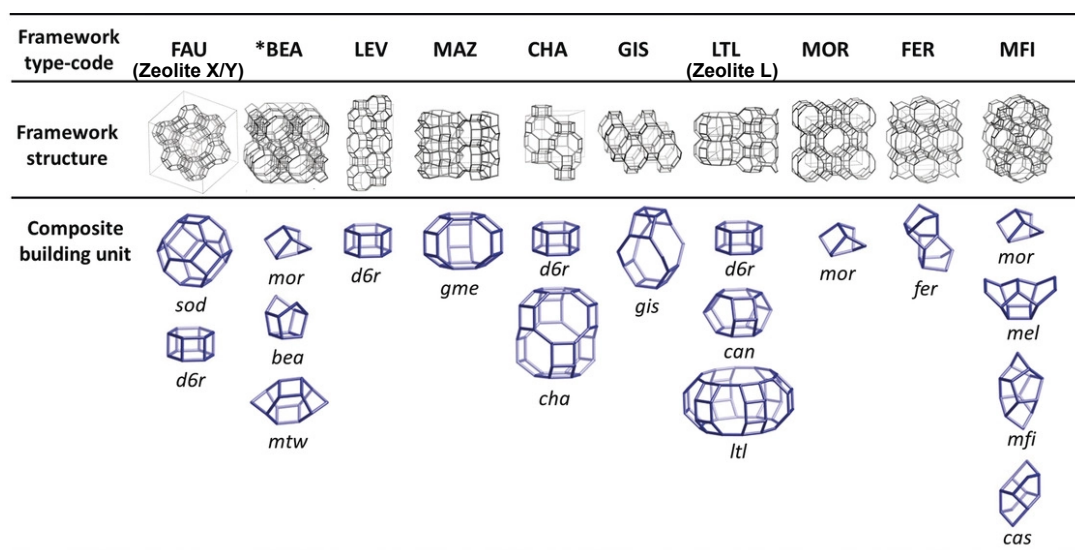


Figure 2.1: Examples of some zeolite frameworks and the secondary building units they are composed of. [22]

The obtained structures are very stable, even under harsh circumstances. There is no release of silicon and aluminium atoms in a pH-range of 3–10 [23]. Zeolites withstand very high

2. Theoretical Background

temperatures. For instance, no lattice collapse is observed below 750°C in zeolite L [14]. Furthermore, the rigid structure is resilient against radiolysis. The crystallinity of zeolite X is maintained up to a fluence of 10^{19} neutrons cm^{-2} [21].

Some of the silicon atoms are replaced by aluminium atoms, resulting in a negatively charged AlO_4^- tetrahedron, instead of the neutral SiO_4 tetrahedron. The number of replaced atoms is expressed in the Si/Al ratio, which is an important property of a zeolite. For example, zeolites with a low Si/Al ratio have a higher cation density, but a lower thermal and acidic stability compared to more siliceous ones [14]. The minimal Si/Al ratio is limited by Löwenstein's rule, that forbids two aluminium ions to share the same oxygen ion [24]. Consequently, AlO_4^- building blocks can not be adjacent and at most half of the silicon atoms can be replaced by aluminium atoms, limiting the Si/Al ratio to be at least 1.

The negative charge of the AlO_4^- units is neutralised by cations located within the cages. These cations are coordinated to the oxygen atoms in the framework. The water present in the cages can also coordinate the cations, forming an aquo-complex, which increases the effective size of the cations. Whether a cation is able to relocate between different cages of the zeolite or exchange with other cations from outside the zeolite, depends on the surrounding structure of binding site. This is only the case when the windows of the cage are sufficiently large to allow the passage of the cation aquo-complex. These cages that allow a cation exchange are called 'open' cages. On the other hand, when only the dehydrated cations can traverse the windows of a cage, it is called a 'closed' cage. [21]

For most zeolites there are multiple positions for cations within the structure. The sites present in a zeolite depend on the specific structure of that zeolite. Every zeolite has its own denomination for the different sites present. Some sites are in the open cages, while other in the closed cages. Even for a specific zeolite the positions that are occupied and the number of cations per site differ for the type of cation and the hydration state of the zeolite. The cation positions are usually determined using X-ray diffraction techniques and/or ^{29}Si -MAS-NMR [21, 25].

2.1.2. Cation exchange

As mentioned above, not all cations are exchangeable with a surrounding solution, due to the structure of a zeolite. Nevertheless, the exchange behaviour of cations in the open cages, that are exchangeable, is not only influenced by the zeolite structure, but also by other factors such as [14]:

- The cation species, mainly its size and charge,
- The temperature,
- The concentration of the cation in the surrounding solution,
- The counter anion species in the solution,
- The surrounding solvent.

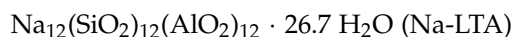
For example, cations are more difficult to exchange for an increasing size and valency [26]. Increasing the temperature seems to facilitate the cation exchange. However, the cation sites that are occupied, differ with the temperature; higher temperatures favour sites that are harder to exchange. Generally water is used as surrounding solvent.

2.1.3. Calcination

Under normal circumstances cations can not enter or leave the closed cages, but upon dehydration this relocation becomes possible. During calcination, a zeolite is dehydrated by increasing the temperature. While during dehydration the crystal lattice remains unchanged, keeping the same window sizes of the cages, the effective diameter of the cations is decreased, since their coordination number is reduced. The diameter of the dehydrated cations is sufficiently reduced in order to pass through the window of the closed cages. Generally, trivalent cations have a higher affinity for the closed cages, resulting in an increase in the number of occupied sites in the closed cages upon calcination. Although in theory these trivalent cations could relocate back to the open cages upon reheating, they will remain in the closed cages due to the higher affinity. [14, 21]

2.1.4. Zeolite A

The official name of zeolite A is Linde type A (LTA). In the remainder of this thesis, both terms will be used interchangeably. Zeolite A has an Si/Al ratio of 1. Taking into account the structure outlined in Section 2.1.4.1, zeolite A is characterised by the molecule formula: $\text{Me}_{12/n}(\text{SiO}_2)_{12}(\text{AlO}_2)_{12} \cdot N \text{H}_2\text{O}$, with Me representing the exchangeable cation of charge n , and N the number of water molecules per unit cell, which varies from 20 to 30 [24]. Consequently, there are at most four trivalent cations per unit cell or maximally 12 monovalent cations. In case of sodium loaded LTA the molecule formula is [18]:



2.1.4.1. Structure of zeolite A

Zeolite A is build from two secondary units: a cube and a truncated-octahedron. It has a cubic unit cell with a lattice constant of 12.32 Å [24]. The structure of zeolite A is depicted in Figure 2.2. This structure is formed by connecting the square faces of the truncated-octahedra with cubes. Consequently, a polyhedron shape is enclosed consisting of: six octagonal faces, eight hexagonal faces and twelve square faces. In zeolite topology this shape is called an α -cage and the truncated-octahedron is called a β -cage. The α -cage has a free diameter of 11.4 Å, resulting in a corresponding free volume of 775 Å³ [24]. The free diameter of the β -cage is 6.6 Å, with a free volume of 157 Å³ [24]. The α -cages are connected by the octagonal faces. This eight-membered-ring opening has an effective diameter of 4.2 Å [27], facilitating the transport of cations through the zeolite. Consequently, the α -cage is an open cage. Cations may enter the β -cage via the hexagonal faces between the α -cage and the β -cage. This window has an effective diameter of 2.2 Å [27]. This opening is sufficiently large for dehydrated cations to pass. However, due to the larger diameter, hydrated cations are unable to pass through this hexagonal face. Therefore, the β -cage is a closed cage.

2.1.4.2. Cation sites in zeolite A

There are three different cation sites in zeolite A. The sites are displayed in Figure 2.2. Site I is inside the closed β -cage, located in the middle of the hexagonal face. Sites II and III are accessed from the open α -cage. Site II is located on the octagonal face, slightly of centre. Site III is positioned in the middle of a square face. Despite, the structure remains unaltered during cation exchange, the number of cations per site type varies for different cations. Reed

2. Theoretical Background

et al. [24] have suggested that the maximum number of cations at site I is 8 per unit cell, and 12 for site II. The distribution of the cations is determined by the charge and size of the cation. Table 2.1 gives an overview of the distribution of cations over the different sites in dehydrated LTA for sodium, calcium and potassium. This distribution also changes upon hydration. [27]

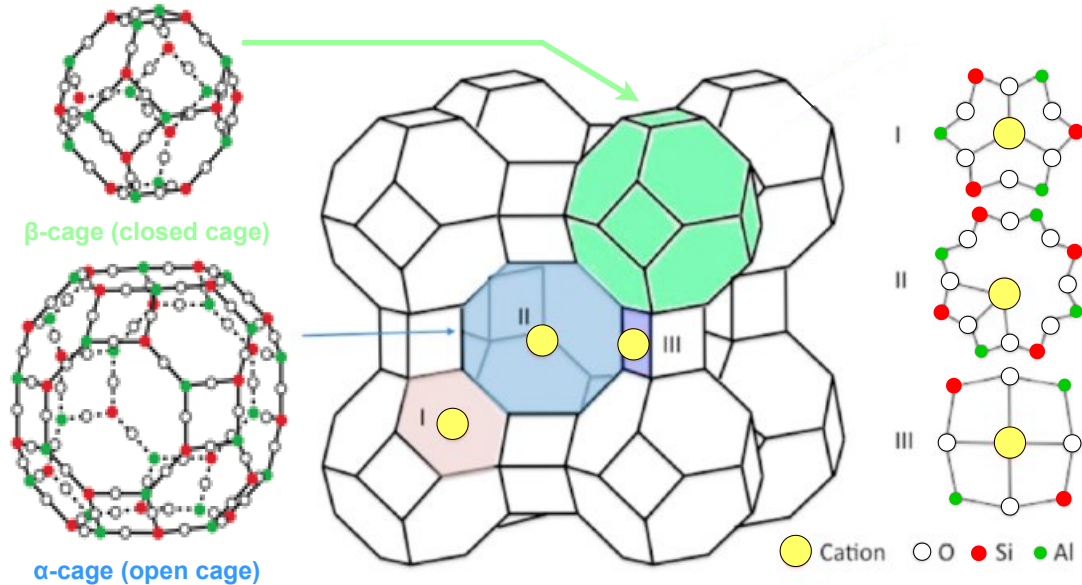


Figure 2.2: Structure of zeolite A, composed of two secondary building blocks: truncated-octahedra and cubes. The truncated-octahedron forms a β -cage, this is a closed cage. The enclosed polyhedron is called an α -cage, which is an open cage. Three cation sites are indicated. Site I is inside the closed cage, it is positioned in the middle of a hexagonal face of the β -cage. Site II and III are reached from the open cage. Site II is positioned on an octagonal face. Site III is in the middle of a square face. [28, 29].

Table 2.1: The distribution of cations over the different sites in dehydrated zeolite A. [27]

cation	cation locations			
	site I	site II	site III	other
Na	8	3	1	-
Ca	5	1	0	-
K	6	3	0	3

2.1.4.3. Selection of zeolite A

For this research zeolite type A is selected for a couple of reasons. There was a choice between two zeolite types that were in stock: zeolite A and L. See Appendix A for an image of the structure of zeolite L. Zeolite L was not chosen, since Newell [14] has indicated that zeolite L is unsuitable for isotopic enrichment, mainly due to the high amount of target nuclides that are released at typical irradiation temperatures (requirement 3 in Section 2.4.1). This resulted in an extraction of 10–20% of the target nuclides after irradiation, which is high compared to the 1% extracted with zeolite X [21].

In contrast, zeolite A is expected to have promising characteristics for isotopic enrichment, since it resembles zeolite X. Campbell [19] successfully applied zeolite X for the enrichment of praseodymium-142. Lai [21] investigated the exchange and recoil of cations in zeolite X further and found that zeolite X exhibits promising characteristics for application in isotope enrichment. Unfortunately, cations located in 'site I' of zeolite X, which is inside a hexagonal-prism (see Appendix A), have a much lower probability to relocate upon recoil than the other sites, which adversely effects the enrichment. The structure of zeolite A is comparable to that of zeolite X, but it has no site similar to 'site I' in zeolite X. The difference is that for zeolite X the β -cages are connected with hexagonal-prisms, while for zeolite A the β -cages are connected with cubes. Since the dimensions of these cubes are too small to have a cation binding site, zeolite A does not have a site similar to site I of zeolite X. This is favourable for isotope enrichment. For these reasons zeolite A is selected for this research.

2.2. Holmium

Holmium has an atomic number 67 and has only one stable isotope: holmium-165 with a natural abundance of 100% [6]. It has an atomic mass of 164.9 u [30]. Holmium is part of the lanthanide series. All lanthanide elements have similar electronic configurations, resulting in comparable chemical and physical characteristics. Therefore, the methods applied in this thesis for holmium, should be easily transferable to other lanthanide elements [9]. These similar properties include strong paramagnetism. Holmium has the highest magnetic moment of any naturally occurring element, making it suitable for applications with MRI [31]. Just as most lanthanide elements, holmium in an aqueous solution has an oxidation state of +3 and is coordinated by 9 water molecules. The ionic radius of holmium is 0.901 Å [32], while the radius of holmium coordinated by 9 water molecules is 2.42 Å [33]. Therefore, hydrated holmium ions are unable to enter the closed cage of LTA with an opening of only 2.2 Å [27], but dehydrated holmium ions can pass the hexagonal window to the closed cage. The eight-membered-ring connecting the open cages of LTA has a diameter of 4.2 Å, allowing the transportation of hydrated holmium ions through the zeolite.

2.2.1. Holmium-166

Holmium-166 has one neutron more than the stable holmium-165. ^{166}Ho has an atomic mass of 165.9 u [30]. The neutron rich holmium-166 decays to Erbium-166 by beta-decay. An overview of the decay characteristics is given in Figure 2.3. Holmium-166 has a half-life of 26.79 hours [2]. The emitted β -particles have a maximum energy of 1.84 MeV and 85% of the emitted β -particles are within the energy range of 1.76–1.84 MeV. Also gamma photons are emitted during decay, with an energy of: 80.6 keV with a yield of 6.56%, 1.38 MeV with a yield of 0.922% or other energies with a yield lower than 0.2% [30].

2.2.1.1. Production routes for ^{166}Ho

Holmium-166 can be produced by irradiation in a reactor via two different routes, which are displayed in Figure 2.3. The first route consist of the neutron activation of ^{165}Ho . This (n,γ) reaction has a cross section of 64.4 b for thermal neutrons [30]. After neutron absorption, a cascade of γ -photons is emitted with an energy between 19.8 keV and 6.19 MeV [34]. The resulting ^{166}Ho is obtained with a high isotopic purity because ^{165}Ho has a natural abundance of 100% [6]. The only by-product is ^{166m}Ho , which is a metastable version with a much

2. Theoretical Background

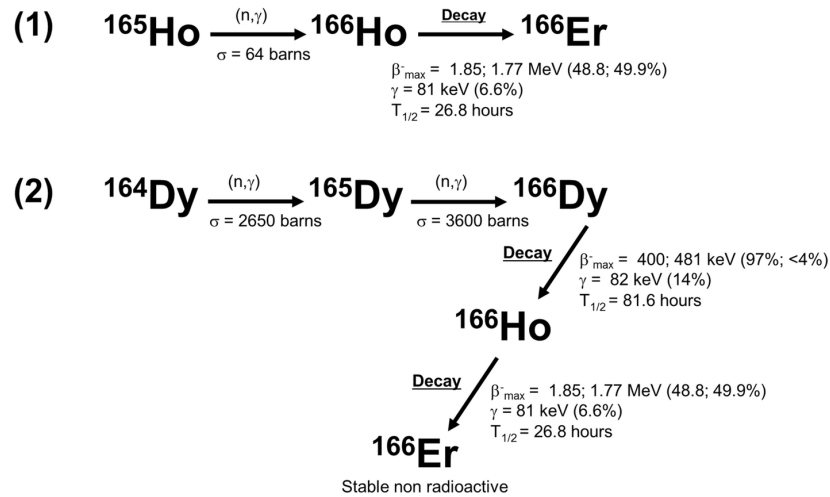


Figure 2.3: Production and decay scheme for holmium-166. (1) Represents the production via a direct (n,γ) reaction. (2) Involves the production via a double neutron capture starting with dysprosium-164. [6].

longer half-life of 1200 years [10]. Fortunately the reaction $^{165}\text{Ho}(n,\gamma)^{166m}\text{Ho}$ has a lower cross section of 3.4 b for thermal neutrons [6] and ^{166m}Ho has a much longer half-life, which cause the activity of the produced ^{166m}Ho to be insignificant. Immediately after production, the activity of ^{166m}Ho is a million times smaller than the activity of ^{166}Ho . Nonetheless, this production route yields a low specific activity because only a minor fraction of the target nuclides, ^{165}Ho , undergoes conversion to ^{166}Ho and these isotopes are inseparable using conventional chemical methods, since they are of the same element (see Section 2.3).

Via a second route, no-carrier-added ^{166}Ho can be produced. This route contains a double neutron capture starting with dysprosium-164. The reaction $^{164}\text{Dy}(n,\gamma)^{165}\text{Dy}$ has a high cross section of 2650 b. The formed ^{165}Dy can either decay to ^{165}Ho with a half-life of 2.3 hours or capture another neutron with a cross section of 3900 b, resulting in ^{166}Dy , which then decays to ^{166}Ho with a half-life of 81.6 hours. A radionuclide generator could be made, from which the ^{166}Ho is extracted. However, this generator system needs to be replaced frequently, due to the short half-life of ^{166}Dy . Moreover, an extremely high neutron flux is required, due to the double neutron capture via a decaying nuclide. Consequently, this method is unsuitable for large scale production. [6]

2.2.1.2. Medical applications of ^{166}Ho

The decay characteristics mentioned above make holmium-166 a promising radionuclide for medical applications. The emitted β -particle is used for therapy, while the γ -photon is used for imaging, making holmium-166 a theranostic radionuclide. ^{166}Ho is applied in a variety of medical fields, including rheumatism, vasculopathy and oncology. For example, a ^{166}Ho labelled chitosan or FHMA-complex is applied in radiosynoviorthesis, treating rheumatoid arthritis. The radiation induces necrosis of the synovium. For the treatment of vasculopathy diseases, a ^{166}Ho coating on a stent or a dilatation balloon is used for intraluminal irradiation, preventing re-stenosis or treating blood vessel wall abnormalities. Holmium-166

compounds are also extensively used in oncology, for instance in patches to treat skin cancer and in many intratumoural treatments of different cancers. [6]

Firstly, ^{166}Ho is conjugated to bone-seeking agents for bone marrow treatment of patients with multiple myelomas or for metastatic bone pain palliation [35]. Secondly, a ^{166}Ho chitosan complex injected with a needle directly into the tumour is applied in the treatment of prostate cancer, renal cysts, hepatocellular carcinomas and cystic brain tumours [5]. Thirdly, micro-spheres with ^{166}Ho are used to treat head and neck tumours, pancreas tumours, lung tumours and liver tumours [10]. Fourthly, ^{166}Ho containing ceramic materials are applied in brachytherapy of for instance brain or breast tumours [36]. Furthermore, ^{166}Ho labelled antibodies and tumour-seeking peptides are used in targeted therapy [6]. These applications would benefit from a higher specific activity. With a higher specific activity ^{166}Ho could be applied in even more treatments. For example, currently lutetium-177 is used more often in targeted therapy, due to a higher specific activity [6].

2.3. Specific activity

Specific activity is defined by the International Union of Pure and Applied Chemistry (IUPAC) as the activity of a specified radionuclide per unit mass of that element [37]. In the case of holmium-166 the specific activity, SA in Bq/g, is calculated with Equation 2.1:

$$SA = \frac{A_{^{166}\text{Ho}}}{m_{^{165}\text{Ho}} + m_{^{166}\text{Ho}}} \quad (2.1)$$

Where A is the activity in Bq and m the mass in g, with the subscripts denoting specific nuclides.

The specific activity has a theoretical maximum value for a carrier free radionuclide, since the denominator of Equation 2.1 is minimal. This carrier free specific activity, $CFSA$ in Bq/g, is calculated with Equation 2.2 [8]:

$$CFSA = \frac{\ln(2) N_{av}}{t_{1/2} M} \quad (2.2)$$

$t_{1/2}$ is the half-life of the nuclide in seconds, N_{av} denotes Avogadro's constant equal to $6.022 \cdot 10^{23} \text{ mol}^{-1}$ and M is the molar mass of the nuclide in g/mol. Substituting the numbers for holmium-166 results in a theoretical maximal specific activity of $9.390 \cdot 10^{19} \text{ Bq/g}$.

2.3.1. Specific activity for production via a direct (n, γ) reaction

The produced specific activity immediately after irradiation for the production of radionuclides by a direct (n, γ) reaction, depends on characteristics of the target nuclide and on the irradiation circumstances. Characteristics of the target nuclide include its abundance, h , molar mass and cross section, σ in b. The influencing factors during irradiation are the neutron flux, Φ in $\text{cm}^{-2} \text{ s}^{-1}$ and the irradiation time relative to the half-life of the produced nuclide, $t_{irr}/t_{1/2}$. The obtained specific activity is calculated using Equation 2.3 [8]:

$$SA = \frac{hN_{av}}{M} \Phi \sigma \left[1 - \frac{1}{2}^{t_{irr}/t_{1/2}} \right] \quad (2.3)$$

2. Theoretical Background

In this formula it is assumed that the mass of the target nuclides does not change significantly. For example, irradiating ^{165}Ho for 3 minutes in the TU Delft reactor institute with a thermal neutron flux of $4.69 \cdot 10^{12} \text{ cm}^{-2} \text{ s}^{-1}$ results in a ^{166}Ho specific activity of $1.43 \cdot 10^9 \text{ Bq/g}$. A longer irradiation period would increase this value. However, the specific activity converges to the limit SA_{sat} , in Bq/g, as the nuclides produced by irradiation is in equilibrium with the number of decaying nuclides.

$$SA_{sat} = \frac{hN_{av}}{M} \Phi \sigma \quad (2.4)$$

In the example of the ^{166}Ho production with a thermal neutron flux of $4.69 \cdot 10^{12} \text{ cm}^{-2} \text{ s}^{-1}$, this results in a maximum produced specific activity of $1.10 \cdot 10^{12} \text{ Bq/g}$. This is a factor 10^8 lower than the maximum specific activity calculated before. If the maximum specific activity produced with neutron activation (Equation 2.4) is compared with the theoretical maximum specific activity (Equation 2.2), it becomes clear that for a high specific activity $h\Phi\sigma$ should approach $\frac{\ln(2)}{t_{1/2}}$. For ^{166}Ho this would require a neutron flux with a magnitude in the order of $10^{17} \text{ cm}^{-2} \text{ s}^{-1}$. However, this is not feasible as the neutron flux in production reactors is in the order of 10^{14} to $10^{15} \text{ cm}^{-2} \text{ s}^{-1}$ [38].

Since the achievable neutron flux is limited, other methods are applied to increase the specific activity. One method is the separation of the target nuclide and the produced radioactive nuclide using the Szilard-Chalmers effect, described in Section 2.4. The increase in specific activity is expressed by the enrichment factor. This is the ratio of the increased specific activity obtained with separation of target nuclide and produced nuclide divided by the specific activity that would be obtained without separation under similar irradiation conditions.

2.4. Szilard-Chalmers effect

In order to increase the specific activity, separation of the target and produced nuclides is required. After a direct (n,γ) reaction a conventional chemical separation is not feasible, since the isotopes are of the same element and vary only about 1 u in mass [9, 11]. The Szilard-Chalmers effect could be used to increase the specific activity of radionuclides produced by a direct (n,γ) reaction [2, 11, 14, 19, 21, 39]. The IUPAC defined the Szilard-Chalmers effect as: "Rupture of the chemical bond between an atom and the molecule of which the atom is a part as a result of nuclear reaction of that atom." [37] Szilard and Chalmers [39] first observed this new principle of separation, obtaining isolated iodine radioisotopes by irradiating ethyl iodide.

The processes immediately after neutron capture are essential for the the Szilard-Chalmers effect, causing a different chemical state between the target and produced nuclides. When a chemically bound target nuclide captures a thermal neutron, transforming it into the produced radionuclide, the energy of the nucleus is increased by the binding energy of the neutron. A cascade of prompt γ -rays is emitted to release this excess energy of about 8 MeV. This emission of γ -photons results in the recoil of the radionuclide. The recoil energy produced by one γ -photon, E_R in J, depends on: the energy of the γ -photon, E_γ in J, the atomic mass of the radionuclide, m_a in kg, and the speed of light, c , equal to $3.0 \cdot 10^8 \text{ m s}^{-1}$. The

recoil energy is calculated with the left side of formula 2.5 [34].

$$E_R = \frac{E_\gamma^2}{2 \cdot m_a \cdot c^2} \approx \frac{E_\gamma^2}{2 \cdot m_a \cdot 931.5} \quad (2.5)$$

Often the energy and atomic mass are given in the non-SI units MeV and u. The right side of Equation 2.5 is applied for these units.

However, the distribution in the total recoil energy is difficult to predict, because a cascade of γ -photons is emitted with a complex spectrum of photons having different directions and energies [21]. If a cascade of n isotropically emitted photons with equal energy is assumed, the mean total recoil energy, $\overline{E_{R,tot}}$ in eV is approximated by [40]:

$$\overline{E_{R,tot}} \cong \frac{537 \cdot E_{\gamma,tot}^2}{m_a \cdot n} \quad (2.6)$$

Where $E_{\gamma,tot}$ is the sum of γ -photon energies in MeV. For this formula m_a is in the units u. This would result in a typical recoil energy in the order of a few hundred electron volts. Although this cascade with γ -photons of the same energy is very unlikely, this approach gives an idea about the order of magnitude of the recoil energy. Upon making the assumptions that n is the sum of all partial cross sections of each gamma photon energy divided by the neutron capture cross section, and $E_{\gamma,tot}$ is equal to the neutron separation energy; then $E_{\gamma,tot}$ is 6.244 MeV and n is 1.15 for the prompt γ -rays emitted by ^{166}Ho [41]. Using Equation 2.6 results in a $\overline{E_{R,tot}}$ of 108 eV. On the other hand, Safavi [34] determined the range in recoil energies by using Equation 2.5 with the lowest and highest energy in the prompt γ -photon spectrum, neglecting the effects of the emission of multiple photons. This method results in a recoil energy range between 0.0026 and 124.7 eV for neutron activation of ^{165}Ho . Similarly, Braun and Rausch [12] found a maximum recoil energy of 126 eV.

In general, the prompt gamma emission results in an abundant recoil energy for bond rupture, since chemical bonds typically have an energy in the range of 1–5 eV [42]. Only if all emitted γ -photons have an energy below 1.2 eV (see Equation 2.5) or all higher energies are emitted simultaneously in opposite directions, then the recoil energy would be insufficient. Fortunately, these conditions have a very low probability [42]. The chemical bond rupture produces a difference in chemical state between the recoiled radionuclide and the still bound target nuclides, facilitating separation of the two by conventional chemical separation methods. Therefore, a high specific activity is achieved. [9]

2.4.1. Requirements for applying the Szilard-Chalmers method

For achieving a higher specific activity with the Szilard-Chalmers effect, the following general conditions need to be satisfied [34]:

1. Upon formation, the produced radionuclide has to be capable of changing its chemical state compared to the target material.
2. The produced radionuclide is not allowed to recombine with the target material, nor to interchange with the inactive target nuclides.
3. The target material has to be chemically and radiolytically stable, preventing the release of target nuclides unless undergoing the Szilard-Chalmers effect.

2. Theoretical Background

4. A method is required that separates the produced radionuclide in its new chemical form from the target material.

To meet these requirements Lai [21], Newell [14] and Zhernosekov et al. [11] found that the following production conditions are required for previously studied target compounds: a low temperature during irradiation and storage before processing, as well as a short storage time between irradiation and processing are required to limit the interchange and recombination; a high ratio of thermal neutrons to γ -rays, a limited flux of neutrons and short irradiation periods are needed to reduce radiolysis. In general these conditions induce low yields, hampering the application for large scale production of radionuclides. However, zeolites are expected to ease these required conditions.

2.4.2. Szilard-Chalmers effect in zeolites

The general concept is to produce a zeolite with the target nuclides locked in the closed cages and none in the open cages. Upon neutron capture, the produced radionuclide is expected to recoil from a closed cage to an open cage. After irradiation, the produced radionuclide is extracted from the open cage, while the target nuclides remain locked in the closed cages. This results in a high specific activity. The four requirements mentioned in Section 2.4.1 are expected to be fulfilled, due to the promising characteristics of zeolites. Sections 2.4.2.1 through 2.4.2.4 will elaborate on this for the specific activity enhancement of holmium-166 in zeolite A. The mentioned characteristics of zeolite A are explained in Section 2.1.4.

2.4.2.1. Requirement 1: chemical state change of produced radionuclide upon recoil

Holmium-166 is expected to change its chemical state during recoil in a zeolite, considering its recoil energies discussed in Section 2.4. Previous studies proved the relocation of other ions in zeolites due to recoil effects. Dyer et al. [18] proved the relocation of monovalent ions Na, K and Rb upon recoil in zeolite A. Similarly, both Lai [21] and Newell [43] showed the recoil from the open to the closed cages and visa versa in respectively zeolite X and L for: these and other monovalent ions; for some divalent ions; and even for one trivalent ion, lanthanum. To analyse the relocation of holmium-166 upon recoil more closely the mean free path of a recoiling ^{166}Ho in zeolite A is considered. For a recoiling ^{24}Na nuclide with a recoil energy of 218 eV in zeolite X or L, the mean free path is respectively 1.72 or 1.84 nm, calculated using a hard sphere model [40, 43]. Recoiling ^{166}Ho in zeolite A is assumed to have a mean free path in the same order of magnitude as these sodium ions, because zeolite A largely resembles zeolite X, and ^{166}Ho has a comparable recoil energy and ionic radius as ^{24}Na . Since zeolite A has an unit cell dimension of 12.3 Å [24], recoiling holmium radionuclides presumably traverse the whole unit cell. Consequently, the probability for a recoiling holmium radionuclide coming to rest in an open or a closed cage is expected to be governed by the free volume of that cage compared to the total free volume. This has been observed to be the case for cation recoil in zeolite X [17, 40]. With the free volumes of zeolite A mentioned in Section 2.1.4.1, this would result in a probability of 83% for a recoiling atom to end up in an open cage and 17% to end up in a closed cage.

2.4.2.2. Requirement 2: no recombination or interchange

The effect of recombination and interchange is expected to be limited, due to the cage structure of zeolites. In this case, recombination would mean, that the radionuclide in the open cage moves back to the closed cage. As explained in Section 2.1.3, hydrated holmium is

too large to pass through the hexagonal face into the locked cage. Higher temperatures are needed to dehydrate holmium to allow it to move to the locked cages. Temperatures during irradiation are presumed to be insufficient, since a minimal temperature of 60°C is needed to move lanthanum ions through the six-membered ring in zeolite Y [16]. Interchange of a produced radionuclide with a target nuclide is improbable, because in that case both have to pass through the window of a closed cage.

2.4.2.3. Requirement 3: no release of target nuclides

The release of target nuclides during irradiation is anticipated to be low, due to the excellent thermal, acidic and radiolytic stability of zeolites. No structural changes have been observed in zeolite A up to a temperature of 800°C [44]. No release of Si and Al atoms of zeolite A has been observed for a pH range of 3 to 10 [23]. Zeolite X, which closely resembles zeolite A, maintains its crystallinity and exchange properties up to a neutron fluence of 10^{19} neutrons cm^{-2} [21].

The target nuclides are expected to have a good chemical stability, because in the locked cages they can not be exchanged or extracted [45], due to their size compared to the limited size of the six-membered ring.

2.4.2.4. Requirement 4: separation of produced and target nuclides

The difference in the cation position, the recoiled radionuclides in open cages and the target nuclides within the closed cages, is exploited for their separation. Ions in the closed cages are not removed during extraction, while ions in the open cages are exchangeable [45]. Extracting will remove the produced radionuclides from the open cages, while leaving the target nuclides in the closed cages. Before irradiation all target nuclides have to be locked in the closed cages, without target nuclides in the open cages, to restrict the extraction of target nuclides after irradiation.

To sum up, zeolites possess promising characteristics to increase the specific activity, meeting all four requirements of successful application of the Szilard-Chalmers method. Campbell [19] already made a proof of concept by increasing the specific activity of Praseodymium-141 with a factor 50 using zeolite X. This study poses that the same methods should be applicable for other trivalent rare earth elements. Therefore, in this study the application of zeolite A to increase the specific activity of holmium-166 is investigated.

2.5. Measurement devices

This section gives an overview of the general working principles of the applied measurement devices. How the apparatus are applied in this research is described in Chapter 3.

2.5.1. ICP

An inductively coupled plasma (ICP) can be applied as ionisation source for the measurement of concentrations in a sample. A plasma is created with electric currents induced by varying magnetic fields. Measurement devices usually contain a plasma of ionised argon atoms, with temperatures of about 7000 K. The sample is nebulised and this is inserted into the plasma, where collisions with the high density of electrons result in the ionisation of the sample. The sample's molecules are reduced to their atoms, which are then ionised. Either the emission spectrum or the mass-to-charge ratio of these ions is measured. [46]

2. Theoretical Background

2.5.1.1. ICP-OES

Inductively coupled plasma optical emission spectroscopy (ICP-OES) utilises the photons emitted by the ionised atoms to make a qualitative and a quantitative measurement. The high temperature of the plasma causes the ions to excite. When the ions de-excite to the ground state, photons with a characteristic wavelength are emitted. By measuring the emitted spectrum, the elements within a sample are determined, since the emission spectrum is element specific. The intensity of the emitted wave lengths is used to quantify. By comparing the intensities of the sample's spectrum with that of reference solutions with a known concentration, the sample's concentration is determined. [46]

2.5.1.2. ICP-MS

Inductively coupled plasma mass spectrometry (ICP-MS) separates the ions based on mass differences, allowing to measure the isotope composition of a sample. The ions are first accelerated in a vacuum region. Then the path is adjusted by an alternating current and a direct current over four electrodes along the flight path. It depends on the mass of the ion, which currents result in a stable flight path. Inversely, the mass of the ion is determined by measuring this stable region. Hence, different isotopes of the same element are distinguishable. However, isotopes of different elements with the same mass number interfere with each other. By collecting the ions at the end of the flight path an intensity of this mass is determined. The sample's concentration is determined by comparison with the intensities of know concentrations. [46]

2.5.2. Wallac gamma counter

The Wallac gamma counter is used to determine the (relative) activity of gamma emitting nuclides in a sample by measuring the emitted gamma spectrum. The gamma spectrum is recorded with a NaI(Tl) scintillation detector. The absorption of a γ -photon by the scintillator medium results in the emission of visible light. This is converted by a photomultiplier tube in an electrical pulse, of which the voltage is related to the energy of the absorbed γ -photon. The emitted gamma spectrum is composed by counting the individual pulses. This spectrum is integrated over a region of interest to obtain the count-rate for a specific nuclide. The resolution of the spectrum is poor, making the Wallac unsuitable for qualitative analysis. If multiple nuclides are measured simultaneously, the energy of the emitted γ -photons should differ sufficiently. A good counting efficiency is achieved by measuring with a well-type detector. This geometry also limits effects of the sample position and volume. However, especially low emitted photon energies are subjected to self-absorption, which should be corrected for. The efficiency of the detector depends on the gamma energy and sample geometry, resulting only in a relative activity. These results may only be compared between samples of the same nuclide and geometry. Despite the detector is shielded with 3 cm of lead against radiation from samples outside the detector, a background correction is needed. The background is determined by measuring an empty sample. Since this varies with the amount and activity of the samples outside the detector, it should be determined for each measurement series. To conclude, the Wallac gamma counter is an effective device for quantitative comparison of the same nuclide in samples with comparable geometries. [47]

2.5.3. HPGe detector

The high purity germanium (HPGe) detector measures the emitted gamma spectrum with a high resolution. The device allows for measuring with easy adjustable distance to the detector and with samples of varying shapes. However, the efficiency is very sensitive to this applied geometry and must be similar to compare the activity of samples with each other. The detector consists of a semiconductor diode of germanium, which is subjected to a reversed bias. The interaction with a photon creates electron-hole pairs, these are measured to determine the energy of the incoming photon. The required energy to form an electron-hole pair is low, resulting in a high energy resolution. On the downside, it requires cooling of the device with liquid nitrogen. Since the energy of a γ -photon emitted during decay is nuclide specific, the obtained gamma spectrum could be used for qualitative analysis. The (relative) activity of a specific nuclide in the sample is determined by integrating the gamma spectrum around a peak of the gamma energy emitted by this nuclide. However, the efficiency of the detector at the energy of the emitted γ -photon and for the applied geometry is needed to determine the real activity of the sample. [48]

2.5.4. INAA

Instrumental neutron activation analysis (INAA) can be used to qualitatively and quantitatively measure chemical elements in a sample by measuring the gamma spectrum emitted during the decay of the sample's nuclides that have absorbed a neutron. First the sample is irradiated with neutrons, converting stable nuclides into radioactive nuclides. Flux-meters are inserted between the samples to measure the received neutron fluence. By a subsequent measurement of the gamma spectrum, emitted by the decaying radioactive nuclei, the composition and amount of each isotope in the sample is determined. The energy of an emitted γ -photon is used to determine the type of isotope. The intensity of the measured gamma emission is proportional to the amount of that isotope present. Together with the efficiency of the detector and the received neutron fluence, the quantity of an isotope is determined. If the emitted gamma energies of different activated isotopes overlap, the gamma spectrum could be measured after various periods of time. By correlating the decrease of intensity with the half-lives of the isotopes, the individual quantities can be determined.

2.5.5. XRD

X-ray diffraction (XRD) can be used to analyse the crystal structure of a sample. XRD measures the distances between lattice planes by using Bragg's law. The incoming X-rays are scattered at subsequent lattice planes, resulting in a different path length. Since the wavelength of the X-rays (λ) is of the same order of magnitude as the distance between lattice planes (d), this results in constructive and destructive interference. There is constructive interference when this path length difference is a multiple of the wavelength, which is the case if: $n\lambda = 2d\sin(\theta)$, with n an integer and θ the angle of the incoming X-ray compared to the lattice plane. In powder samples all orientations of the crystal structure are present. By measuring the angles at which constructive interference occurs, the distance between the lattice planes is determined. [49] Degradation of the crystal structure due to radiolysis might be determined, by measuring a sample before and after irradiation.

2.5.6. MAS-NMR

Nuclear magnetic resonance (NMR) techniques use the physical phenomena that nuclides with a nonzero nuclear spin in a strong magnetic field produce an electromagnetic signal, when perturbed by a weak oscillating magnetic field. The emitted frequency is characteristic for the magnetic field at the nucleus, which depends on the applied magnetic field and on the magnetic properties of the isotope and its chemical environment. Consequently, measuring the emitted electromagnetic signal provides information about the structure of a sample. [50]. In magic-angle-spinning nuclear magnetic resonance (MAS-NMR) a better resolution is obtained by spinning the sample with an axis of $54^{\circ}44'$ with respect to the applied magnetic field. [51]

^{29}Si - and ^{27}Al -MAS-NMR are useful for the quantitative determination of zeolite framework. ^{29}Si -MAS-NMR can identify $\text{Si}(\text{OAl})_n(\text{OSi})_{4-n}$ structural groups in the zeolite framework ($n=0,1,\dots,4$). ^{27}Al -MAS-NMR is used to determine the coordination of the aluminium atoms, revealing the ordering of Al and Si atoms within the structure. With the Si/Al ratio of 1 for zeolite A and the corresponding strict ordering of alternating Si and Al atoms, the ^{29}Si -MAS-NMR spectrum consists of a single peak. However, processes that change the structure, such as dealumination, will introduce other peaks, corresponding to silicon environments with less than 4 aluminium atoms. [51]

3. Experimental Method

In this chapter the utilised experimental methods are discussed. First a specification of the chemicals and the devices is listed in Section 3.1. It was required to obtain holmium loaded zeolite and the extraction characteristics before zeolite could be applied for specific activity enhancement. Therefore the loading, calcination and extraction procedures are discussed in Section 3.2. In order to determine the efficiencies of these procedures, it was important to measure the amount of holmium in samples. The different methods for this are considered in Section 3.4. Hereafter, Section 3.5 explains the procedure for irradiating holmium loaded zeolite and determining the obtained activity of ^{166}Ho . Subsequently, Section 3.6 presents the formulas which utilise the measured quantities for the calculation of values such as the wt% holmium, the probability of relocation upon recoil, and the specific activity.

All experiments were performed at room-temperature (between 18°C and 23°C), unless another temperature is specified. Most experiments were performed in triplicate. Unless stated otherwise, the result of an experiment is the mean of the triplicate and the corresponding error is one standard deviation from the mean.

3.1. Specifications of applied materials and devices

The used chemicals are listed in Table 3.1. Table 3.2 provides an overview of the applied apparatus.

Table 3.1: Specification of the applied chemicals.

Product name	Chemical formula	Supplier
Ammonium chloride	NH_4Cl	Merck
Erbium, AAS standard solution, Specpure, Er 1000 µg/ml	Er_2O_3 in HNO_3 5%	Alfa Aesar
Holmium(III) chloride hexahydrate, REacton r 99.9% (REO)	$\text{HoCl}_3 \cdot 6 \text{H}_2\text{O}$	Thermo Fisher Scientific
Holmium (III) oxide powder pure	Ho_2O_3	Riedel-de Haën
Holmium ICP standard certipur, traceable to SRM from NIST	Ho_2O_3 in HNO_3 2–3%	Merck
Hydrochloric acid 30%, Suprapur	HCl	Supelco
Hydrofluoric acid puriss. p.a., ACS reagent, ISO, Ph. EUR., $\geq 48\%$	HF	Sigma-Aldrich
MilliQ	H_2O	Ultrapure water system, Advantage A10, Merck
Na-LTA	$\text{Na}_{12}(\text{SiO}_2)_{12}(\text{AlO}_2)_{12} \cdot 26.7 \text{H}_2\text{O}$	NanoScape AG.
Nitric acid 65% Reag. ISO, Reag. Ph. Eur	HNO_3	Honeywell

3. Experimental Method

Table 3.2: Specification of the applied devices.

Device	Product name	Manufacturer
Balance	Semi-Micro Analytical balance GR-202	A&D instruments LTD.
Centrifuge 15 ml tubes	Mega Star 600R centrifuge	VWR
Centrifuge Eppendorf tubes	Micro Star 17R microcentrifuge	VWR
Desiccator	Vacuum desiccator	
Flask shaker	Griffin Flask Shaker	Griffin & George LTD.
Freeze dryer	EZ-DRY EZ550Q; GVD 5 vacuum pump	Kinetic; Atlas Co
Furnace	ThermoLab Furnace 1100-8	Borel Swiss SA
HPGe detector	Ge(Li) detector model LG22	Princeton Gamma-Tech
ICP-MS	NexION 2000 ICP-MS	PerkinElmer
ICP-OES	Optima 8000 ICP-OES	PerkinElmer
Magnetic stirrer	Heater and magnetic stirrer Arc. T with timer	Velp Scientifica
Microwave	Microwave Reaction System, Multiwave PRO	Anton Paar
NMR spectrometer	500 MHz (11.7 Tesla) wide bore NMR spectrometer	Bruker
Oven	Ventricell ecol line	MMM Group
pH meter	Metrohm 744 pH meter	Gemini BV
pipette 1 ml	Pipetman P1000, 100–1000 μ l, Metal Ejector	Gilson
pipette 0.2 ml	Pipetman P200, 20–200 μ l, Metal Ejector	Gilson
pipette 20 μ l	Proline Single Channel Pipette 2–20 μ l	Biohit
pipette 10 ml	2–10 ml Laboratory Dropper Single Channel Adjustable Micro Pipette	ZHIBANG
Sonicator	5800 Ultrasonic cleaner	Branson
Thermo shaker	PHMT PSC24N Thermo Shaker	Grant-bio
Vortex mixer	Vibrofix VF1 Vortex	IKA
Wallac gamma counter	2480 Wallac Wizard2 Automatic Gamma Counter	PerkinElmer
Well-type germanium detector	Ge(Li) detector model GWL-220-15-S	Ortec
X-Ray Powder Diffractometer	X'Pert Pro MPD TTK-450	PANalytical

3.2. Characterising zeolite A

In the rest of this thesis the state of a zeolite A sample will be represented by the following abbreviation:

$\text{Ho}(T_{load}, t_{load}) \text{LTA} [T_{cal}] \text{IR} \text{NH}_4(T_{ex}, n \times V_{ex}, t_{ex})$

Where $\text{Ho}()$ denotes the loading procedure, with T_{load} the temperature during loading and t_{load} the loading time. $[T_{cal}]$ describes the calcination temperature. This part is omitted if the sample was not calcined. IR is included if the zeolite sample was irradiated. $\text{NH}_4()$ denotes an extraction procedure, with n the number of extractions of a volume V_{ex} for a time t_{ex} at a temperature T_{ex} . If the sample was not extracted, then $\text{NH}_4()$ is also omitted. The performed steps are stated in chronological order.

3.2.1. Loading

In this section the loading of holmium into the open cages is described. The efficiency of loading was characterised by the holmium wt% in the zeolite, see Section 3.6.1 for the corresponding formula. The effects of temperature, time, concentration, pH and number of fresh solutions were studied. If no other parameters are specified, then the following procedure was applied: 1.001 ± 0.002 ml of 0.1998 ± 0.005 M holmium chloride with a pH of 5.7 was added to 66.69 ± 0.07 mg of Na-LTA in an Eppendorf tube. This tube was placed in the thermoshaker at a setting of 1400 rpm and 80°C for 1 hour, after which it was centrifuged for 10 min at $10k \times g$. The supernatant was removed with a pipette. The remaining holmium outside the zeolite was removed by washing it three times with milliQ. This sample is denoted as $\text{Ho}(80^\circ\text{C}, 1 \text{ h}) \text{LTA}$. When the efficiency of loading was determined, the zeolite was weighted after drying.

A loading time of 1 h, 3 h and 1 d was examined at room-temperature and at 80°C . The loading time is defined as the time between adding holmium chloride and putting the sample in the centrifuge. For loading at 80°C , the temperature of the sample was assumed to be equal to the temperature setting of the thermoshaker. Additionally, a loading time of 2 h, 2 d, 3 d, 4 d and 8 d were studied at room-temperature.

The effect of the holmium concentration during the loading was investigated. The concentration of the added holmium chloride solution (0.020, 0.050, 0.10, 0.15 or 0.20 M) was varied during loading at room-temperature for 1 d or 3 d. The holmium concentration of the solution surrounding the zeolite decreased during loading, possibly decreasing the rate of the reaction. A possibly more favourable loading efficiency was studied by daily refreshing the 0.2 M holmium solution for a loading time of 1, 2, 3 or 4 days. The total loading time is defined as the time spend in the thermoshaker, without the time needed to centrifuge or exchange the solution.

The influence of adjusting the pH of the added holmium chloride solution was studied for loading for 70 ± 1 h. pH values of 1.25, 2.98, 4.13 and 5.7 were applied. Holmium chloride hexahydrate dissolved in milliQ had a pH of 5.7. The pH of the added holmium chloride solution was altered by adding either 1 M or 0.01 M HCl.

3.2.2. Calcination

To relocate the holmium ions from the open to the closed cages, the following calcination procedure was applied. A dried Ho(80°C, 1 h) LTA sample was transferred from the Eppendorf tube to a crucible. To prevent structural damage of the zeolite, the temperature needed to be increased slowly ($1^{\circ}\text{C min}^{-1}$) [14, 21, 45] to 100°C, in order to allow water to escape the zeolite. Since the furnace had no program with varying heating rates, the temperature remained at 100°C for 0–3 hours until the next step was programmed. After this, the temperature was increased to 600°C at a rate of $10^{\circ}\text{C min}^{-1}$ or to 300°C at a rate of $1^{\circ}\text{C min}^{-1}$. The furnace was kept for 6 h at the final temperature. Then the furnace was turned off, slowly cooling down to room-temperature, which took about 10 hours.

After drying, the LTA sample formed a solid block that stuck to the walls of the Eppendorf tube. The sample was detached from the walls and formed into a powder by tapping against the walls of a closed tube in different orientations. However, in case of insufficient drying, the sample stayed attached to the walls of the Eppendorf tube and was not transferred to the crucible. A larger crucible was placed over the crucible with the sample in order to shield the sample from the dirty environment in the furnace and to prevent contamination of the furnace in the case of the tracer study.

A variation of this calcination method was tested, where the sample was not dried before calcination. Instead, after the loaded zeolite was washed, 0.2 ml milliQ was added to be able to pipette the zeolite from the Eppendorf tube into the crucible. Hereafter, the normal calcination procedure at 600°C was applied. The holmium left in the Eppendorf tube and on the pipette tip was measured to determine the amount of zeolite added to the crucible.

The effectiveness of the calcination procedure was determined by comparing subsequent extraction experiments. The sample was transferred from the crucible to the tube for extraction by pipetting. In case of the extraction with 1 ml, three times 0.25 ml ammonium chloride solution was added to the crucible and transferred to the Eppendorf tube with a 1 ml pipette tip which was cut off to prevent blockage. The fourth time a 0.2 ml pipette was used for transferring, to limit the loss of ammonium chloride solution in the crucible. In case of an extraction with 15 ml of ammonium chloride solution, a similar method was applied as for the transfer from an Eppendorf tube, which is described in Section 3.2.3.2.

If no extraction was performed after calcination, then the zeolite was transferred for storage from the crucible to an Eppendorf tube with a paper folded funnel. $98\pm 1\%$ of the sample which was added to the crucible, was found in the Eppendorf tube after the calcination. The mass of this zeolite was used to calculate the water extracted in the furnace, which is described in Section 3.6.2.

3.2.3. Holmium extraction

A procedure to extract holmium from the open cages of zeolite A was investigated, which was applied both before and after irradiation. To determine the most efficient method, extractions were performed on zeolite samples that were not calcined, consequently it only had holmium ions in the open cages. The characteristics of extraction were determined for varying time, temperature and volume during the extraction of samples with different loading temperatures and loading times. The extraction was characterised by:

1. The percentage of holmium extracted per eluate,
2. The percentage of holmium extracted in total,

3. The concentration holmium in the eluates,
4. The total amount of extracted holmium,
5. The amount of holmium in an eluate normalised to the first eluate,
6. The decrease in wt% holmium of the zeolite sample.

3.2.3.1. Extraction with 1 ml ammonium chloride solution

The general procedure for the extraction with 1 ml started by adding 1.001 ± 0.002 ml of saturated (5.4 M) ammonium chloride solution to the sample. First, the sample was mixed, then it was placed in the thermoshaker at a setting of 1400 rpm and 50°C . After 0.5 h the sample was centrifuged at $10k \times g$ for 10 min. The eluate was removed by pipetting and collected in a separate Eppendorf tube. This separate vial with the eluate was centrifuged at $10k \times g$ for 10 min. The upper 0.792 ± 0.003 ml of this vial was pipetted in another vial, which was measured for holmium content. This extraction process was repeated four more times. Thereafter the zeolite was washed three times. If it was necessary, then the sample was stored in this stage until the radioactivity had decreased to background levels, which took 2–4 weeks. Hereafter the sample was dried and weighted.

An efficient extraction method was sought by altering the time and temperature during the extraction of Ho(20°C , 1 d) LTA. An extraction temperature of 20°C , 50°C or 80°C was investigated. The actual temperature of the samples was not measured. The temperature was assumed to be equal to the setting of the thermoshaker. All samples were centrifuged at room-temperature. At the beginning of each eluate, the temperature of the sample differed from the intended temperature, since the added ammonium chloride solution was at room-temperature.

An extraction time of 0.5 h, 1 h and 2 h was studied. The extraction time is defined as the time a sample was in the thermoshaker, which excludes the time required to centrifuge or change solutions. The total number of eluates also changed for different extraction times, as the total extraction was performed within one day.

To consider whether different loading procedures resulted in different binding sites for holmium, an extraction at 50°C for 0.5 h and 1 h was repeated for Ho(20°C , 1 h) LTA and Ho(80°C , 1 h) LTA samples. Since Ho(80°C , 1 h) LTA NH_4 (50°C , 5×1 ml, 0.5 h) became the standard, this result was also used to compare with extraction after calcination or irradiation.

3.2.3.2. Extraction with 15 ml ammonium chloride solution

The general procedure for the extraction with 15 ml started by transferring the sample to a 15 ml tube. First three times 1 ml saturated (5.4 M) ammonium chloride was added to the Eppendorf tube before it was transferred with a 1 ml pipette tip which was cut off to prevent blockage. Again three times 1 ml of NH_4Cl was added, but now it was transferred with a full 1 ml pipette tip. The remaining 9 ml was added directly to the 15 ml tube. The tube was attached to the flask shaker and mixed for 1 d. The flask shaker was on the maximum speed without moving the shaker itself, which was speed setting 6. Hereafter, the samples were centrifuged at $12k \times g$ for 15 min. The upper 1 ml of the eluate was pipetted to an Eppendorf tube for measurement. The rest of the eluate was decanted. This process was repeated two more times without transferring the zeolite and by adding 15.11 ± 0.06 ml NH_4Cl directly to the 15 ml tube. The zeolite was washed three times with 10 ml milliQ. If necessary, the sample was stored in this stage until the radioactivity had decreased to background levels, which took 1–3 weeks. Afterwards the zeolite was dried and weighted.

3. Experimental Method

The required extraction time was estimated by measuring the increase of holmium concentration in the ammonium chloride solution. This experiment was performed with just one sample. A Ho(80°C, 1 h) LTA sample was transferred to the 15 ml tube as describe above, with 15 ml NH₄Cl solution. For an extraction time of: 0.5 h, 0.75 h, 1 h, 1 d, 2 d, 3 d and 4 d the following steps were repeated: the sample was centrifuged; the upper 0.988±0.002 ml of the eluate was pipetted into a separate vial for measurement; the sample was mixed; and placed back in the flask shaker. Consequently, for each measurement point the extraction volume decreased with 1 ml.

The efficiency of the 15 ml extraction was analysed by extracting a Ho(80°C, 1 h) LTA sample. The influence of the extraction volume was investigated by repeating this process for adding 10 ml of saturated (5.4 M) ammonium chloride to a Ho(80°C, 1 h) LTA [600°C] sample. It was studied whether daily changing the ammonium chloride solution was required by extracting a Ho(80°C, 1 h) LTA [600°C] sample for 3 days with one NH₄Cl solution.

During the removal of a liquid from a zeolite sample after centrifuging, either for washing or extracting, a small amount of LTA was removed as well. Residual amounts of zeolite were present for example in the extracted liquid or on a pipette tip. The effect of this zeolite loss on the extraction characteristics was neglected. For a 1 ml extraction, in order to minimise the amount of zeolite present in the eluate during the measurement of holmium: the Eppendorf tube with the eluate was centrifuged; and the upper 0.792±0.003 ml was pipetted into a separate vial. This vial was measured to characterise the eluate. The remaining 0.2 ml could be measured to determine the loss of zeolite. For a 15 ml extraction, the presence of zeolite in the measured eluate solution was prevented by collecting the upper 1 ml ammonium chloride solution with a pipette in a separate vial, before the remaining liquid was decanted.

3.2.4. Recombination and interchange of holmium ions

A preliminary examination was conducted in order to investigate the additional uptake of holmium ions by zeolite that had already been loaded, as well as the interchange of holmium ions within the open cages with external holmium ions. The study involved recontacting two dried samples of Ho(80°C, 1 d) LTA and one sample of Ho(20°C, 3 d) LTA [600°C] with a 0.01 M holmium chloride solution containing a tracer of ¹⁶⁶Ho at 50°C for 0.75 h, 3 h and 1 d respectively. Subsequently, these samples were extracted with five times 1 ml of saturated ammonium chloride solution for 0.5 h at 50°C. The activity measurements of the tracer of ¹⁶⁶Ho were compared to the holmium concentration measured with ICP-MS.

3.3. General applied steps

3.3.1. Mixing

After centrifuging the zeolite formed a chunk attached to the bottom of the Eppendorf tube or 15 ml tube. In order to re-suspend the zeolite, the sample was either stirred with a cocktail stick or a vortex mixer. The sample was held horizontally or up side down on the vortex mixer, such that air and liquid was contacting the zeolite.

3.3.2. Washing

The holmium ions that were present outside the zeolite, for example after loading or extraction, were removed by washing. Washing in an Eppendorf tube was done by adding 1.001 ± 0.002 ml of milliQ to the sample, before mixing. The sample was centrifuged at $10k \times g$ for 10 min, after which the water was removed with a pipette. This was repeated two more times. There could be a waiting time between mixing and centrifuging. The influence of washing with or without a 0.5 h waiting time was analysed. In case an experiment could not be completed before the closure of the lab, the sample was left overnight between washing repetitions.

In case of washing with a 15 ml tube, 10 ml of milliQ was added to the sample. This was mixed and then centrifuged at $12k \times g$ for 15 min. The water was decanted. This was repeated twice more. The third time not all water was removed at once. The zeolite sample with approximately 0.5 ml water was centrifuged at $12k \times g$ for 15 min. Then the last water was removed with a pipette.

3.3.3. Drying

A zeolite sample was dried before calcination and at the end of every experiment. The drying procedure started with a washed zeolite sample and resulted in a zeolite in powder form. Two devices were utilised: a freeze dryer or a vacuum desiccator.

3.3.3.1. Freeze dryer

First, the sample was frozen at -50°C in a freezer for at least 24 h. The sample was put in ice for transport from the freezer to the freeze dryer. The tube was covered with parafilm containing small holes, before placing it in the freeze drying chamber. The chamber with the sample was then depressurised to a vacuum of about 0.1 Pa for minimally a day. Hereafter, the parafilm was replaced by the tube's screw cap. The zeolite was stored in this way.

3.3.3.2. Vacuum desiccator

The open tube with the zeolite sample was placed in the desiccator with blue silica gel at the bottom. Then the desiccator was put under vacuum. For subsequent calcination, the samples were removed after 1 or 2 days in the desiccator. For drying at the end of an experiment, the samples were in the desiccator for 3–5 days. If some of the silica gel crystals had turned pink, then the absorbed water was removed by heating the silica gel to 110°C for 3 hours.

3.4. Measuring holmium

Four methods were applied to measure the amount of holmium in a sample: ICP-OES, ICP-MS, INAA and a tracer of ^{166}Ho .

3.4.1. ICP-OES

ICP-OES was applied for measuring the amount of holmium in a zeolite sample or in an eluate. A sample was not measured directly with the ICP-OES, but a solution containing part of the sample was analysed. This sample solution needed to contain a similar measurement matrix as the used references. For this research aqua regia, with a concentration of 2.7% hydrochloric acid and 2.0% nitric acid, was used as matrix. The sample had to be completely dissolved. Therefore the structure of the zeolite had to be broken down to Al and Si ions in order to measure a zeolite sample. For measuring a zeolite sample, the sample solution was made as follows: 30 mg of zeolite sample with 4.5 ml of 30% hydrochloric acid, 1.5 ml of 65% nitric acid and for some samples a droplet of hydrogen fluoride was added. This was heated in a microwave. The heating was controlled by the applied power. The utilised microwave programme consisted of a linear power increase to 1300 W in 30 min. Then the power was kept constant for 1 hour, after which the samples were left for 15 min to cool down. Hereafter, the sample with acids was transferred to a volumetric flask by rinsing it three times with milliQ. Then milliQ was directly added to the flask, filling it up to the 50 ml mark. The flask was shaken and then transferred to a 50 ml tube for storage. Before measuring, the sample solution was left minimally overnight to homogenise.

To prepare the solution for measuring an eluate with the ICP-OES, the following procedure was implemented: first, the zeolite present in the eluate was removed through filtration using a syringe filter with a pore size of 0.2 μm . From this filtered solution 0.1-0.9 ml was added to 0.9 ml HCl and 0.3 ml HNO₃. Then the volume was increased with milliQ to 10 ml. This was shaken and minimally left overnight to homogenise before measurement.

A measurement series started by making calibration curves for each measured element at each measured wavelength. For the measurement of holmium, the intensity at a wavelength of 339.9 and 345.6 nm was measured. Reference solutions with a concentration of 1.0, 3.0, 6.9, 9.1, 51 and 103 mg/l were used. Thereafter the sample solutions were measured and the holmium concentration was determined by comparing the measured intensity with the calibration curve. After measuring about ten samples, the functioning of the ICP-OES was checked by measuring a reference solution. If the measured holmium concentration in a sample solution was higher than 100 mg/l, then a dilution of this solution was made and this was measured again. The sample solution was diluted with the measurement matrix. The ICP-OES software calculated the amount of holmium in the initial sample from the measured concentration in the sample solution, if information was given about: the added sample mass or volume; the total volume of the sample solution; and if necessary the dilution volumes.

3.4.2. ICP-MS

The holmium concentration in the eluates was measured with ICP-MS. If necessary, a sufficient waiting time was applied such that all activity had decayed to the background level. The eluates could not be measured directly, but again a sample solution with a fixed measurement matrix was required. For ICP-MS nitric acid with a concentration of 0.65% was used as matrix. Furthermore, the eluates had to be diluted such that the ammonium chloride concentration was at most 0.05 M and the holmium concentration was in a range of 25–500 $\mu\text{g/l}$. Therefore the eluates were diluted with a factor 100, 1000, 2000 or 10000 \times , corresponding to the expected concentration. The first three dilutions were made by adding: 0.1 ml 65% HNO₃; 9.8 ml milliQ; and respectively 0.1 ml, 10 μl or 5 μl of the eluate. The

10000× dilution was made by diluting two times 100×. The sample solutions were shaken and left overnight to homogenise before measurement.

New calibration curves were made, every time when the ICP-MS machine was started up. Holmium reference solutions were used with a concentration of 0.97, 4.9, 9.9, 25, 50, 98, 246 and 500 µg/l. These reference solutions had the same measurement matrix of 0.65% HNO₃, but did not contain NH₄Cl. The influence of ammonium chloride on the measured concentration was investigated by measuring reference solutions prepared with 0.05 M NH₄Cl. The holmium concentration was determined by measuring a mass of 165 u. A mass of 166 u was also measured to possibly detect ¹⁶⁶Er, the decay product of ¹⁶⁶Ho. This was compared to the measurement of erbium with a mass of 168 u. For this, erbium reference solutions of 1, 5 and 10 µg/l were applied.

The holmium concentrations of the sample solutions were determined by comparing the measured mass intensity with the calibration curve. With this concentration of the sample solution, the ICP-MS software calculated the holmium concentration in the eluate, if the added eluate volume and total sample solution volume were given. A blank, only containing the measurement matrix, was measured and the corresponding mass intensity was subtracted from the subsequent measurements of the sample solutions. After about 15 samples, a new blank intensity was measured and the blank correction was adjusted. Also a reference solution was measured after every blank to check the functioning of the ICP-MS device.

3.4.3. INAA

The amount of holmium in a zeolite sample was measured with INAA. First 18±2 mg of a zeolite sample was added to a cylindrical HDPE capsule with a diameter of 8 mm and height of 5 mm. In the rest of this thesis, this capsule will be denoted as 'INAA cup'. The capsule was sealed by heating the edges of the lid. The samples were sandwiched between flux monitors and this was inserted in a tube made of HDPE foil. The flux monitors consisted of filter paper with a dried zinc standard solution in an INAA cup. Also an in-house developed holmium standard was included for quality control. The tubes were irradiated for 5 min in the BP3 pneumatic irradiation facility of the 2.3 MW nuclear research reactor (Hoger Onderwijs Reactor) of the Reactor Institute Delft. Hereafter, this irradiation facility will be indicated as BP3. A specification of the flux is provided in Section 3.5. After 5 days of decay time, the samples and flux monitors were removed from the tube and placed in a larger capsule. The gamma spectrum emitted by the irradiated samples and flux monitors, was measured with a well-type germanium detector for 15 min each. The spectrum was only measured once, since there was no need to correlate the decrease in intensity with a half-life, in order to separate nuclides with overlapping energies. The dead time was maximally 26%, which was measured with the pulser method. For this method an artificial peak at the high-energy end of the spectrum was introduced by a 25 Hz pulser peak.

An in-house INAA software was used to determine the exact thermal neutron flux received by a sample with the spectrum of the adjacent flux monitors and to analyse the gamma-ray spectrum of the samples. This information was combined by the software, to determine the amount of holmium in the sample. In the same way, the sodium content of the zeolite sample was determined by the INAA software.

3. Experimental Method

3.4.4. Tracer of ^{166}Ho

A tracer of ^{166}Ho was applied to measure the amount of holmium in a zeolite sample or eluate by relating the activity of ^{166}Ho to the amount of holmium. The ^{166}Ho was produced by irradiating 24 ± 4 mg of holmium chloride hexahydrate in an INAA cup at BP3. The produced ^{34}P , ^{38}Cl and ^{164}Ho had decayed away before use by waiting 1–3 days. The irradiation time was adjusted from 1 to 5 min to produce an activity of 3–5 MBq after the waiting time. After loosening the lid, the INAA cup, lid and irradiated holmium chloride hexahydrate were added to a non-radioactive holmium solution and stirred for minimally 30 min. This solution had a holmium concentration of 0.1998 ± 0.005 M and is referred to as the stock solution. The count-rate of 1.001 \pm 0.002 ml of this stock solution added to 66.69 \pm 0.07 mg of Na-LTA in an Eppendorf tube, was measured with the Wallac gamma counter for at least 6 samples per stock solution. The average of this, together with the concentration of the stock solution, was used to calculate a factor $F_{N/A}$, which is the amount of holmium per count-rate measured with the Wallac [mol Ho/CPM]. The amount of holmium in a sample, N_{Ho} [mol], was then calculated by using Equation 3.1.

$$N_{\text{Ho}} = A_{\text{cor}} \cdot F_{N/A} \quad (3.1)$$

Where A_{cor} in CPM, is the count-rate of a sample measured with the Wallac gamma counter as described in Section 3.4.4.1. This method was validated by comparing the concentration measured both with the tracer and the ICP-MS for at least three eluates produced from three different stock solutions.

3.4.4.1. Wallac gamma counter

The count-rate of a sample was measured with the Wallac gamma counter. Samples with a similar expected count-rate were loaded together in one sample rack. If a rack had samples with a different expected count-rate than the previous rack, then an empty slot was added to measure the background count-rate, $A_{\text{background}}$ in CPM. The Wallac gamma counter automatically took one sample from the rack and measured its emitted gamma spectrum. The measurement time was between 1 and 30 min. The 80.6 keV gamma photon, emitted by the holmium, was measured by integrating this spectrum over an interval from 60 to 90 keV. The output of the Wallac, A_{meas} in CPM, was this integral divided by the measurement time. Although this is not the number of disintegrations of holmium, due to the efficiency of the Wallac and the yield of the emitted gamma photon, this 'relative' activity of ^{166}Ho was used for analysis. All measured count-rates were corrected for the time between irradiation and measurement, t_{meas} in seconds, to compare samples and to relate the measured count-rate with the amount of holmium. The count-rate of a sample with a correction for the background and the time of measurement, A_{Wallac} in CPM, was calculated with Equation 3.2.

$$A_{\text{Wallac}} = \left(A_{\text{meas}} - A_{\text{background}} \right) \cdot 2^{t_{\text{meas}}/t_{1/2}} \quad (3.2)$$

The measured count-rate depended on the geometry of the sample. If samples were measured with the large sample rack, then they were placed in the rack with a second vial, that kept the Eppendorf or 15 ml tube upright and centred. Geometry differences due to varying filling volumes were corrected by a factor, $F_{\text{cor},V}$ in ml^{-1} . The determination of this factor is

3.5. Irradiating zeolite A containing holmium

described in Section 3.4.4.2. The count-rate with a correction for the background, time of measurement and filling volume, A_{cor} in CPM, was computed with Equation 3.3.

$$A_{cor} = \frac{A_{Wallac}}{1 - F_{cor,V} \cdot V_{meas}} \quad (3.3)$$

Where V_{meas} is the volume of the measured sample in ml. The volume of zeolite in the sample was taken to be equal to 0.2 ml.

3.4.4.2. Filling volume correction

The effect of the filling volume on the measured count-rate, expressed by the factor $F_{cor,V}$, was determined by measuring the count-rate of a certain amount of stock solution for different added volumes of milliQ. This was performed for the small and large sample racks of the Wallac and with 0.1993 ± 0.0001 ml or 0.494 ± 0.001 ml of stock solution. First the volume of stock solution was added to an Eppendorf tube and the count-rate was measured. Then 0.2509 ± 0.0004 ml of milliQ was added and the count-rate was measured, which was repeated until a total volume of 1.5 ml was achieved. A_{Wallac} was plotted for the different filling volumes and a linear square fit, $A_{Wallac} = c_1 \cdot V_{meas} + c_2$, was made. $F_{cor,V}$ is then defined as $-c_1/c_2$, such that A_{cor} corresponds to the count-rate measured with a filling volume of zero.

3.5. Irradiating zeolite A containing holmium

Several holmium loaded zeolite samples obtained by the procedures described in Section 3.2, were irradiated to determine the probability of relocation upon recoil and to investigate the obtained specific activity. First, Section 3.5.1 mentions the applied irradiation procedure. Then Section 3.5.2 explains the extraction of holmium-166 after irradiation, of which the activity was measured as is described in Section 3.5.3 and 3.5.4. Finally, Section 3.5.5 describes the measurements performed to study radiolysis.

3.5.1. Irradiation procedure

After drying, the complete zeolite sample was transferred to an INAA cup. On average 66 ± 8 mg zeolite sample was added. Six INAA cups were inserted in a tube made of HDPE foil. This was irradiated at BP3 for 3 min. The neutron fluxes at BP3 are given in Table 3.3. A decay time of 2-4 days was applied before the samples were processed. The different type of zeolite samples that were irradiated, are listed in Table 3.4. The samples differed whether they were calcined and/or extracted with NH_4Cl before irradiation.

Table 3.3: Neutron fluxes in the BP3 pneumatic irradiation facility of the 2.3 MW nuclear research reactor (Hoger Onderwijs Reactor) of the Reactor Institute Delft.

Type of neutrons	Flux ($\text{s}^{-1} \text{cm}^{-2}$)
Thermal neutrons (0–0.55 eV)	$4.69 \cdot 10^{12}$
Epithermal neutrons (0.55 eV– 100 keV)	$8.7 \cdot 10^{10}$
Fast neutrons (100 keV–20 MeV)	$3.38 \cdot 10^{11}$

3. Experimental Method

Table 3.4: Irradiated zeolite samples and subsequent performed extractions.

#	Sample irradiated	Extraction after irradiation	Deviating extraction times
1	Ho(80°C, 1 h) LTA	NH ₄ (50°C, 5×1 ml, 0.5 h)	E1 15 min on shaker
2	Ho(80°C, 1 h) LTA NH ₄ (50°C, 6×1 ml, 0.5 h)	NH ₄ (50°C, 5×1 ml, 0.5 h)	E1 15 min on shaker, E3 1 h
3	Ho(80°C, 1 h) LTA [600°C]	NH ₄ (50°C, 5×1 ml, 0.5 h)	E1 15 min on shaker
4	Ho(80°C, 1 h) LTA [600°C] NH ₄ (50°C, 5×1 ml, 0.5 h)	NH ₄ (50°C, 5×1 ml, 0.5 h)	E1 15 min on shaker
5	Ho(80°C, 1 h) LTA	NH ₄ (20°C, 3×15 ml, 1 d)	
6	Ho(80°C, 1 h) LTA NH ₄ (20°C, 3×15 ml, 1 d)	NH ₄ (20°C, 3×15 ml, 1 d)	
7	Ho(80°C, 1 h) LTA [600°C]	NH ₄ (20°C, 3×15 ml, 1 d)	
8	Ho(80°C, 1 h) LTA [600°C] NH ₄ (20°C, 3×15 ml, 1 d)	NH ₄ (20°C, 3×15 ml, 1 d)	before irradiation E3 4 h
9	Ho(20°C, 1 d) LTA	NH ₄ (50°C, 5×1 ml, 0.5 h)	E1 45 min, E4 36 min, E5 41 min
10	Ho(20°C, 1 d) LTA	NH ₄ (50°C, 5×1 ml, 1 h)	E1 75 min
11	Ho(80°C, 3 h) LTA	MilliQ (20°C, 3×1 ml, 0)	

3.5.2. Extraction after irradiation

The extraction after irradiation was similar to the general extraction procedure applied for characterising zeolite A described in Section 3.2.3.1 for extraction with 1 ml and in Section 3.2.3.2 for extraction with 15 ml. However, the procedure differed for the first eluate. Additionally the sample was measured with the HPGe detector before adding a new ammonium chloride solution.

In case of the extraction with 1 ml, the irradiated zeolite was transferred from the 10 mm high INAA cup to the Eppendorf tube by pipetting. First, 0.1993 ± 0.0001 ml of saturated (5.4 M) ammonium chloride solution was added to the INAA cup by flushing it over the lit of the INAA cup. This was transferred to the Eppendorf tube with a 1 ml pipette of which the tip was cut off to prevent blockage. Then three times 0.1993 ± 0.0001 ml of NH₄Cl was added directly to the INAA cup and transferred to the Eppendorf tube with the cutoff pipette tip. Lastly, 0.1993 ± 0.0001 ml of NH₄Cl was added and transferred to the Eppendorf tube with a 0.2 ml pipette tip. In total 1 ml of saturated (5.4 M) ammonium chloride was added. This was then centrifuged at $10k \times g$ for 5 min, measured with the HPGe detector, mixed and placed in the thermoshaker at a setting of 1400 rpm and 50°C. It took about 0.5 h between adding the first ammonium chloride solution and placing the sample in the thermoshaker. After 15 min in the thermoshaker, the sample was centrifuged at $10k \times g$ for 10 min. The eluate was removed by pipetting and collected in a separate Eppendorf tube. For the following eluates, the procedure given in Section 3.2.3.1 was used.

In case of the extraction with 15 ml, the lit of the 5 mm high INAA cup was loosened. The INAA cup, lit and irradiated zeolite were added to a tube with 15.11 ± 0.06 ml of saturated

(5.4 M) ammonium chloride solution. This was centrifuged at $5k \times g$ for 5 min, measured with the HPGe detector, mixed and attached to the flask shaker. Hereafter, the general procedure in Section 3.2.3.2 was applied.

One experiment was also performed where the irradiated Ho(80°C, 3 h) LTA was washed with 1 ml of milliQ. The same transfer from INAA cup to Eppendorf tube was applied with milliQ instead of NH_4Cl . This was mixed before centrifuging it for 10 min at $10k \times g$. The total count-rate was measured with the HPGe detector. The water was removed by pipetting and collected in a separate vial. The count-rate of the zeolite was measured with the HPGe detector. Then 1 ml of milliQ was added to the zeolite and this was mixed. The sample was centrifuged for 10 min at $10k \times g$ before the water was removed and collected in a separate vial. This washing was repeated three times in total. The separate vials containing the wash were centrifuged for 10 min at $10k \times g$ and the upper 0.8 ml was pipetted in another vial of which the count-rate was measured with the Wallac gamma counter.

The extraction after irradiation was characterised in a similar way as the extraction with the tracer study, but for the extraction after irradiation a difference between ^{165}Ho and ^{166}Ho isotopes was made.

1. The percentage of ^{166}Ho extracted per eluate,
2. The percentage of ^{166}Ho extracted in total,
3. The concentration ^{165}Ho in the eluates,
4. The total amount of extracted ^{165}Ho ,
5. The amount of ^{166}Ho in an eluate normalised to the first eluate,
6. The specific activity of ^{166}Ho in each eluate.

3.5.3. Activity measurements with the Wallac gamma counter

The count-rate of the eluates and zeolite was measured with the Wallac gamma counter. By using Equation 3.3, the count-rate was corrected for the background radiation, the time of measurement and the filling volume. If A_{meas} exceeded 10^6 CPM, then the sample was measured again after a sufficient decay time. This resulted in a time between irradiation and measurement of about one week for zeolite samples. Therefore the total count-rate of a zeolite sample after irradiation before the extraction experiment could not be measured directly with the Wallac gamma counter. This total count-rate was calculated with the removed fractions and the zeolite after extraction and washing. In case of the 1 ml extraction, the total count-rate was equal to the sum of the count-rates measured in: the extracted and washed zeolite; the 0.8 ml centrifuged eluates; the remaining 0.2 ml eluate with zeolite loss; and the three washes. For the 15 ml extraction, the total count-rate was equal to the sum of: the extracted and washed zeolite; 1 ml of the eluates $\times 15$; 1 ml of the washes $\times 10$; and the last 0.5 ml of wash. The count-rate that was measured in the eluates and zeolite, was compared to this total count-rate.

3.5.3.1. Detector efficiency

The detector efficiency of the Wallac gamma counter for measuring ^{166}Ho was determined to relate the measured count-rate to the number of disintegrations per second. This was needed to calculate the specific activity. For this purpose 0.4 ml of stock solution was added to a 10 mm high INAA cup. This cup was placed in a slightly larger capsule. The count-rate was measured with the Wallac and corrected with Equation 3.3 for: the background radiation, the time of measurement and the filling volume. Then the emitted gamma spectrum was

3. Experimental Method

measured with a well-type germanium detector for 1 hour with a dead time of 0.6%. The efficiency of this detector was known and the INAA software was used to calculate the ^{166}Ho activity. A factor $F_{A/\text{counts}}$ in Bq/CPM was determined that relates the count-rate measured with the Wallac to the disintegrations of ^{166}Ho per second. This factor was used to calculate the activity of a sample, $A_{166\text{Ho}}$ in Bq.

$$A_{166\text{Ho}} = F_{A/\text{counts}} \cdot A_{\text{corr}} \quad (3.4)$$

3.5.4. Activity measurements with the HPGe detector

To analyse the extraction process more directly, the zeolite samples were measured with the HPGe detector. The distance between the detector and the sample was adjusted such that the total count-rate after irradiation before extraction was measured with a dead time below 12%. The same distance was used to compare measured count-rates with each other. Hence, the same distance was used for all measurements of the samples obtained from the same irradiated zeolite. To measure the total count-rate, first the sample was centrifuged for 5 min at $10\text{k} \times \text{g}$ for a 1 ml extraction or at $12\text{k} \times \text{g}$ for a 15 ml extraction. The sample was measured on the HPGe detector, ensuring that the part of the surface that was raised during centrifugation was facing downwards. The decrease of activity in the zeolite during the extraction procedure was studied by measuring it with the HPGe detector before the subsequent addition of the ammonium chloride solution. The position of the zeolite during measurement was similar to that used for measuring the total count-rate with the raised surface facing downwards. The 0.8 ml centrifuged eluate for the 1 ml extraction and the upper 1 ml eluate for the 15 ml extraction were also measured. The zeolite was also measured before and after washing.

The HPGe detector measured the emitted gamma spectrum. A measurement time, t_{det} in s, of 120–480 s was used. The number of counts, $\#C_{\text{HPGe}}$, was obtained by integrating this spectrum between 77.0 and 84.0 keV. A background correction was included by integrating the spectrum above the line connecting the counts at edges of the interval. The count-rate, A_{HPGe} in CPM, with a correction for the time between irradiation and the measurement, t_{meas} in s, was calculated with Equation 3.5.

$$A_{\text{HPGe}} = 60 \cdot \frac{\#C_{\text{HPGe}} \cdot 2^{t_{\text{meas}}/t_{1/2}}}{t_{\text{det}}} \quad (3.5)$$

3.5.4.1. Geometry effects

The HPGe detector was sensitive to the applied geometry during measurement. The effect of this was studied by subsequent measurements of the same sample. For example, a sample with zeolite suspended in an ammonium chloride solution was measured for different waiting times after shaking or centrifuging. The influence of the filling volume for measuring with a 15 ml tube or an Eppendorf tube at a detector distance with either two or three 5 cm high spacers, was analysed with a comparable method as applied for the determination of the filling volume correction factor that has been described in Section 3.4.4.2. 0.5 ml of milliQ was added to 26 mg of irradiated holmium chloride hexahydrate in an INAA cup and this was stirred. 0.2 ml was pipetted in an Eppendorf tube and in a 15 ml tube. The count-rate was measured with the HPGe detector at a total volume of: 0.2, 0.4, 0.6, 0.8, 1.0, 1.2 and 1.4 ml for the Eppendorf tube and at a total volume of: 0.2, 0.4, 0.6, 0.8, 1.0, 2.0, 3.0, 4.0, 5.0, 7.5, 10.0 and 15.0 ml for the 15 ml tube. The volume was increased by adding milliQ. Each measurement was performed for a detector distance with two and three spacers.

3.5.5. Radiolysis

The effect of radiolysis was inspected by a structural analysis with XRD and MAS-NMR. Na-LTA in powder form was measured before and after irradiation for 3 min at BP3. A decay time of minimally 4 weeks was applied to reduce the activity to background level before the second measurement was performed.

3.5.5.1. XRD

The Na-LTA was placed in the sample holder. The surface was smoothed with a glass plate and any residual powder was brushed away. The sample was measured for 50 min with the X-ray powder diffractometer. The scattering angles in a range of 2.5 to 45° were measured. The diffractogram was measured before and after irradiation in order to be able to make a comparison.

3.5.5.2. MAS-NMR

The ²⁹Si- and ²⁷Al-MAS-NMR spectra were measured with a Bruker 500 MHz (11.7 Tesla) wide bore NMR spectrometer. A 3.2 mm MAS 3 channel probe was used which was tuned to aluminium at 130 MHz and silicon at 99 MHz, the proton channel was idle. The 90 degree pulse was calibrated for ²⁷Al and ²⁹Si using an aluminium nitrate solution in water and neat TMS respectively. A spinning rate of 15 kHz was applied. The measurement parameters are given in Table 3.5. By comparing the ²⁹Si- and ²⁷Al-MAS-NMR spectra before and after irradiation, information about radiolysis was obtained.

Table 3.5: Parameters for MAS-NMR measurements

Nucleus	Pulse	Scans	Relax. Delay	Frequency	Acq. Time
²⁹ Si	6.4 μs (90°)	2048	150 s	99 MHz	0.1 s
²⁷ Al	1.4 μs (15°)	1024	20 s	130 MHz	0.025 s

3.6. Calculations with measured quantities

This section describes how the previous mentioned measurements were used to calculate the weight percentage of holmium, the decrease of water content in the furnace, the probability of relocation upon recoil and the specific activity.

3.6.1. Holmium weight percentage

The weight percentage of holmium, wt% Ho, was measured to characterise the loading and extraction efficiency. In case of INAA, the software calculated the wt% with the initial sample mass and the measured amount of holmium concluded from the gamma spectrum. The wt% Ho at the tracer study was calculated with Equation 3.6.

$$wt\%Ho = \frac{N_{Ho} \cdot M_{165Ho}}{m_{sample}} \quad (3.6)$$

3. Experimental Method

N_{Ho} followed from Equation 3.1, obtained with a count-rate measured after washing the zeolite sample. The molar mass of ^{165}Ho was used, since the amount of ^{166}Ho nuclides was negligible. m_{sample} is the mass of the zeolite. This mass was obtained by measuring the zeolite with the Eppendorf tube after drying and subtracting the mass of the Eppendorf tube, which had been weighted before starting the experiment. The error was taken equal to one standard deviation from the mean of the triplicate experiment.

3.6.2. Decrease of water in zeolite during heating in furnace

In the furnace, water was extracted from the zeolite. The decrease in water content was determined with the difference in the mass of the zeolite before and after the calcination procedure at 600°C. Due to the radioactivity at the tracer studies, these masses could not be measured directly, but they were determined by weighing closed Eppendorf tubes. The count-rates measured for the tracer study, were used to determine the zeolite loss. This resulted in a corrected mass before heating in the furnace, $m_{before,corr}$ in g, of which the calculation is described in Appendix B.1. The zeolite mass after heating in the furnace, m_{after} in g, was measured after a decay time of 2 weeks during which the zeolite was stored in a closed Eppendorf tube. The removed water, R_{H_2O} in %, is expressed in Equation 3.7 as the decrease in mass of the zeolite during heating in the furnace relative to the initial mass of the zeolite.

$$R_{H_2O} = \frac{m_{before,corr} - m_{after}}{m_{before,corr}} \quad (3.7)$$

3.6.3. Characterising holmium extraction

This section describes the calculation of the characteristics for the holmium extraction at the tracer study specified in Section 3.2.3 and after irradiation specified in Section 3.5.2. A difference was made between a 1 ml or a 15 ml extraction.

3.6.3.1. Characterising the 1 ml extraction

1. The percentage of holmium or ^{166}Ho extracted per eluate, was calculated by dividing A_{corr} of the centrifuged eluate by its volume of 0.792 ± 0.003 ml and by A_{corr} of the zeolite before extraction.
2. The percentage of holmium or ^{166}Ho extracted in total was calculated by adding the percentages calculated in point 1 with a small volume correction. The first eluate was assumed to be 0.9 ml if the ammonium chloride solution was added to a dry zeolite powder. The last eluate was assumed to be 1.1 ml. All other eluates were taken to be equal to 1 ml.
3. The concentration of holmium in the tracer study was calculated by dividing the amount of holmium in the centrifuged eluate by the centrifuged eluate's volume of 0.792 ± 0.003 ml. The amount of holmium in the centrifuged eluate was calculated with its corrected count-rate via Equation 3.1. The concentration of ^{165}Ho in the eluates after irradiation was determined with ICP-MS.
4. The total amount of extracted holmium or ^{165}Ho was calculated by addition of the concentrations calculated in point 3 multiplied with the volumes such as described in point 2.
5. The eluates were normalised to the first eluate by dividing A_{corr} of the centrifuged eluate by A_{corr} of the first centrifuged eluate.

6. For the tracer study, the decrease in wt% Ho was determined by subtracting the wt% Ho measured after the extraction from the wt% Ho measured for a similar loading procedure. The wt% Ho was calculated with Equation 3.6. The calculation of the specific activity is discussed in Section 3.6.4.

3.6.3.2. Characterising the 15 ml extraction

1. The percentage of holmium or ^{166}Ho extracted per eluate was calculated by multiplying A_{corr} of the 1 ml eluate with 15 and dividing this by the total count-rate of the zeolite before extraction.
2. The percentage of holmium or ^{166}Ho extracted in total was calculated by adding the percentages calculated in point 1.
3. The concentration of holmium in the tracer study was calculated by dividing the amount of holmium in the 1 ml eluate by its volume. The amount of holmium in the 1 ml eluate was calculated with its corrected count-rate via Equation 3.1. The concentration of ^{165}Ho in the eluates after irradiation was determined with ICP-MS.
4. The total amount of extracted holmium or ^{165}Ho was calculated by adding the concentrations calculated in point 3 multiplied with 0.015.
5. The eluates were normalised to the first eluate by dividing A_{corr} of the 1 ml eluate by A_{corr} of the first 1 ml eluate.
6. For the tracer study the decrease in wt% Ho was determined by subtracting the wt% Ho measured after the extraction from the wt% Ho measured for a similar loading procedure. The wt%Ho was calculated with Equation 3.6. The calculation of the specific activity is discussed in Section 3.6.4.

3.6.4. Specific activity

The specific activity of the eluates, obtained after irradiation of the zeolite, was calculated with Equation 2.1. Where $A_{166\text{Ho}}$ was computed with Equation 3.4. In the experiments performed for this thesis, $m_{165\text{Ho}}$ was significantly larger than $m_{166\text{Ho}}$, which meant that $m_{166\text{Ho}}$ could be neglected in the calculation of the specific activity. $m_{165\text{Ho}}$ was calculated with the ^{165}Ho concentration of the eluate, $C_{165\text{Ho}}$ in M, measured with the ICP-MS.

$$m_{165\text{Ho}} = V_{meas} \cdot 10^{-3} \cdot C_{165\text{Ho}} \cdot M_{165\text{Ho}} \quad (3.8)$$

The specific activity was calculated with a measured activity corrected for the time between measurement and irradiation. Hence, it represents the specific activity that would be obtained if the processing time would be zero, $SA(t_0)$ in Bq/g. The specific activity after processing, $SA(t_{proc})$ in Bq/g, could be calculated with formula 3.9.

$$SA(t_{proc}) = SA(t_0) * \frac{1}{2}^{t_{proc}/t_{1/2}} \quad (3.9)$$

Where t_{proc} is the time required to process the zeolite after irradiation.

To determine the obtained specific activity without the Szilard-Chalmers effect for similar irradiation conditions, 11.95 mg of holmium chloride hexahydrate was irradiated at BP3 for 3 min. This was transferred from the INAA cup to an Eppendorf tube in a similar way as the irradiated zeolite was transferred with an ammonium chloride solution. The specific activity of this was determined in the same way as for the eluates. The specific activity of

3. Experimental Method

this irradiated holmium chloride hexahydrate was used for the calculation of the enrichment factor.

3.6.5. Relocation of ^{166}Ho between open and closed cages upon recoil

The percentage of ^{166}Ho that was extracted after irradiation, $\%Ex$, depended on the probability that holmium was extracted from an open cage, $P(O_f \rightarrow Ex)$, and the percent of ^{166}Ho nuclides present in the open cages after irradiation, O_f .

$$\%Ex = P(O_f \rightarrow Ex) \cdot O_f \quad (3.10)$$

O_f depended on the initial position of the holmium ions before irradiation and the probability of relocation to an open cage upon recoil.

$$O_f = O_i \cdot P(O_i \rightarrow O_f) + C_i \cdot P(C_i \rightarrow O_f) \quad (3.11)$$

Where O_i is the percentage of holmium in the open cages before irradiation; C_i is the percentage of holmium in the closed cages before irradiation; $P(O_i \rightarrow O_f)$ is the probability of a ^{166}Ho nuclide to remain in its open cage or to relocate to another open cage upon recoil; and $P(C_i \rightarrow O_f)$ is the probability of a ^{166}Ho nuclide to relocate from a closed cage to an open cage upon recoil.

3.6.5.1. Recoil from open to open cages

$P(O_i \rightarrow O_f)$ was determined with the extraction experiments after irradiating zeolite that was not calcined. Consequently, all the holmium ions were located in the open cages: $O_i = 1$ and $C_i = 0$. Therefore Equation 3.10 and 3.11 simplified to:

$$P(O_i \rightarrow O_f) = \frac{\%Ex}{P(O_f \rightarrow Ex)} \quad (3.12)$$

$\%Ex$ and $P(O_f \rightarrow Ex)$ were determined with the description in point 2 of Section 3.6.3. The measurements of the extraction after irradiation and at a corresponding tracer studies were used to determine $\%Ex$ and $P(O_f \rightarrow Ex)$ respectively. $P(O_i \rightarrow O_f)$ was determined with experiments 1, 2, 5, 6, 9 and 10 of Table 3.4. The calculation of the error of $P(O_i \rightarrow O_f)$ is described in Appendix B.3.

3.6.5.2. Recoil from closed to open cages

$P(C_i \rightarrow O_f)$ was calculated for measurements with zeolite that had been calcined before irradiation with: either with or without holmium extraction before irradiation; and a 1 ml or a 15 ml extraction volume. This corresponds with experiments 3, 4, 7 and 8 of Table 3.4. Rewriting Equations 3.10 and 3.11 results in Equation 3.13 for $P(C_i \rightarrow O_f)$:

$$P(C_i \rightarrow O_f) = \frac{\frac{\%Ex}{P(O_f \rightarrow Ex)} - O_i \cdot P(O_i \rightarrow O_f)}{C_i} \quad (3.13)$$

$\%Ex$ and $P(O_f \rightarrow Ex)$ were determined with the description in point 2 of Section 3.6.3. The measurements of the extraction after irradiation and at a corresponding tracer studies were used to determine $\%Ex$ and $P(O_f \rightarrow Ex)$ respectively. O_i after calcination was determined

3.6. Calculations with measured quantities

with the percentage of holmium extracted for calcined zeolite at the tracer study, which is described in Appendix B.2 and $C_i = 1 - O_i$. The value of $P(O_i \rightarrow O_f)$, obtained with the extraction experiments after irradiating non-calcined zeolite, was also applied in the calculation of $P(C_i \rightarrow O_f)$. The calculation of the error in $P(C_i \rightarrow O_f)$ is described in Appendix B.3.

4. Results and Discussion

In this chapter the results obtained by performing the experiments described in Chapter 3 are discussed. In this thesis the experiments were only performed with zeolite A. Consequently, if in this chapter zeolite is mentioned without specifying the specific type, then zeolite A is meant. The chapter is divided in three sections; first the applied methods are discussed, then the characterisation of processing zeolite A is given and finally the irradiation experiments are analysed.

4.1. Characterisation of applied methods

4.1.1. Triplicate experiments

It should be noted that the triplicate experiments were not completely independent, since they were conducted simultaneously. Hence, factors such as temperature fluctuations or incorrect timing were similar within the triplicate. The given standard deviation could be too low. Some triplicate experiments were repeated to validate the obtained standard deviation. For example, the triplicate experiment with loading for 1 h at 80°C was performed twice. The obtained wt% differed 0.1%, which was equal to the standard deviation from both experiments. The extraction at 50°C for 1 h was also repeated. The results of both experiments agreed within the given standard deviation. This indicated that the standard deviation could be adequately determined with triplicate experiments performed simultaneously.

4.1.2. Washing

Two washing methods were studied: with and without shaking for 0.5 h between mixing and centrifuging. The resulting holmium concentrations in the washing solutions are presented in Figure 4.1. The two methods resulted in a similar holmium concentration in the washing solutions. Therefore, it was concluded that no shaking during the washing procedure was required. Furthermore, it is shown that for washing three times, the holmium concentration in the wash decreased by more than a factor thousand. Hence, washing three times was sufficient. The lack of decrease in the holmium concentration for wash 4 and 5, could be caused by traces of LTA containing holmium in the measured washing solution. Comparing the concentration of holmium in the supernatant with the concentration in the washes revealed that an equivalent of about 0.1 ml of the supernatant was not removed with pipetting.

4.1.3. Drying

Two methods were tested for removing water from the zeolite samples by applying either a freeze dryer or a vacuum desiccator. Drying with the vacuum desiccator is a simpler procedure and is better compatible for working with radioactivity because it can be performed in a fume hood behind lead shielding and does not require the freezing of radioactive samples. Therefore, it was investigated whether drying with the desiccator sufficed. A sample was first dried for 3 days in the vacuum desiccator. Hereafter, the sample was dried a second time with the freeze dryer. After drying with the desiccator, another 5 wt% H₂O was extracted with the freeze dryer. The additional extracted water with the freeze dryer was presumed to be sufficiently minor, justifying the utilisation of the desiccator.

4. Results and Discussion

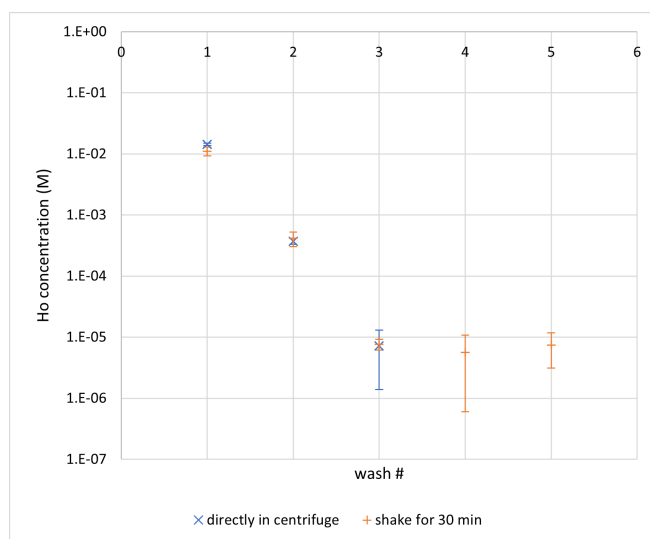


Figure 4.1: Holmium concentration in washing solutions. Washing was performed with and without shaking for 0.5 h between mixing and centrifuging. The holmium concentration was measured with the tracer study. The error is given as one standard deviation from the mean of a triplicate.

The water content in the zeolite after drying with the desiccator was studied by calculations based on the holmium and sodium content of the zeolite measured with INAA. Considering the general formula of zeolite A provided in Section 2.1.4, the number of Si, AL and O atoms of the zeolite could be determined, if information about the holmium and sodium content of a sample was known. For this, it was assumed that holmium and sodium were the only cations in the zeolite sample and that the zeolite had a Si/Al ratio of 1. By subtracting the mass of these atoms from the mass of the sample, the water content was determined. These calculations resulted in an average of 52 ± 4 H₂O molecules per unit cell, which deviates from the range of 20–30 water molecules per unit cell of zeolite A reported in literature [18, 24]. This discrepancy could be explained by the incomplete water extraction with the vacuum desiccator.

Heating the zeolite samples in a furnace to 600°C for calcination resulted in a reduction of $9.4 \pm 0.9\%$ of the mass after two days in the desiccator. For 52 ± 4 H₂O molecules per unit cell, the wt% H₂O in holmium loaded zeolite A would be 30–35%. Hence, not all water in the zeolite was removed in the furnace. After the furnace, the number of water molecules per unit cell would correspond better to the literature. It is also expected that the water content after the oven is more consistent than after drying in the desiccator. Therefore it would be advisable for future research to determine weight percentages with the mass obtained after drying in an oven. A disadvantage of this method is that the zeolite samples dried in an oven can not be reused for further experiments, due to relocation of the cations between the open and closed cages.

4.1.3.1. Time in vacuum desiccator

The time required for drying in the vacuum desiccator was determined by weighing 27 samples for increasing times inside the desiccator. The difference in weight was assumed to be

the extracted water. Zeolite samples with varying holmium weight percentages were used as well as some samples also containing ammonium ions. No significant difference was observed between these cases. If the amount of water extracted after 14 days in the desiccator is considered as 100%, then the percentage of extracted water for shorter time periods in the desiccator is visualised in Figure 4.2. It can be seen that after one day already most of the water was extracted (95%). Hence, drying for 1 day in the desiccator was satisfactory for subsequent calcination. However, this corresponds to a total weight of 108% compared to the weight after 14 days in the desiccator. For a true wt% Ho of 15%, the calculation with the incorrect mass after 1 d in the desiccator would result in a 1% lower calculated wt%. Furthermore, there was a large variation in the extracted water. It is concluded that 1 day in the desiccator is insufficient for determination of weight percentages.

After two days in the desiccator, 99% of the water was extracted. This corresponds to a total weight of 101% compared to the weight after 14 days in the desiccator. The error in the calculated wt% Ho is then merely 0.1%. Moreover, the variation in the extracted water was less. Therefore, the weight after two days in the desiccator could be used for the calculation of the wt%, even though a systematic error of -0.1% should be kept in mind.

For three days in the desiccator the systematic error in the wt% calculations was even decreased to -0.05% . For this reason, the difference in extracted water for 3 days or more in the desiccator, was assumed to be sufficiently minor. Consequently, the mass of the zeolite after minimally three days in the desiccator was used for the wt% calculations.

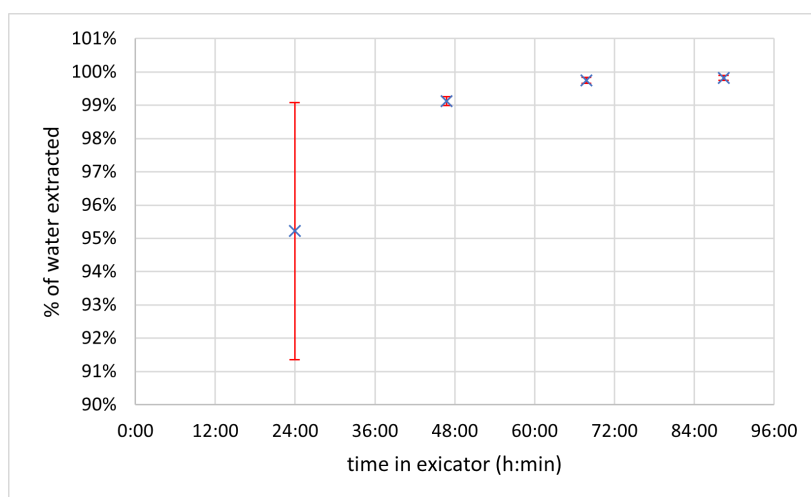


Figure 4.2: Percentage of water extracted for increasing time periods in the desiccator. The water extracted after 14 days in the desiccator is regarded as 100%. The error is given as one standard deviation from the mean of 27 samples containing different weight percentages of holmium.

It should be noted that this experiment was performed for non-calcined samples loaded and extracted at room-temperature, while also calcined samples or samples loaded and extracted at higher temperatures were dried with the desiccator. Therefore, the water extraction for 1 day versus 4 days in the desiccator was considered for three samples loaded at 80°C . This gave similar results as the extensive analysis above. In view of this, the characterisation of drying with the desiccator was assumed to be valid for all types of applied zeolite samples.

4. Results and Discussion

After 14 days in the desiccator 0.11 ± 0.02 g water was removed. Hence, about 0.1 ml of liquid was not removed after pipetting. Therefore during the extraction procedure of holmium it was assumed, that when 1 ml liquid was added to dried zeolite, only 0.9 ml was removed by pipetting. Also the last eluate was assumed to have a volume of 1.1 ml, since washing removed the last 0.1 ml, which was not removed by pipetting.

4.1.4. Measuring holmium

4.1.4.1. ICP-OES

ICP-OES was not suitable to measure holmium in zeolite. To measure the correct amount of holmium, the zeolite has to be dissolved, such that the holmium ions are free in the solution. In order to dissolve the zeolite hydrofluoric acid was needed. However, HF reacted with holmium forming a precipitate, which resulted in a lower measured value. When it was attempted to dissolve the zeolite without HF by using nitric and/or hydrochloric acid, with or without a microwave treatment, then small flakes of zeolite were observed in the solution. Even after applying an ultrasound bath for 4.5 hours, small flakes of zeolite were visible at the bottom of the vial. After a microwave treatment of zeolite in aqua regia with a drop of HF, no flakes were visible. Adding water resulted in a clear solution. However, within an hour a yellow precipitate became visible at the bottom of the vial. The same kind of precipitate was observed when this treatment was repeated with holmium chloride or holmium oxide. The ICP-OES measurements of this holmium chloride solution resulted in a concentration less than half of what was expected and for holmium oxide even less than a fifth of the expected concentration. On the other hand, the ICP-OES measurements after the same treatment without HF gave the expected concentrations. Furthermore, the ICP-OES machine can be damaged, when measuring solutions with incompletely dissolved zeolite or holmium-fluoride precipitate; the particles in the solution clog up the channel towards the argon torch.

Nevertheless, a holmium content higher than the theoretical value was calculated when the amount of holmium in the zeolite was determined by: the difference between the initial added holmium chloride solution, and the ICP-OES measurements of the holmium in the supernatant and washing solutions. The amount of holmium lost during the experiment resulted in a large error. Hence, it was not feasible to determine the holmium content in this manner.

To conclude, the ICP-OES was not suitable to determine the holmium content in zeolite. The obtained results had a substantial error, and/or the measurements could damage the machine.

Measurement of the holmium concentration in eluates with ICP-OES was also not feasible. The eluates contained a high concentration of NH_4 , requiring a dilution of at least a factor of 50 to ensure that the ammonium chloride concentration remained below 0.1 M. Higher concentrations of ammonium chloride would introduce an excess of ions into the plasma, resulting in the malfunctioning of the ICP-OES machine. However, with this dilution the concentration of holmium became too low to be measured accurately with the ICP-OES (below 1 mg/l). Therefore, ICP-MS was used for measuring the holmium concentration in eluates.

4.1.4.2. ICP-MS

The reference solutions with a concentration below 10 µg/l had a large residual error in the obtained calibration curves. Moreover, a concentration of 1 µg/l was measured for a blank. For reliable measurements, the sample solutions should have a concentration in the range of 25–500 µg/l, since the reference solutions in this range did result in an accurate linear calibration curve. Measuring the concentration of the reference solutions with 0.05 M ammonium chloride resulted in the expected values within the error of ICP-MS. It was therefore expected that an ammonium chloride concentration below 0.05 M did not influence the measured holmium concentration. Consequently, eluates needed to be diluted minimally by a factor 100.

For measuring the same sample successively ten times, the minimal and maximal measured value differed by $1.2 \pm 0.4\%$ from the average, which corresponded to the error given by the ICP-MS. However, measuring the same sample at separate days with new calibration curves could give significantly varying results, up to a difference of 20%.

The measurement of erbium was influenced by the ^{165}Ho in the sample. For an increasing concentration of holmium in the sample, the erbium concentration measured with a mass of both 166 u and 168 u, increased. No relative increase of measured ^{166}Er compared to ^{168}Ho was observed. Consequently, Erbium-166 in the samples could not be detected with the ICP-MS. This is not surprising, since the concentration of ^{166}Er was more than a million times smaller than the holmium concentration for the specific activities applied in this research.

4.1.4.3. INAA

The INAA measurements gave good results for the determination of the sodium and holmium content of zeolite samples. However, it is a relative complex and time demanding procedure. Therefore, experiments using INAA were performed merely once. The error only includes the error of the INAA measurement. Furthermore, INAA can only be applied on solid samples without ammonium ions, which excluded measuring the holmium content through out the course of an experiment, zeolite samples extracted with ammonium chloride or eluates. In conclusion, INAA facilitates the verification of other techniques measuring the holmium content in zeolite samples, but was not preferred as the standard measuring method.

4.1.4.4. Tracer study

The tracer study utilising ^{166}Ho was selected as the preferred method for measuring holmium, due to its rapid measurements and straightforward application. The measurement of 13 eluates from three distinct stock solutions yielded consistent results, when measuring with the tracer study and ICP-MS. The measured holmium concentrations exhibited a variation of $2.4 \pm 0.4\%$, which fell within the error of the ICP-MS. There was also a good agreement between the holmium content measured using the tracer study and INAA for zeolite samples produced under similar experimental conditions, as evidenced by the experiments conducted for different loading times and concentrations.

However, the tracer study has certain disadvantages. Because of the relative short half-life of ^{166}Ho , a stock solution had a restricted processing time of one week. For low concentrations

4. Results and Discussion

this was even less. As a result, the tracer study is not suitable for longer experiments involving extended loading, extraction or stability investigations. Furthermore, only holmium that is added via the stock solution to a sample, can be measured to provide a known ratio between the measured count-rate and amount of holmium. However, this required starting every experiment with holmium loading in the zeolite, which limited the time left for subsequent experiments. It should also be noted that during the count-rate measurement of 1 ml of stock solution, in order to determine $F_{A/\text{counts}}$, the sample was not in the thermoshaker and hence the sample was not shaken or heated. The influence of this on the loading was neglected. This influence was limited by using a short measurement time of 1 min per sample. Some supplementary comments about the tracer study are given in Appendix D.

4.1.5. Wallac gamma counter

The Wallac gamma counter was applied for both the tracer study and activity measurements after the irradiation of zeolite. The measured count-rates ranged from 10^2 to 10^6 CPM. A higher activity caused a slight shift in the measured peak energy, while the same integrating window was applied. Nevertheless, the effect of this energy shift on $F_{N/A}$, $F_{cor,V}$ and $F_{A/\text{counts}}$, which were determined at count-rates of respectively 10^5 , 10^5 and 10^4 CPM, was neglected.

Samples with A_{meas} exceeding 10^6 CPM were either discarded or remeasured after a waiting period. Nevertheless, it is probable that this upper limit was inadequate. A mean discrepancy of 5% was observed in the decay-time corrected count-rates, when remeasuring samples with A_{meas} initially in the order of 10^5 CPM and subsequently in the order of 10^3 CPM. In the future, it would be advisable to apply a limit of 10^6 CPM for the total counts measured by the Wallac, instead of applying this limit on the integrated counts.

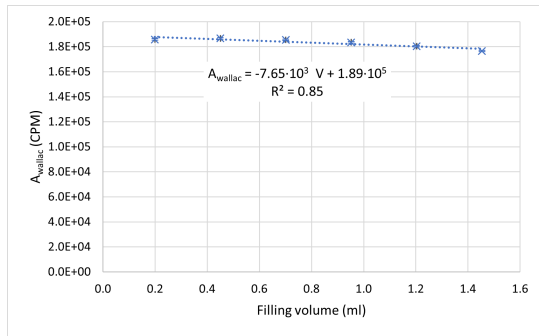
4.1.5.1. Filling volume

The influence of the filling volume on the count-rate measured with the Wallac is demonstrated in Figure 4.3. Increasing the filling volume decreased the measured count-rate, which was probably induced by the amplified impact of self-shielding and greater distance to the detector. The difference in self-shielding between water or zeolite was neglected, when applying the filling volume correction. The linear regression analysis of the graphs yielded filling volume correction factors, $F_{cor,V}$ of 0.091 ± 0.002 for the large sample rack and 0.040 ± 0.001 for the small sample rack. The error is one standard deviation from the mean of the two measurements (0.2 ml and 0.5 ml of stock solution). These correction factors were applied for both the tracer study and the activity measurements after irradiating zeolite.

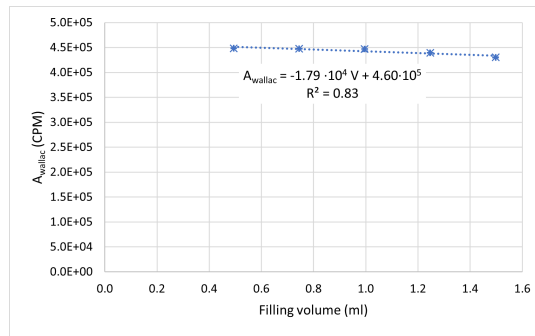
4.1.5.2. Detector efficiency

The detector efficiency, expressed as $F_{A/\text{counts}}$, was measured to be 0.263 ± 0.005 Bq/CPM. However, this was determined with merely one measurement. The error was calculated with the uncertainty of the Wallac and well-type germanium detector, but a triplicate should be performed to investigate the real error. Furthermore, it was assumed that the same filling volume correction factor could be applied for the INAA cup. Additionally, the shielding difference between an INAA cup or other plastic vials was neglected.

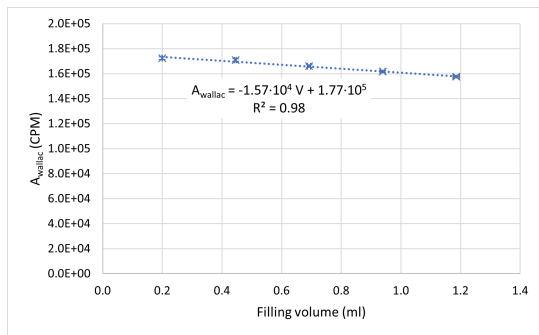
4.1. Characterisation of applied methods



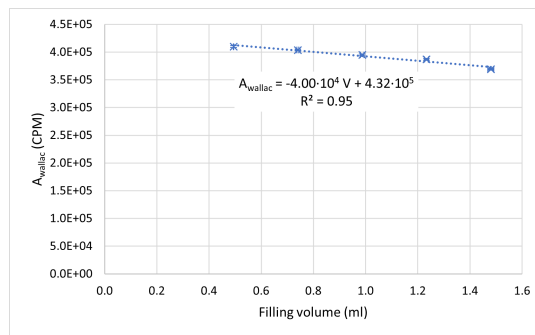
(a) Small rack: 0.2 ml stock solution



(b) Small rack: 0.5 ml stock solution



(c) Large rack: 0.2 ml stock solution



(d) Large rack: 0.5 ml stock solution

Figure 4.3: Influence of the filling volume on the measured count-rate with the Wallac gamma counter. The measured count-rates were corrected for the measurement time and background radiation. (a) and (b) were made with a different stock solution than (c) and (d). A linear fit is included. The error of the count-rate was determined with the relative error of one standard deviation from the total measured counts following from the counting statistics. The error of the volume was calculated with one standard deviation determined with the calibration of the pipette.

4.1.6. HPGe detector

The measurements with the HPGe detector were very sensitive to geometric differences. For instance, there was a noticeable difference of 6.5% in count-rate, when measuring an Eppendorf tube containing eluate in an upright or upside-down position. Additionally, the location of the activity within the sample significantly influenced the measured count-rate. For measuring irradiated zeolite in a 15 ml ammonium chloride solution, there was a 23% difference in count-rate between measurements taken immediately after shaking versus 8 minutes after shaking. Furthermore, if the sample was centrifuged before the measurement, this difference increased to 43%. However, even when measuring after centrifugation, the measured count-rate was greatly influenced by whether the activity resides in the zeolite or the ammonium chloride solution. Measuring a centrifuged zeolite sample directly after adding ammonium chloride solution or after 1 day, resulted in a 9% difference in count-rate.

Nevertheless, measuring zeolite without a solution on top also gave unsatisfactory results. The orientation of the sloped surface resulting from centrifugation caused a 3% difference

4. Results and Discussion

in measured count-rate. Additionally, subsequent measuring of a zeolite sample without a solution on top, before and after removing a fraction containing activity, often resulted in an equal or higher count-rate than before. Even if the measured count-rate did decrease, this decrease could not be related to the count-rate of the removed fraction. This indicated that the geometry differences between samples were too large to compare with each other. Furthermore, due to the lower efficiency of the HPGe detector, the eluates of the 15 ml extraction could not be measured with sufficient counts.

All in all, it was concluded that uncertainties associated with measurements using the HPGe detector were too large for the purposes of this study. Therefore, the Wallac measurements were used for analysing the results, despite being less direct and requiring additional calculations and assumptions. The results obtained from the HPGe detector aligned with the values calculated using the Wallac measurements within the considerable error margin of the HPGe detection method. This indicated that the applied calculations with the Wallac measurements, closely resembled reality.

4.1.6.1. Filling volume

In Figure 4.4 the impact of the filling volume on the measured count-rate for the HPGe detector is given. Each volume was measured at two distances from the detector, using either two or three 5 cm high spacers. When measuring with three spacer blocks, the count rate was less than half compared to measuring with two spacers. Nonetheless, there was no consistent ratio between the measurements at the two distances, and as a result, measurements at different detector distances can not be related to each other.

The count-rate also clearly depended on the filling volume. Up to a filling volume of 1.4 ml, this relation was approximately linear, see Figure 4.5. Following the same calculation as for the Wallac, the linear fit yielded a filling volume correction factor of 0.22 ± 0.01 for measuring with two spacers and of 0.19 ± 0.02 for measuring with three spacers. These larger correction factors indicated that the HPGe detector was much more sensitive to geometry differences than the Wallac gamma counter. For larger filling volumes the linear approximation was not valid anymore. Consequently, the filling volume correction can not be applied for volumes above 1.4 ml. The measured points seemed to follow a logarithmic regression. Measuring with a filling volume of 15 ml substantially deviated from smaller filling volumes and can therefore not be compared with each other.

It is noteworthy that for two spacers, the filling volume had a greater impact than for measuring with three spacers. In Figure 4.5, this is seen by the steeper slope of measuring with two spacers instead of with three spacers. Also the deviation between the maximum measured count-rate (for the smallest filling volume) and the minimum measured count-rate (for the largest filling volume) relative to the mean, was larger for measuring with two spacers. It is expected that geometry effects have a smaller influence for measuring with three spacers.

Measuring in a Eppendorf tube or in a 15 ml tube resulted in comparable count-rates for a filling volume between 0.2 and 1 ml. This was observed for measurement with both two and three spacers. For measuring with two spacers the count-rate was about 3% lower in the Eppendorf than in the 15 ml tube, and about 2% for three spacers. This difference could be caused by geometric or shielding differences between the two vials, but could also be a result of a pipetting error or inhomogeneities, which was likely due to the small dimensions of mixing the irradiated holmium chloride in an INAA cup. To investigate the cause, the experiment should be repeated, preferably with a stock solution that is mixed better.

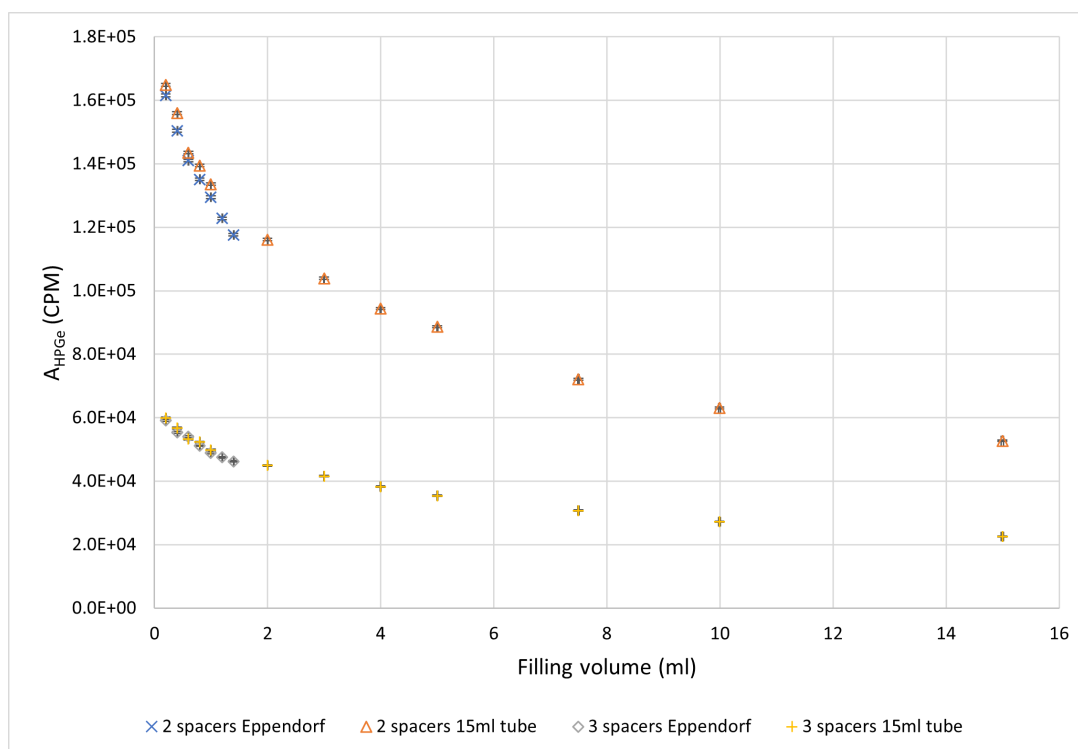


Figure 4.4: Influence of the filling volume on the measured count-rate with the HPGe detector. The count-rates were measured at two distances between the sample and the detector, as well as with an Eppendorf tube and 15 ml tube. The count-rates were corrected for the measurement time. The error of the count-rate is given as the error in determining the area in the emitted gamma-spectrum, depending on the total number of counts and on the background. The error of the volume was calculated with one standard deviation determined with the calibration of the pipette.

From this analysis it follows that samples measured in either an Eppendorf tube or a 15 ml tube, at the same distance from the detector and with a filling volume below 1.4 ml should be relatable with each other. However, this analysis was performed for homogeneous solutions. As mentioned before, the measurements of inhomogeneous samples of zeolite was not feasible.

4.2. Characterising zeolite A

As described in Section 2.4.2, the general concept consisted of irradiating zeolite with holmium in the closed cages, without holmium in the open cages and the subsequent extraction of radioactive holmium from the open cages. To produce a zeolite with holmium in the closed cages, first the holmium had to be loaded into the open cages, which will be discussed in Section 4.2.1. Then the ions had to be relocated within the zeolite by calcination, as described in Section 4.2.3. The holmium that remained in the open cages after calcination and radioactive holmium that recoiled to the open cages upon irradiation had to be extracted, which is examined in Section 4.2.2.

4. Results and Discussion

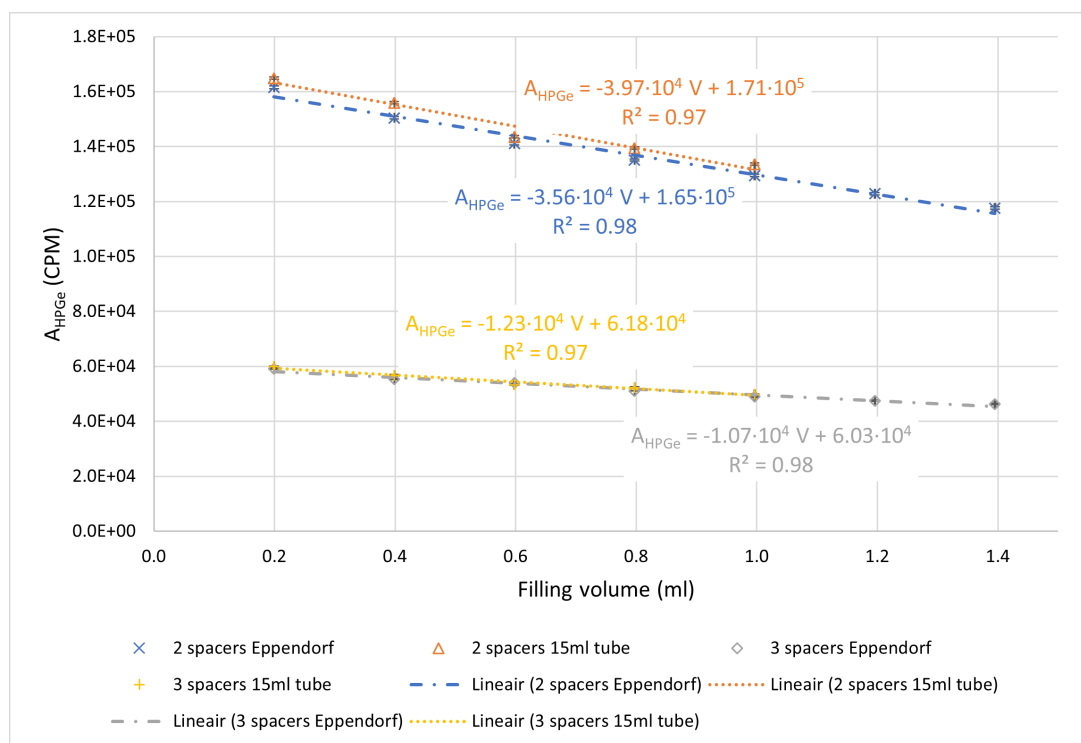


Figure 4.5: Influence of the filling volume on the measured count-rate with the HPGe detector, zoomed in for a range of 0.2–1.4 ml. The count-rates were measured at two distances between the sample and the detector, as well as with an Eppendorf tube and 15 ml tube. The count-rates were corrected for the measurement time. A linear fit per measurement was made. The error of the count-rate is given as the error in determining the area in the emitted gamma-spectrum, depending on the total number of counts and on the background. The error of the volume was calculated with one standard deviation determined with the calibration of the pipette.

4.2.1. Loading

The influence of the temperature, time, holmium chloride concentration and pH on the amount of holmium in the zeolite after loading was analysed. As explained in Section 2.1.4, maximally four holmium ions can be loaded per unit cell, resulting in a molecule formula: $\text{Ho}_4(\text{SiO}_2)_{12}(\text{AlO}_2)_{12} \cdot \text{N H}_2\text{O}$. From the INAA measurements of the holmium and sodium content in zeolite A followed that N was 52 ± 4 . Consequently, the theoretical maximum wt% Ho for zeolite A is 22%.

4.2.1.1. Loading time and temperature

Increasing the loading time resulted in a slight increase of the holmium content in zeolite A, as is shown in Figure 4.6. The wt% holmium seemed to converge to a limit for longer loading times. However, the INAA results indicated that for a loading longer than 4 days, the amount of holmium in the zeolite started to decrease again. This might be caused by the replacement of cations with H_3O^+ ions. The measurement of sodium content with INAA supported this, since the sum of holmium and sodium content in the zeolite loaded for 4 and

8 days was lower than expected. This cation deficiency has also been reported by Lai [21] and Newell [14] for zeolite X and L respectively. This would mean that loading for longer than 4 days is undesirable. It should be noted that the INAA measurement were performed with just one sample, and could not be reproduced with the tracer study due to the limited processing time for the tracer study related to the half-life of holmium of about a day.

From Figure 4.6 it is evident, that the temperature had a greater influence on the holmium content loaded into the zeolite. After a loading time of only 1 hour at 80°C, already a wt% Ho of $18.3 \pm 0.1\%$ was achieved, which was noticeably higher than the $13.7 \pm 0.5\%$ wt% Ho obtained for 1 hour loading at room-temperature and which was quite close to the theoretical maximum of 22%. Loading for 1 day at 80°C increased the wt% Ho by merely $1.1 \pm 0.1\%$ compared to loading for 1 hour. This increase was assumed to be small enough to use 1 h loading at 80°C as the general procedure.

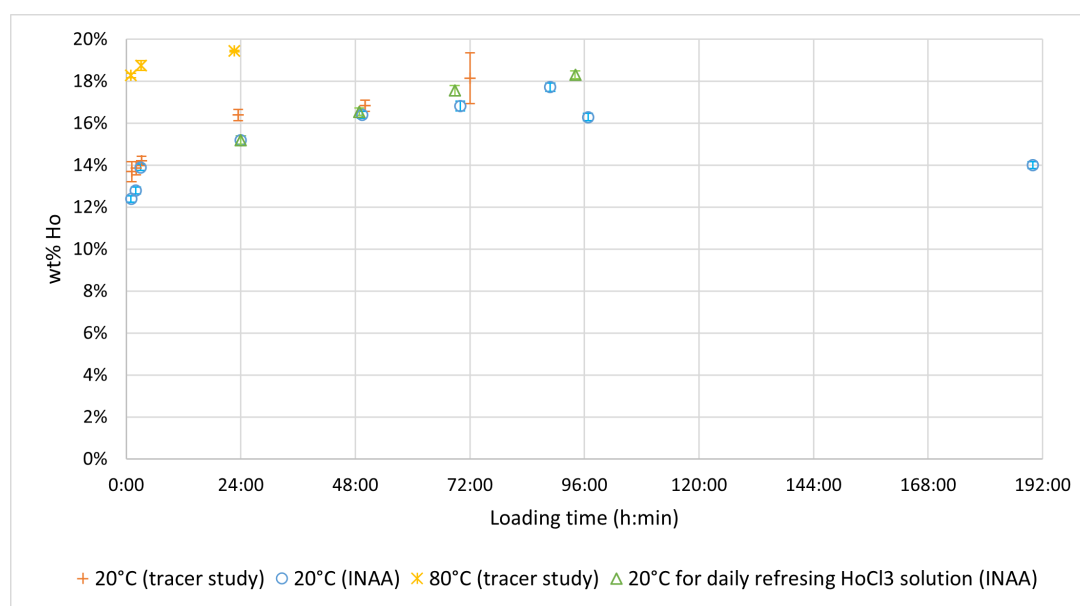


Figure 4.6: The wt% Ho in zeolite A after loading with different loading times at 20°C and 80°C, measured with the tracer study or INAA. The wt% Ho after loading for exchanging the holmium chloride solution daily is also included. The error of the tracer study is given as one standard deviation from the mean of a triplicate. The error for INAA only includes the error of the measuring method.

4.2.1.2. Holmium concentration

Figure 4.7 displays the amount of holmium in the zeolite after loading with varying concentrations of added holmium chloride solution. Even though the difference in loading time, the tracer study and INAA gave similar wt% Ho. This indicated that the holmium concentration was the limiting factor in these experiments instead of the loading time. There was an increase of loaded holmium up to an added concentration of 0.1 M. For higher concentrations the wt% Ho stayed approximately constant. Hence, for an efficient loading procedure a concentration of 0.1 M would suffice. A closer observation of the tracer study of experiments involving loading with 0.2 M, showed that about 40% of the initially added holmium

4. Results and Discussion

was absorbed by the zeolite. If all holmium could be absorbed by the zeolite, this means that a minimal concentration of 0.08 M is needed for the applied volume and zeolite mass. Nevertheless, loading with 0.02 M and 0.05 M suggested that maximally 90% of the initially added holmium was absorbed. This would indicate that a minimum holmium concentration of 0.09 M is required for efficient loading. Loading with varying concentrations close to 0.09 M are needed to verify this.

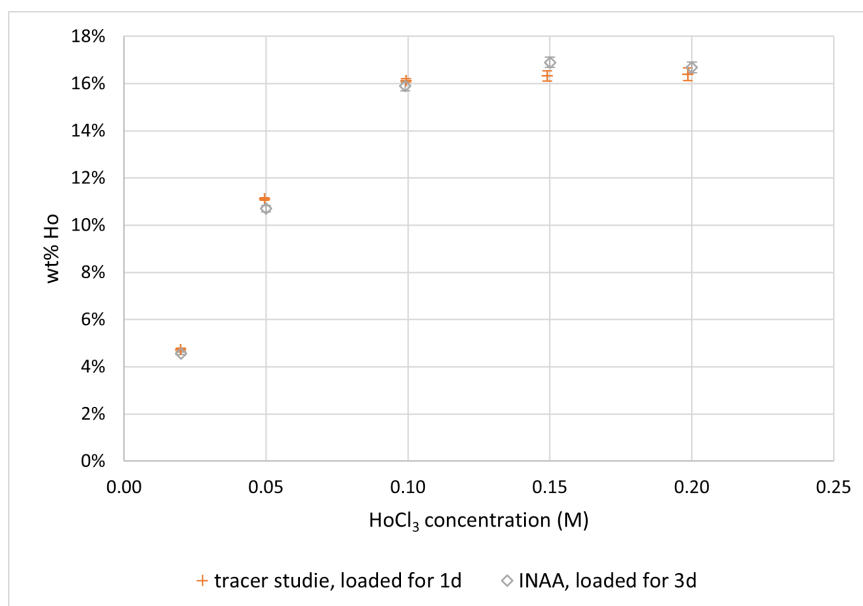


Figure 4.7: The wt% Ho for loading with different concentrations of holmium chloride solution. The loading was performed at room-temperature. For the tracer study a loading time of 1 day was used, while the measurements with INAA had a loading time of 67 ± 1 h. The error of the tracer study is given as one standard deviation from the mean of the triplicate. For INAA only the error of the measurement method is included.

The influence of the holmium concentration during loading was also studied by refreshing the holmium chloride solution. As shown in Figure 4.6, daily changing the holmium chloride solution resulted in a minimal increase of loaded holmium. It was concluded that changing the holmium chloride solution during loading was superfluous.

4.2.1.3. pH

The results of varying the pH of the added 0.2 M holmium chloride solution is depicted in Figure 4.8. The loading was performed at room-temperature for 70 ± 1 h. The change in holmium concentration due to the added hydrochloric acid was neglected, since a holmium concentration above 0.1 M gave similar results, see Section 4.2.1.2. No clear relation between pH and wt% Ho was observed. The lower wt% Ho measured at a pH of 2.98 could be an experimental error caused by adding only 0.8 ml HoCl₃ to 54.2 mg Na-LTA, instead of the normal procedure. Nevertheless, the sum of the holmium and sodium content of the zeolite measured with INAA, was lower than expected for lower pHs, which could indicate the replacement of the cations by H₃O⁺ ions. Therefore, for the general loading procedure the pH of the HoCl₃ solution was not adjusted, corresponding to a pH of 5.7.

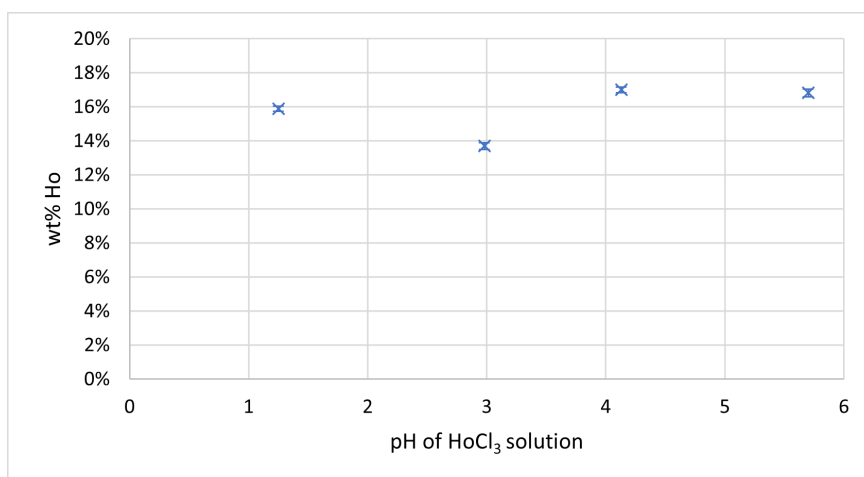


Figure 4.8: The wt% Ho for loading with holmium chloride solutions of varying pH. The loading was performed at room-temperature for 70 ± 1 h. The holmium content was measured with INAA. The given errors only include the error of the measurement method.

4.2.2. Extraction

The extraction of holmium from the open cages by an ammonium chloride solution was analysed. The most relevant extraction characteristics will be discussed in this section, an overview of all six characteristics mentioned in Section 3.2.3 is given in Appendix C. The effect of extraction time, temperature and volume was studied and the extraction of samples that were loaded differently is discussed.

4.2.2.1. Extraction time and temperature

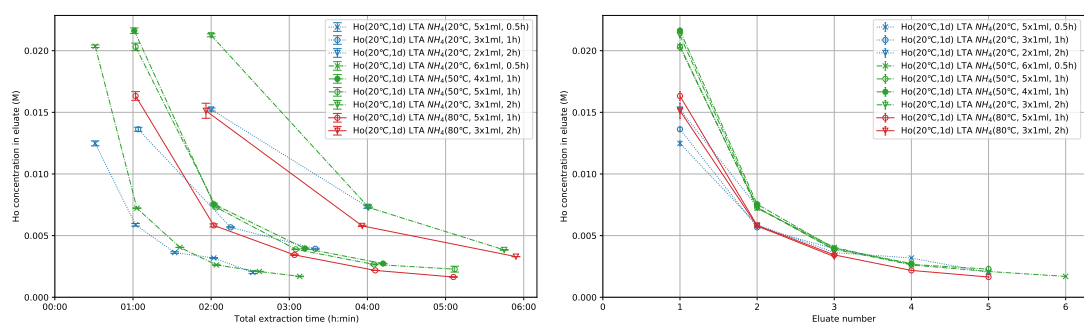
The holmium concentration in the eluates for an extraction of Ho(20°C, 1 d) LTA samples with a 1 ml saturated ammonium chloride solution, for varying extraction times and temperatures is given in Figure 4.9a. The holmium concentration was the highest in the first eluate and decreased for further eluates. The total amount of extracted holmium was determined with the concentrations in each eluate, see Appendix C. This was compared with the amount of holmium initially present in the zeolite to obtain the percentage of holmium extracted from the open cages, which is illustrated in Figure 4.9c. The extraction procedure is the most efficient for a high percentage of extracted holmium for a short extraction time. This was the case for an extraction of 0.5 h at 50°C.

The extraction process appeared to rely less on the extraction time, instead the number of the eluate seemed to be of greater importance. Therefore, the holmium concentration in the eluates and the percentage of holmium extracted, are plotted as function of the eluate number in Figures 4.9b and 4.9d. Merely a small difference was present between the experiments with varying extraction times. For 20°C, the longer extraction time removed slightly more holmium per eluate. This could indicate that the process of extracting holmium was slower at 20°C and for this temperature a longer extraction time could increase the extraction. For 50°C there was no clear difference between the extraction times. Hence, to reduce the processing time, an extraction time of 0.5 h is favourable. Moreover, at 80°C a longer extraction time negatively effected the holmium extraction.

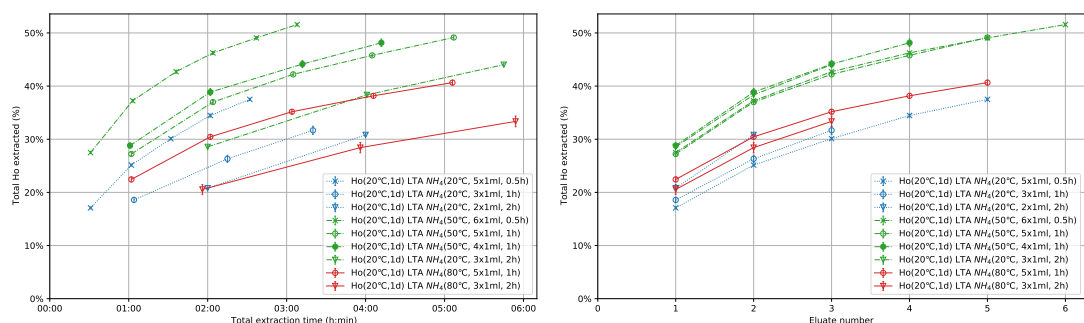
4. Results and Discussion

On the other hand, Figure 4.9b and 4.9d show that the temperature had a greater influence on the extraction process, especially for the first eluates. The extraction was most efficient at a temperature of 50°C. Surprisingly for increasing the temperature to 80°C less holmium was extracted. This and the decrease in extraction for a longer extraction time, might point to a change in the number of cations per binding site at 80°C. To this end, the extraction after loading at 80°C is studied in Section 4.2.2.2.

To sum up, it was concluded that an extraction time of 0.5 h at a temperature of 50°C was the most efficient. Therefore, this was taken as the standard extraction procedure for the 1 ml extraction.



(a) Holmium concentration in eluates at different extraction times (b) Holmium concentration in eluates as function of the eluate number



(c) Total percentage of holmium extracted at different extraction times (d) Total percentage of holmium extracted as function of the eluate number

Figure 4.9: Holmium extraction from the open cages for different extraction times and temperatures. Each point represents a change of the ammonium chloride solution. They are connected by lines to clarify the measurement points of one experiment. The notation as described in Section 3.2, is applied to specify the extraction procedure. All samples were loaded at 20°C for 1 d before extraction with 1 ml saturated ammonium chloride solution. Extraction at 20°C is given in blue with dotted lines, at 50°C in green with dash-dotted lines and at 80°C in red with solid lines. The markers indicate the applied extraction time: crosses for 0.5 h; circles for 1 h; and triangles for 2 h. The holmium was measured with the tracer study and the error is given as one standard deviation from the mean of the triplicate.

4.2.2.2. Different loading

The holmium concentration in the eluates for the extraction of zeolite A samples with varying loading procedures, is depicted in Figure 4.10a. If the first eluate was excluded from the analysis, then it appeared that the holmium concentration in an eluate was influenced by the wt% Ho in the zeolite prior to extraction, rather than by the loading temperature. Ho(20°C, 1 d) LTA and Ho(80°C, 1 h) LTA with similar holmium weight percentages, but with varying loading temperatures, exhibited comparable extraction characteristics (also see Appendix C). In contrast, a lower percentage of holmium was extracted per eluate for Ho(20°C, 1 h) LTA, which had an equal loading temperature, but a lower wt% than Ho(20°C, 1 d) LTA. Furthermore, the wt% Ho in n times extracted Ho(20°C, 1 h) LTA was comparable with the wt% Ho in $n + 1$ times extracted Ho(20°C, 1 d) LTA or Ho(80°C, 1 h) LTA; and as is seen in Figure 4.10a, the m^{th} eluate of Ho(20°C, 1 h) LTA was comparable with the $m + 1^{\text{th}}$ eluate of Ho(20°C, 1 d) LTA or Ho(80°C, 1 h) LTA.

As mentioned in Section 4.2.2.1 the extraction time was less important than the number of eluates for the extraction of Ho(20°C, 1 d) LTA. Figure 4.10a shows that this was also the case for the extraction of Ho(20°C, 1 h) LTA, since the results for an extraction time of 0.5 h and 1 h were similar. However, for the extraction of Ho(80°C, 1 h) LTA, the concentration of the first eluate increased for an extraction time of 1 h instead of 0.5 h, which indicated an insufficient extraction time. For the subsequent eluates, an extraction time of 0.5 h or 1 h resulted in similar concentrations.

It is unclear why the holmium concentration in first eluate of zeolite loaded at 80°C was lower than expected. However, it seemed unlikely that this was caused by a measurement error of the first eluate, since the decrease in the wt% Ho during the total extraction process was lower for the extraction of Ho(80°C, 1 h) LTA ($5.8 \pm 0.2\%$) than that for Ho(20°C, 1 d) LTA ($6.5 \pm 0.3\%$). The wt% Ho was determined by measuring the activity in the zeolite, which was independent of the activity measurement of the first eluate.

As mentioned in Section 2.1.4.2, there are two cation binding sites in the open cages of zeolite A: site II and site III. The temperature dependence of the extraction (see Section 4.2.2.1) together with the difference in the first eluate of zeolite samples with a similar wt% Ho loaded at 80°C or 20°C, hint that: the extraction efficiency differs between site II and III, and the distribution of cations among these two sites depends on temperature. A change in the distribution of cations over the sites in zeolite X has also been reported by Lai [21] for temperatures above 40°C. In this thesis, only a distinction between open or closed cage was made, neglecting the difference in site II or III. For further research, it would be interesting to apply a model which considers all three binding sites.

The extraction efficiency was compared by considering the total percentage of extracted holmium, as is presented in Figure 4.10b. The extraction efficiency of Ho(20°C, 1 d) LTA was larger compared to that of Ho(20°C, 1 h) LTA, which pointed to a dependence on the wt% Ho. The difference between the extraction efficiency of Ho(20°C, 1 d) LTA and Ho(80°C, 1 h) LTA was caused by the difference in the first eluate. Taking into account the percentage of holmium extracted from Ho(80°C, 1 h) LTA after five eluates, in the rest of this thesis it is assumed that $39.3 \pm 0.7\%$ of the holmium ions can be extracted from the open cages by extraction five times with 1 ml for 0.5 h each at 50°C. However, this neglects the influence of the wt% Ho on the extraction efficiency.

4. Results and Discussion

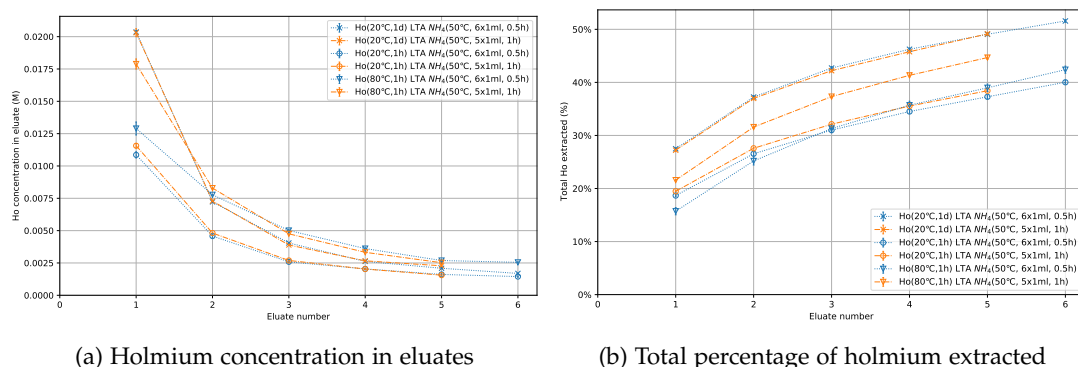


Figure 4.10: Holmium extraction from the open cages for different loading procedures. Each point represents a change of the ammonium chloride solution. They are connected by lines to clarify the measurement points of one experiment. The notation as described in Section 3.2, is applied to specify the loading and extraction procedure. All the extractions were performed at 50°C with 1 ml saturated ammonium chloride solution. An extraction time of 0.5 h is denoted in blue with dotted lines and of 1 h in orange with dash-dotted lines. The markers indicate the loading procedure: crosses for 1 d at 20°C; plus signs for 1 h at 20°C; and triangles for 1 h at 80°C. The holmium was measured with the tracer study and the error is given as one standard deviation from the mean of the triplicate.

4.2.2.3. Extraction volume

To increase the extraction of holmium from the open cages, another extraction procedure with a 15 ml saturated ammonium chloride solution per eluate was tested. First, an estimation of the required extraction time was made by measuring the holmium concentration of the first eluate for an increasing extraction time, as is illustrated in Figure 4.11. The experiment started with Ho(80°C, 1 h) LTA and was performed at room-temperature. It should be noted that this experiment was only performed with one sample. Moreover, the total extraction volume was decreased by 1 ml for each measurement point, while the influence of this volume change was neglected. Consequently, the results should be interpreted as a rough estimation and the obtained concentrations were unrealistically high compared to the other 15 ml extractions. The holmium concentration was expected to approach an equilibrium after sufficiently long extraction times. Therefore, a least square fit of the formula $b(1 - a^{t_{ex}})$ was applied, where b indicated the equilibrium concentration and a was a measure for the time required to reach the equilibrium. A value of 0.25 was found for a , which implied that 75% of the equilibrium concentration was reached for an extraction time of 1 day. For this reason, an extraction time of 1 day per eluate was applied for the general extraction procedure with 15 ml.

The holmium concentration in the eluates and the total percentage of extracted holmium for the extraction of Ho(80°C, 1 h) LTA with three times 15 ml saturated ammonium chloride solution are given in Figure 4.12. The large errors were induced by poor counting statistics due to: measuring the count-rate of only a fraction of the eluate, and a relative long decay time between irradiation of the holmium in the stock solution and the count-rate measurements. This extraction was compared to the extraction of Ho(80°C, 1 h) LTA with 1 ml of saturated ammonium chloride solution, shown in Figure 4.10. The concentrations in the eluates were much lower for the extraction with 15 ml than for 1 ml, although more holmium was extracted per eluate for the 15 ml extraction if the difference in volume was considered.

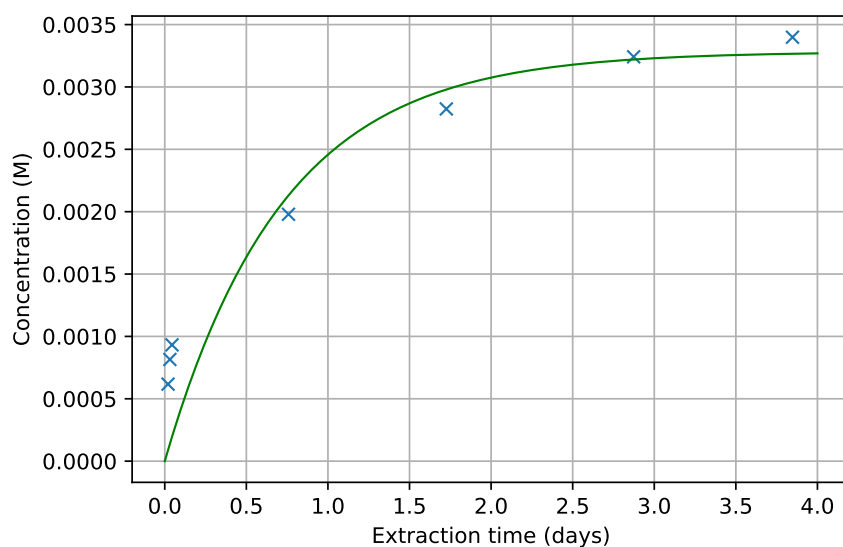


Figure 4.11: Holmium concentration in the first eluate for different extraction times. The extraction started with 15 ml of saturated ammonium chloride solution added to Ho(80°C, 1 h) LTA. For each measurement point 1 ml was removed, resulting in a decrease of the extraction volume. The line represents a least square fit of the formula $b(1 - a^{t_{ex}})$, with $b = 0.0033$ and $a = 0.25$. No errors are included, since the experiment was only performed once.

After extracting three times with 15 ml for 1 day per eluate, $55 \pm 1\%$ of the holmium was extracted from the open cages. This was better than the $39.3 \pm 0.7\%$ extracted with five times 1 ml for 0.5 h per eluate at 50°C. Another advantage of the 15 ml extraction was that it was less labour-intensive. However, it should be noted that the extraction procedure with 15 ml took three days, while the extraction with 1 ml could be performed within a single day. This is especially disadvantageous for processing after irradiation. Furthermore, this obtained extraction efficiency is still lower than that of La^{3+} in zeolite X of 70% for an extraction time of 20 h [21], and La^{3+} in zeolite L of 80% for 16 h and 98% for 3 d [52].

The influence of the extraction volume was further investigated by comparing a 10 ml and a 15 ml extraction of Ho(80°C, 1 h) LTA [600°C]. Figure 4.13 shows the total extracted holmium from the zeolite, by zooming in on Figure 4.12b. Since the difference between 10 and 15 ml was within one standard deviation, the data suggested that for a 15 ml extraction the limiting factor was time instead of the holmium concentration of the ammonium chloride solution. A 15 ml extraction of Ho(80°C, 1 h) LTA [600°C] for 3 days without changing the ammonium chloride solution resulted in a removal of $3.4 \pm 0.2\%$ of the holmium (see Figure 4.12b). This was higher than for changing the ammonium chloride solution daily, which supported that the extraction time was the limiting factor. However, there was a large error due to extremely poor counting statistics. The measured count-rates for the first eluates had an error of 9% and the count-rates of the third eluates had decreased to merely twice the background. Better counting statistics would have been obtained if the extraction was performed on Ho(80°C, 1 h) LTA, because the shorter processing time and larger removed fraction would have resulted in a higher count-rate.

4. Results and Discussion

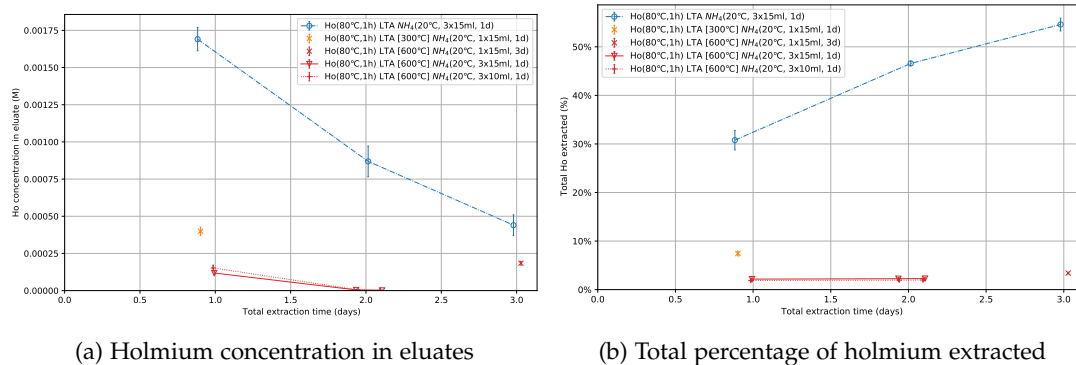


Figure 4.12: Holmium concentration in the eluates and the total percentage of holmium extracted for an extraction with 15 ml saturated ammonium chloride solution at room-temperature. Each point represents a change of the ammonium chloride solution. The lines clarify, which points belong to the same experiment. The notation as described in Section 3.2, is applied to specify the loading and extraction procedure. Blue represents non-calcined samples, yellow was calcined at 300°C and red was calcined at 600°C. Also an extraction with 10 ml saturated ammonium chloride solution is included (+). The holmium was measured with the tracer study and the error is given as one standard deviation from the mean of the triplicate.

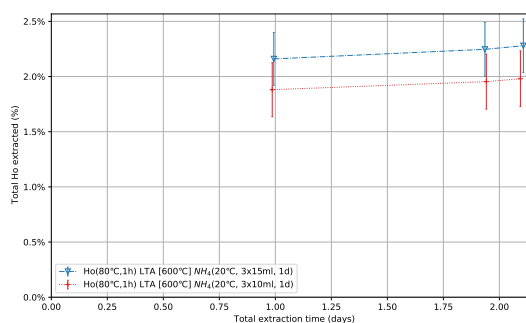


Figure 4.13: Total percentage of holmium extracted from Ho(80°C, 1 h) LTA [600°C] with an extraction volume of 10 ml (∇ with a dash-dotted line) or 15 ml (+ with a dotted line). Each point represents a change of the ammonium chloride solution. They are connected by lines to clarify the measurement points of one experiment. The percentage was measured with the tracer study, with 100% equal to the holmium in the open and closed cages of the zeolite before extraction. The error is given as one standard deviation from the mean of the triplicate.

4.2.3. Calcination

Different calcination procedures were studied by analysing subsequent extraction, which is displayed in Figure 4.14. The samples were loaded at 80°C for 1 h and the extraction was performed with a volume of 1 ml at 50°C for 0.5 h per eluate. The decrease in the amount of holmium extracted after calcination points to the relocation of the holmium ions from the open to the closed cages. The extraction of $2.64 \pm 0.02\%$ of the holmium ions after a calcination at 600°C indicated that $93.3 \pm 0.1\%$ of the holmium ions were in the closed cages after

calcination, under the assumption that for the applied extraction procedure $39.3 \pm 0.7\%$ of the holmium ions were removed from the open cages (see Figure 4.10b). The high percentage of holmium ions found in the closed cages after calcination corresponds with the findings of Lai [21] and Newell [14], that La^{3+} ions primarily occupy the closed cages in zeolite X and L upon dehydration. Furthermore, it was observed that the calcination at 300°C was less effective, than at 600°C . After calcination at 300°C a larger percentage of the holmium ions was extracted, indicating that a smaller fraction of holmium ions was in the closed cages after calcination ($75.2 \pm 0.4\%$). Therefore, a calcination temperature of 600°C was applied in this thesis.

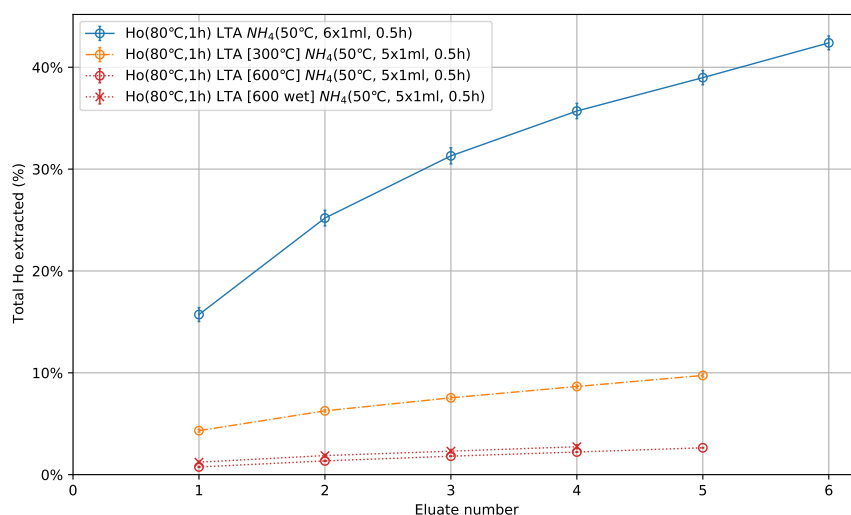


Figure 4.14: Influence of calcination on the percentage of extracted holmium. All samples were loaded for 1 h at 80°C and extracted with 1 ml for 0.5 h per eluate at 50°C . Each point represents a change of the ammonium chloride solution. They are connected by lines to clarify the measurement points of one experiment. Calcination at 600°C is denoted in red with dotted lines, at 300°C in orange with a dash-dotted line and no calcination in blue with a solid line. The circles represent samples that were dried before calcination, while the samples denoted by crosses were put in the oven with 0.2 ml of milliQ. The percentage was measured with the tracer study, with 100% equal to the holmium in the open and closed cages of the zeolite before extraction. The error is given as one standard deviation from the mean of the triplicate.

A similar behaviour was also noticed for the extraction with 15 ml, shown in Figure 4.12. After calcination at 600°C only a few percent of the holmium was extracted, suggesting that approximately $93 \pm 1\%$ of the holmium ions were locked in the closed cages. For calcination at 300°C more holmium was extracted, indicating that only $76 \pm 2\%$ of the holmium ions were locked in the closed cages. For these calculations only the first extraction was considered, because of the poor counting statistics for 600°C , and the lacking experimental data for 300°C .

The variant of the calcination procedure without drying the sample before the furnace gave similar results as with drying. The slightly higher extraction of holmium by the first eluate of the sample without drying before the furnace, could be attributed to the longer extraction time of 3 h instead of 0.5 h. Hence, the drying step, taking 1–2 days, could be omitted

4. Results and Discussion

to reduce the process time. However, without drying a considerably larger fraction of the sample was not transferred from the Eppendorf tube into the crucible ($23\pm 3\%$) compared to that with drying ($2\pm 1\%$). Therefore zeolite samples were dried before calcination for the rest of the thesis.

4.2.3.1. Dehydration

As mentioned in Section 4.1.3 the zeolite was dehydrated in the furnace. The rehydration of the zeolite appeared to be a slow process. This corresponds to the finding of Peters and Djanashvili [53] about the slow water exchange between open and closed cages in zeolite L. Dyer et al. [18] have reported that the complete rehydration of zeolite A can take up to one month. Before calcination the wt% holmium was $18.3\pm 0.1\%$, due to the dehydration this increased to $20.6\pm 0.6\%$ after calcination. Since no holmium is removed during calcination, rehydration should result in the same wt% as before calcination. However, a holmium wt% of $20.2\pm 0.2\%$ was found after being in contact with a 1 ml ammonium chloride solution for 2–5 h during extraction and with approximately 0.1 ml of milliQ for 2 weeks during decay before drying. While a wt% lower than before calcination was expected, since $3.4\pm 0.2\%$ of the initial present holmium was extracted. After the 1 ml extraction of zeolite calcined at 300°C , a wt% of $18.4\pm 0.2\%$ was measured. This was similar to the wt% before calcination, although about 10% of the initial holmium was removed. This discrepancy was likely caused by a lack of rehydration of the zeolite. Nevertheless, this hypothesis has to be tested by a more direct method, since the wt% holmium was not only affected by the water content in the zeolite, but also by other factors, especially when extracting with an ammonium chloride solution. The rehydration could for example be analysed by contacting the calcined zeolite with milliQ for different periods of time in combination with subsequently measuring the water content. The latter could be done either with gravimetric analysis or with the sodium and holmium content measured with INAA. Surprisingly, after extraction with 15 ml of ammonium chloride solution for 3 days the zeolite appeared to be rehydrated.

4.2.4. Recombination and interchange of holmium ions

Contacting the dried Ho(80°C , 1 d) LTA with a 0.01 M holmium chloride solution for 0.75 h at 50°C , resulted in an additional holmium uptake of about 1% compared to the holmium content in the zeolite before the extra loading. For an extra loading of 3 h, this was about 3%. Contacting Ho(20°C , 3 d) LTA [600°C] with the 0.01 M holmium chloride solution for 1 d resulted in an additional holmium uptake of about 20%. This was concluded by comparing the holmium concentration in the supernatants measured with ICP-MS with the added holmium concentration. It should be noted that these experiments were performed with merely one sample, hence the error is unknown. The higher uptake of holmium ions for the calcined sample was probably caused by the more empty open cages, since the holmium ions relocated from the open to the closed cages during calcination. It is striking that about 90% of the extra added holmium was loaded into the open cages of the zeolite. This was similar to the loading of Na-LTA with a 0.02 M holmium chloride solution for 1 d at room-temperature, where $90.7\pm 0.5\%$ of the added holmium was loaded into the open cages (see Section 4.2.1.2). For these low concentrations, the loading of holmium ions into the open cages seemed to be unaffected by the holmium ions in the closed cages.

By comparing the measurements of the activity of the ^{166}Ho tracer with the holmium concentration measured using ICP-MS, it became apparent that the ratio of ^{166}Ho to ^{165}Ho

in the supernatants had decreased relative to the added 0.01 M holmium chloride solution. This observation suggested that holmium ions in the zeolite before recontacting, were interchanged with exterior holmium ions. However, the precise quantity of interchanged holmium ions remains unknown. The conducted experiment was unable to determine this quantity, as it could not distinguish whether the activity measured in the zeolite after recontacting resulted from interchange or the additional loading. To get a better understanding of the interchange of holmium ions, it is necessary to repeat the experiment using the tracer of ^{166}Ho loaded into the zeolite before to the extraction with a non-radioactive holmium chloride solution. By evaluating the activity in the supernatant, it would then be feasible to determine the amount of interchanged holmium ions.

About 80% of the holmium ions loaded into Ho(80°C, 1 d) LTA during the contacting with a 0.01 M holmium chloride solution, were removed by the subsequent extraction with a 1 ml saturated ammonium chloride solution for five times 0.5 h at 50°C. Similarly, about 60% of the holmium ions loaded into Ho(20°C, 3 d) LTA [600°C] were extracted. These extraction efficiencies were remarkably higher than the $39.3 \pm 0.7\%$ of holmium ions extracted after a single loading at 80°C for 1 h. This discrepancy pointed again to the presence of different binding sites within the open cages. The additionally loaded holmium seemed to be bound to sites that are more easily exchangeable. Moreover, the ratio of ^{166}Ho to ^{165}Ho in the eluates was lower compared to that in the added 0.01 M holmium chloride solution. This indicated that the holmium ions initially present in the zeolite, prior to the extra loading, were extracted along with the newly added holmium ions. Although, comparing the extracted activity in relation to the holmium concentration measured using the ICP-MS suggested, that a relatively larger proportion of the newly added holmium ions were extracted. In the first eluates, the newly added holmium ions contributed to approximately half of the holmium concentration, whereas before extraction they contributed only a few percent of the holmium content within the open cages of the zeolite.

4.3. Irradiating zeolite A containing holmium

Different samples of zeolite A with holmium were irradiated and subsequently extracted with saturated ammonium chloride. First the extraction of ^{166}Ho and ^{165}Ho is compared to the holmium extraction of non-irradiated zeolite. This extraction was utilised to calculate the specific activity and to analyse the relocation of ^{166}Ho nuclides upon recoil. Finally, the influence of radiolysis is discussed.

The irradiated samples were previously used in the tracer study to characterise zeolite A. The number of ^{166}Ho nuclides in the stock solutions was 10^{10} times less compared to ^{165}Ho nuclides. Therefore it was assumed that the amount of ^{166}Er in the samples was negligible.

4.3.1. Extraction characteristics

To gain insight into the processes occurring within the zeolite during irradiation, the extraction characteristics of irradiated zeolite were compared to those of similar non-irradiated zeolite. Zeolite samples loaded at 80°C for 1 h were irradiated for four different states: with or without calcination and with or without extraction before irradiation. Some of the extraction characteristics for an extraction volume of 1 ml are depicted in Figure 4.15 and for 15 ml in Figure 4.17. The 1 ml extraction of zeolite that had not been calcined and not extracted before irradiation, was repeated for a different loading procedure of 1 d at

4. Results and Discussion

room-temperature, of which some characteristics are presented in Figure 4.16. Additionally, this was also performed with an extraction time of 1 h. In Section 4.2.2.1 it was concluded that the 1 ml extraction was not influenced significantly by the precise extraction time, but more by the number of extractions. Therefore the graphs with a 1 ml extraction are given as function of the eluate number. In the graphs also the results of the tracer study for a corresponding extraction of non-irradiated zeolite are included for comparison. An overview of all six characteristics mentioned in Section 3.5.2 is given in Appendix C.

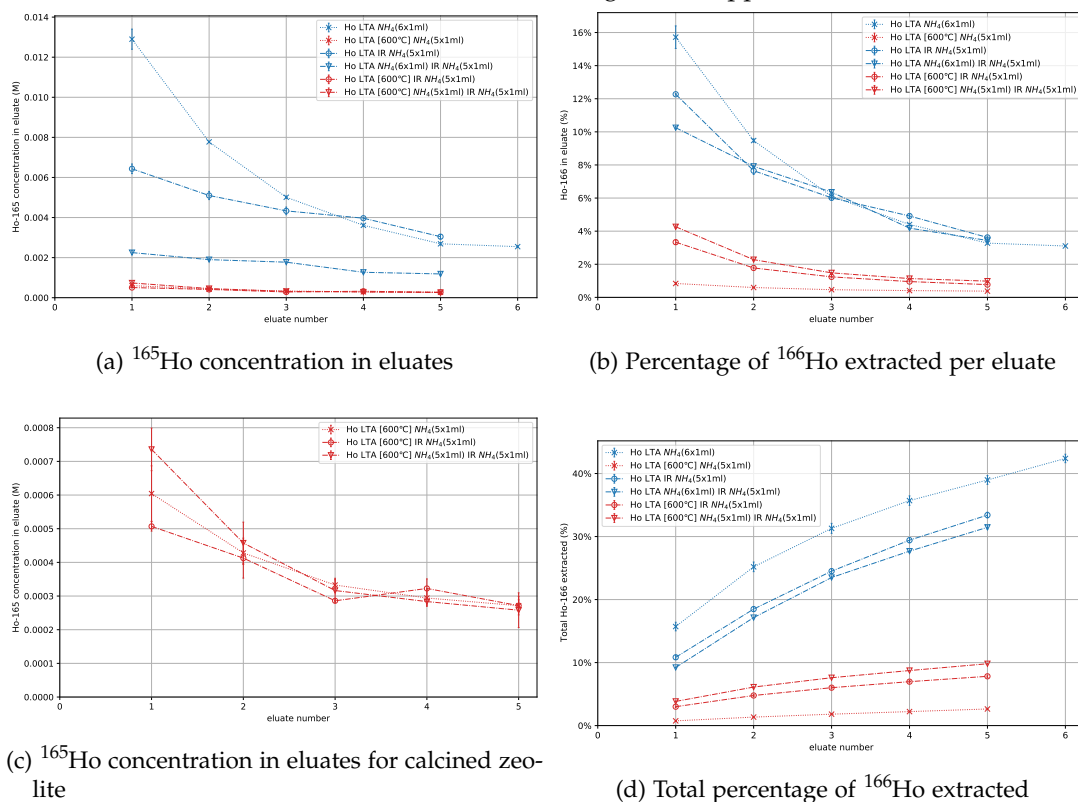


Figure 4.15: ^{165}Ho and ^{166}Ho extraction of irradiated zeolite with a 1 ml ammonium chloride solution. (c) is a zoomed version of (a). For (b) and (d), 100% represents the total amount of ^{166}Ho in the zeolite before extraction. Each point represents a change of the ammonium chloride solution. They are connected by lines to clarify the measurement points of one experiment. A short hand notation similar as described in Section 3.2, is applied to specify the extraction procedure. All samples were loaded at 80°C for 1 h and all extractions were performed at 50°C with an extraction time of 0.5 h. The results from the tracer study for the extraction of holmium from non-irradiated samples are given for comparison by crosses connected by dotted lines. Irradiated samples are represented by dash-dotted lines. Samples that were calcined before irradiation are given in red, blue represents non-calcined samples. The triangles represent samples that were extracted with ammonium chloride before irradiation, the samples denoted by circles were not extracted before irradiation. The activity of ^{166}Ho was measured with the Wallac gamma counter, the concentration of ^{165}Ho with the ICP-MS. The error is given as one standard deviation from the mean of the triplicate.

4.3. Irradiating zeolite A containing holmium

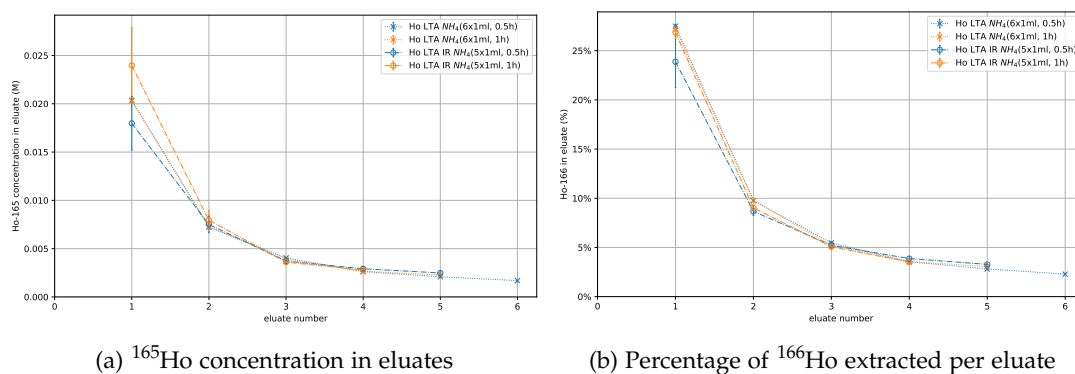


Figure 4.16: ^{165}Ho and ^{166}Ho extraction with a 1 ml ammonium chloride solution of irradiated zeolite loaded at 20°C for 1 d. For (b), 100% represents the total amount of ^{166}Ho in the zeolite before extraction. Each point represents a change of the ammonium chloride solution. The lines clarify, which points belong to the same experiment. A short hand notation similar as described in Section 3.2, is applied to specify the extraction procedure. All samples were loaded at 20°C for 1 d and all extractions were performed at 50°C . An extraction time of 0.5 h is represented in blue and of 1 h in orange. The results from the tracer study for the extraction of holmium from non-irradiated samples are given for comparison by crosses connected by dotted lines. Irradiated samples are represented by circles connected by dash-dotted lines. The activity of ^{166}Ho was measured with the Wal-lac gamma counter, the concentration of ^{165}Ho with the ICP-MS. The error is given as one standard deviation from the mean of the triplicate.

4.3.1.1. Extraction of ^{165}Ho

The extraction of ^{165}Ho target nuclides from the open cages appeared to be similar with or without irradiation, which indicated that there was no significant damage of the zeolite releasing target holmium nuclides. This was concluded from the measured ^{165}Ho concentrations in the eluates, which are illustrated in Figures 4.15, 4.16a and 4.17a.

Firstly, the extractions after irradiation of non-calcined zeolite that had not been extracted before irradiation for the 15 ml extractions and for the samples loaded at room-temperature for 1 d, were comparable with the corresponding tracer study of non-irradiated zeolite. However, the first eluate of Ho(80°C , 1 h) LTA IR NH_4 (50°C , 5×1 ml, 0.5 h) had a lower concentration than expected. Nevertheless, this difference did not have to be caused by irradiation, but was more likely caused by effects of drying and storage before irradiation. Fortunately, a decrease in the extraction of ^{165}Ho is favourable for the specific activity. In order to clarify the cause of the discrepancy, the experiments have to be repeated with and without irradiation. Moreover, the extraction of non-irradiated zeolite that is dried before extraction, has to be performed.

Secondly, the concentration of ^{165}Ho for the extraction of non-calcined zeolite that had been extracted before irradiation, continued the decreasing trend of the extraction of non-irradiated zeolite in Figures 4.15a and 4.17a. This was as if the extraction of non-irradiated zeolite would have been performed for more ammonium chloride solutions without irradiation in between. This was observed for both the 1 ml and the 15 ml extraction.

4. Results and Discussion

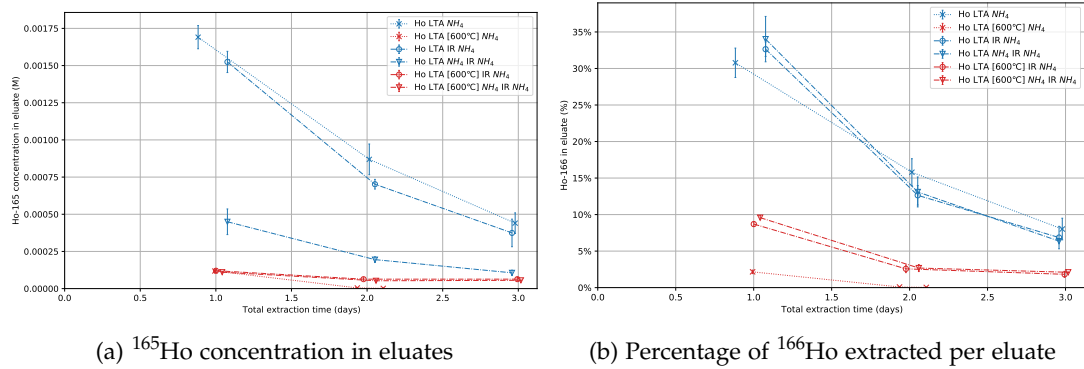


Figure 4.17: ^{165}Ho and ^{166}Ho extraction of irradiated zeolite with a 15 ml ammonium chloride solution. In (b), 100% represents the total amount of ^{166}Ho in the zeolite before extraction. Each point represents a change of the ammonium chloride solution. They are connected by lines to clarify the measurement points of one experiment. A short hand notation similar as described in Section 3.2, is applied to specify the extraction procedure. All samples were loaded at 80°C for 1 h and all extractions were performed three times with 15 ml for 1 d at room-temperature. The results from the tracer study for the extraction of holmium from non-irradiated samples are given for comparison. These are represented with crosses connected by dotted lines. Irradiated samples are represented by dash-dotted lines. Samples that were calcined before irradiation are given in red, blue represents non-calcined samples. The triangles represent samples that were extracted with ammonium chloride before irradiation, the samples denoted by circles were not extracted before irradiation. The activity of ^{166}Ho was measured with the Wallac gamma counter, the concentration of ^{165}Ho with the ICP-MS. The error is given as one standard deviation from the mean of the triplicate.

Thirdly, the 1 ml extraction of calcined irradiated zeolite resulted in a similar concentration of ^{165}Ho in the eluates as that without irradiation, which is demonstrated in Figure 4.15c. This suggested that there was no relocation of the target nuclides upon irradiation between the closed and open cages. The first eluate of the 15 ml extraction was also similar with or without irradiation. The second and third extraction after irradiation seemed to have a higher concentration of ^{165}Ho than without irradiation. Although, it was likely that there was a measurement error in the concentration for the extraction of non-irradiated zeolite, due to the very poor counting statistics as mentioned before in Section 4.2.2.3. Comparing the extracted concentration of ^{165}Ho with the amount present in the zeolite before irradiation revealed that: $\sim 1\%$ of the ^{165}Ho target nuclides was extracted in the first eluate and $\sim 3\%$ in total for a 1 ml extraction; and $\sim 2.5\%$ in the first eluate and $\sim 5\%$ in total for a 15 ml extraction. This is slightly higher than the 1–2% of extracted target nuclides in the studies of Lai [21] and Campbell [19] with zeolite X. Although, it is better than the 10–20% of extracted targets nuclides found by Newell [14] for zeolite L.

Surprisingly, for calcined zeolite that had been extracted prior to irradiation, the concentration of ^{165}Ho in the eluates was comparable to that of zeolite which was not extracted before irradiation. This was observed for both the 1 ml and 15 ml extraction. It seemed that after the extraction of a calcined sample, the holmium ions underwent relocation from the closed cages to the open cages. This is very unfortunately, since the extraction of ^{165}Ho decreases

the obtained specific activity. This relocation could potentially be correlated with the incomplete rehydration after calcination, as discussed in Section 4.2.3.1. The distribution of cations among different sites in zeolite X and L is also known to depend on the residual water content [21, 14]. To prevent the relocation of target nuclides from the closed to the open cages, it is advisable to rehydrate the zeolite between calcination and extraction, as has been done by Lai [21] and Campbell [19]. With this approach, Campbell [19] has achieved low concentrations of target nuclides for subsequent extractions without irradiation. However, with irradiation the concentration of target nuclides increased again. Further research is required to determine whether the relocation of target nuclides from the closed to the open cages occurred before or during irradiation. Moreover, a method to reduce this relocation needs to be investigated.

4.3.1.2. Extraction of ^{166}Ho

The extraction of ^{166}Ho nuclides was examined by the percentage of activity in the eluates compared to total activity of the irradiated zeolite before extraction. The extraction characteristics of ^{166}Ho for non-calcined samples was comparable with that of the holmium extraction for non-irradiated zeolite, for both with and without extraction of the zeolite before irradiation. As demonstrated in Figures 4.15b, 4.16b and 4.17b, the percentage of removed ^{166}Ho was a bit lower than the percentage of holmium extracted without irradiation. This pointed to the relocation of ^{166}Ho nuclides from the open cages to the closed cages upon recoil, since the relocated ions in the closed cages could not be extracted. Nevertheless, the large difference for the 1 ml extraction of Ho(80°C, 1 h) LTA IR was probably due to a diminished extraction efficiency, which was also observed for the extraction of ^{165}Ho .

It is striking that the percentage of ^{166}Ho extracted for the non-calcined sample with or without extraction before irradiation were similar. This implied that the relocation upon recoil of ^{166}Ho from the open cages was not significantly affected by the presence of NH_4^+ ions in the zeolite. Lai [17] has also found that the relocation to the open cages upon recoil in zeolite X is independent of the type of cations present in the open cages.

The percentage of extracted ^{166}Ho for calcined irradiated samples was substantially increased compared to the holmium extraction without irradiation. This indicated that ^{166}Ho nuclides relocated from the closed cages to the open cages upon recoil. The probability of this relocation is calculated in Section 4.3.3. However, the total percentage of extracted ^{166}Ho of about 10% for the 1 ml extraction (Figure 4.15d) and of about 14% for the 15 ml extraction (Figure C.7b) is much lower than the yield of 50–70% found by Lai [21], Newell [14] and Campbell [19] for zeolite X and L.

4.3.2. Specific activity of eluates

The extraction of ^{165}Ho and ^{166}Ho was utilised to determine the specific activity, which is visualised in Figure 4.18. For comparison, the specific activity that was obtained by irradiating holmium chloride hexahydrate equal to 1.4 ± 0.1 GBq/g, is also included in the figure. It should be noted that to be able to compare the different experiments, the given value represents a specific activity that would be obtained directly after irradiation. The actual specific activity was much decreased, due to the decay of ^{166}Ho during the applied decay time of two days and the time needed for the extraction. Even though the time correction was applied, the specific activity decreased with the number of eluates. This meant that the ratio of extracted ^{166}Ho to ^{165}Ho nuclides changed. This reinforced the

4. Results and Discussion

notion of a distinction between cation sites within the open cages. ^{166}Ho nuclides seemed to recoil to the cation sites in the open cages that are extracted more easily.

From Figure 4.18a it is apparent that the state of the zeolite before irradiation influenced the obtained specific activity. For non-calcined samples that were not extracted prior to irradiation, the acquired specific activity was similar to that of the irradiation of holmium chloride hexahydrate. This was the case for loading at 20°C or 80°C , as well as for a 1 ml or a 15 ml extraction. This demonstrated that the recoil of ^{166}Ho nuclides from the open to the closed cages did not have a significant impact, since a lower specific activity would have been observed in that case. With non-calcined zeolite samples that were extracted before irradiation, a slight increase in specific activity was gained of about a factor two for a 1 ml extraction, and one and a half for a 15 ml extraction. Again, this pointed to a distinction between cation sites within the open cages, where ^{166}Ho recoiled to more easily exchangeable sites.

If the zeolite sample was calcined before irradiation, a substantial increase in specific activity was achieved, especially for the first eluate which was about 4 times as high as for an irradiation without zeolite. However, the high specific activity in the first eluate of Ho(80°C , 1 h) LTA [600°C] IR NH_4 (20°C , 3×15 ml, 1 d) is likely too optimistic, due to a too low measured ^{165}Ho concentration. For the 15 ml extraction, the specific activity in the further eluates decreased more rapidly than for the 1 ml extraction. Contrary to the expectations, the experiments with calcined zeolite that had been extracted before irradiation, resulted in a lower specific activity than for calcined zeolite that had not been extracted before irradiation. The lower obtained specific activity was caused by the increase of extracted ^{165}Ho ions, see Section 4.3.1.

However, as observed from the extracted percentage of ^{166}Ho nuclides, the obtained yield was generally poorly. On the one hand, the extractions with the non-calcined irradiated zeolite showed a relative higher yield (for 1 ml: $9.2 \pm 0.1\%$ for the first eluate and $31.5 \pm 0.3\%$ in total; for 15 ml: $34 \pm 3\%$ for the first eluate and $53 \pm 2\%$ in total), but no or only a slight increase in specific activity was obtained. On the other hand, the 1 ml extractions with the calcined irradiated zeolite had a noticeably improved specific activity, but a considerably lower yield ($3.0 \pm 0.1\%$ for the first eluate and $9.8 \pm 0.1\%$ in total). While the 15 ml extractions had a slightly lower specific activity than the 1 ml, they had a better yield ($9.6 \pm 0.3\%$ for the first eluate and $14.4 \pm 0.4\%$ in total).

The incomplete extraction of holmium ions from the open cages by the applied extraction procedure, has a serious adverse effect on the application for isotope enrichment. Because of this, the target nuclides are present in the open cages, which are extracted together with the ^{166}Ho nuclides, decreasing the specific activity. Furthermore, the incomplete extraction results in a low yield, since not all ^{166}Ho nuclides can be extracted from the open cages. For further research it is very important to optimise the extraction of holmium ions from the open cages.

For these experiments, a relative short irradiation time of 3 min was utilised, resulting only in a slight increase of specific activity. It is expected that the enrichment will improve if the irradiation time is extended. The amount of extracted ^{165}Ho target nuclides is assumed to remain approximately constant. This was supported by the data, which suggested that: the extracted amount was primarily determined by the initial quantity of target nuclides in the open cages before irradiation, and no release of target nuclides was observed due to structural damage, as described in Section 4.3.4. If longer irradiation times are employed, more

^{166}Ho will be generated, reducing the relative importance of the extraction of ^{165}Ho nuclides from the open cages. Consequently, a higher enrichment factor is expected for longer irradiation times. Nevertheless, additional research is necessary to optimise the irradiation time, as for a very long irradiation time, the release of ^{165}Ho nuclides is expected to become crucial due to structural damage.

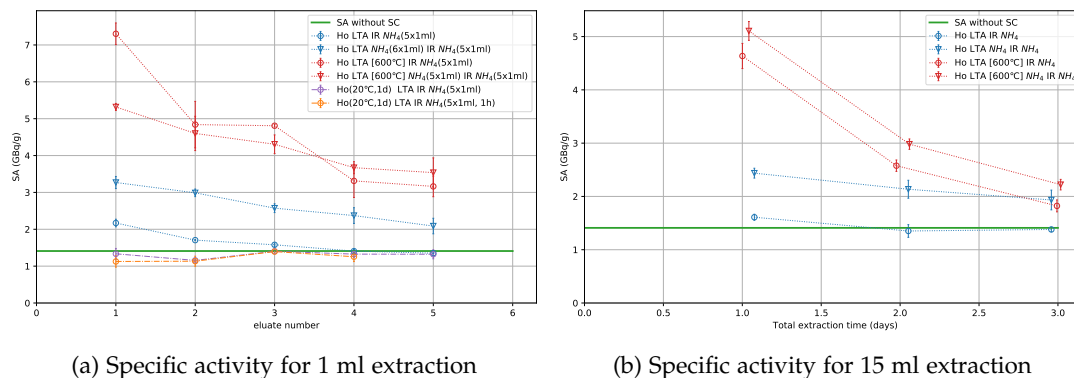


Figure 4.18: Specific activity of ^{166}Ho for a 1 ml and a 15 ml extraction. The given value represents the specific activity that would be obtained directly after irradiation, neglecting the required processing time. Each point represents a change of the ammonium chloride solution. They are connected by lines to clarify the measurement points of one experiment. A short hand notation similar as described in Section 3.2, is applied to specify the extraction procedure. If the notation is omitted, then the samples were loaded at 80°C for 1 h (dotted lines), for (a) extracted at 50°C for five times 0.5 h and for (b) extracted at room-temperature for three times 1 d. The dash-dotted lines represent a loading at 20°C for 1 d. An deviating extraction of 1 h is given in orange. The samples denoted by circles were not extracted before irradiation, while for triangles the samples were extracted with an ammonium chloride solution before extraction. The red colour indicates that the sample was calcined. The specific activity obtained for the irradiation without applying the Szilard-Chalmers method is given by the green line. The error is given as one standard deviation from the mean of the triplicate.

4.3.3. Probability of relocation upon recoil

In order to successfully apply the Szilard-Chalmers method, the produced radionuclide, ^{166}Ho , has to change its chemical state compared to the target material, ^{165}Ho . In case of zeolites, this was realised by the relocation of ^{166}Ho from the closed cages to the open cages upon recoil. The extraction of holmium from the open cages of non-irradiated zeolite A discussed in Section 4.2.2 and the extraction of ^{166}Ho from irradiated zeolite A reported in Section 4.3.1.2, were used to analyse this relocation of ^{166}Ho upon recoil, applying the equations derived in Section 3.6.5.

For the 1 ml extraction procedure, $P(O_f \rightarrow Ex)$ was assumed to be $39.3 \pm 0.7\%$, which was equal to the percentage of holmium ions extracted from the open cages at the tracer study for $\text{Ho}(80^\circ\text{C}, 1 \text{ h}) \text{LTA NH}_4(50^\circ\text{C}, 5 \times 1 \text{ ml}, 1 \text{ h})$. For a 15 ml extraction, $P(O_f \rightarrow Ex)$ was taken to be $55 \pm 1\%$, since this was the percentage of holmium ions extracted from the open cages for $\text{Ho}(80^\circ\text{C}, 1 \text{ h}) \text{LTA NH}_4(20^\circ\text{C}, 3 \times 15 \text{ ml}, 1 \text{ d})$. Nevertheless, as a result it was assumed that $P(O_f \rightarrow Ex)$ was a constant value, neglecting the factors influencing the extraction efficiency

4. Results and Discussion

discussed in Section 4.2.2 (e.g. the influence of the wt% Ho and the distribution of cations between different sites in the open cages). Although $P(O_i \rightarrow O_f)$ was also calculated for a possible different distribution of cations in the open cages by irradiating Ho(20°C, 1 d) LTA and a subsequent extraction with 1 ml for 0.5 h and 1 h. In this case $P(O_f \rightarrow Ex)$ was taken equal to the percentage of extracted holmium at the corresponding tracer study.

Furthermore, the given equations postulated that $P(O_i \rightarrow O_f) + P(O_i \rightarrow C_f) = 1$ and that $P(C_i \rightarrow O_f) + P(C_i \rightarrow C_f) = 1$. In other words, the probability for a ^{166}Ho nuclide to relocate outside the zeolite upon recoil was neglected. This assumption was validated by washing irradiated Ho(80°C, 3 h) LTA. After washing three times, less than 0.1% of the activity was removed from the zeolite. The measured activity was probably caused by traces of zeolite sample in the washing water. Therefore, the probability for a ^{166}Ho to recoil from an open cage to outside the zeolite is negligible. Correspondingly, the recoil from a closed cage to outside the zeolite was neglected. Another possibility is that the ^{166}Ho nuclides that recoiled outside the zeolite were loaded into the open cages before extraction. In this case, the probability of relocation outside the zeolite could be added to the probability of relocation to the open cages, which does not alter the applied calculations. Additionally, the equations did not take into account the holmium outside of the zeolite before irradiation. It was assumed that this could be neglected, due to the sufficiently low holmium concentration in the third wash after the production of the zeolite sample. Yet, no data was obtained whether this was affected by drying and storing the zeolite.

Nevertheless, it should be noted that this model is a simplified version of reality, since solely a distinction between open and closed cages was made, while Section 2.1.4.2 and the extraction characteristics suggested that the open cage consists of two distinct sites. A more elaborate model should distinguish the distribution of holmium ions between these two sites and the corresponding extraction and relocation probabilities. Experiments discriminating between the extraction of the two sites in the open cages might be performed by extracting with other cations than NH_4^+ .

Despite the mentioned limitations, Equations 3.12 and 3.13 were applied to calculate the probability of relocation between the open and closed cages upon recoil. The values calculated with the different irradiation experiments are summarised in Figures 4.19 and 4.20 for $P(O_f \rightarrow Ex)$ and $P(C_i \rightarrow O_f)$ respectively.

On average $P(O_i \rightarrow O_f)$ was found to be $89 \pm 7\%$. A slightly higher value was found for the irradiation experiments with a 15 ml extraction. This could be caused by a too low value of $P(O_f \rightarrow Ex)$, due to the poor counting statistics at the tracer study. The value found for the 1 ml extraction of irradiated zeolite loaded for 1 h at 80°C, was lower than the average value. In this case, $P(O_f \rightarrow Ex)$ was probably taken too high, considering the diminished extraction efficiency observed for the extraction of ^{165}Ho . A similar $P(O_i \rightarrow O_f)$ was found for zeolite A with a different loading, which suggested that the cation distribution over the different sites in the open cages (site II and III) had an insignificant influence on the probability of recoil. Furthermore, similar values were found with and without extraction before irradiation. This indicated that the recoil to the open cages was not affected by the presence of ammonium ions. Moreover, the calculated average value of $P(O_i \rightarrow O_f)$ corresponded to the value of 83%, predicted with the free volumes of the cages in zeolite A. This implied that the recoil energy was sufficiently large to break the bond between the zeolite and a holmium cation in an open site.

4.3. Irradiating zeolite A containing holmium

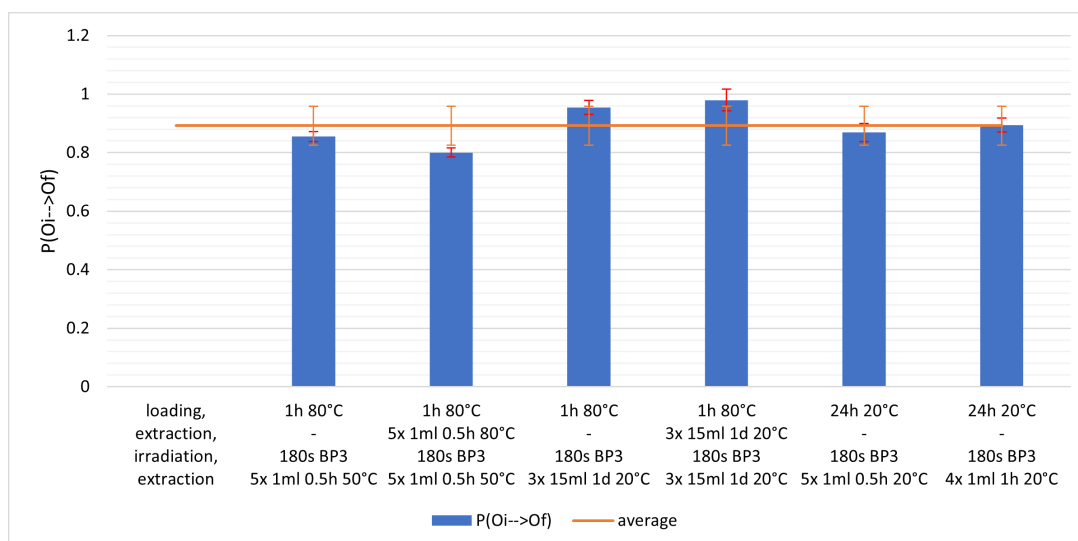


Figure 4.19: Probability of ^{166}Ho relocating from an open cage to an open cage upon recoil, calculated for the irradiation of zeolite samples prepared with varying loading and extracting procedures. The error bars were calculated as described in Appendix B.3 with one standard deviation from the mean of the utilised triplicate experiments. The error of the average is one standard deviation from the mean of these six situations.

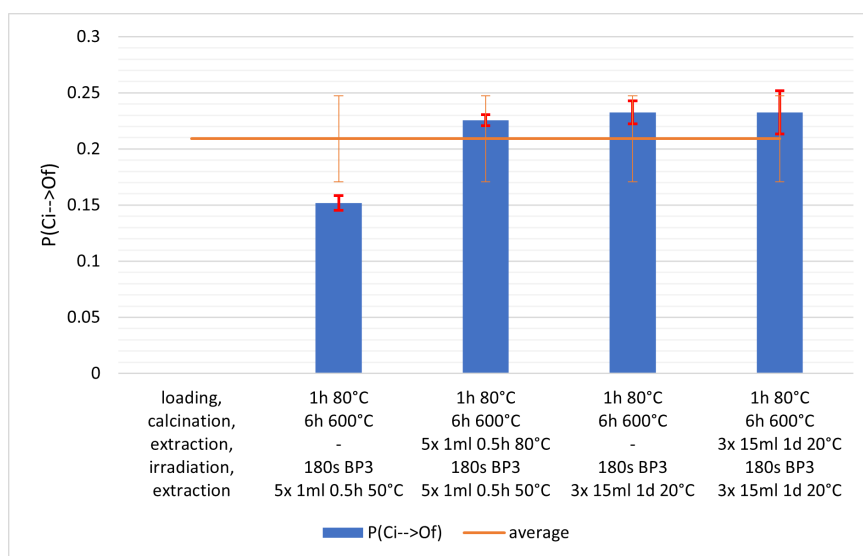


Figure 4.20: Probability of ^{166}Ho relocating from a closed cage to an open cage upon recoil, calculated for the irradiation of calcined zeolite samples prepared with varying extracting procedures. The error bars were calculated as described in Appendix B.3 with one standard deviation from the mean of the utilised triplicate experiments. The error of the average is one standard deviation from the mean of these four situations.

4. Results and Discussion

An average value of $21 \pm 4\%$ was calculated for $P(C_i \rightarrow O_f)$. It is unclear what caused the discrepancy in the value found for Ho(80°C, 1 h) LTA [600°C] IR NH₄(50°C, 5×1 ml, 0.5 h), but this could again be caused by a too high value of $P(O_f \rightarrow Ex)$ applied for this case. The other three results corresponded very well, which indicated that the presence of ammonium ions in the open cages did not influence the relocation to the open cages upon recoil. Nevertheless, the probability to end up in the open cage after recoil was greatly affected by the initial position of the holmium ion; $P(C_i \rightarrow O_f)$ was much lower than $P(O_i \rightarrow O_f)$. Therefore the free space model did not apply for the relocation upon recoil of ¹⁶⁶Ho which was initially in the closed cages. This implied that the recoil energy was often insufficient to break the bond of holmium cations in the closed cages.

There appears to be a correlation between the Si/Al ratio of a zeolite and $P(C_i \rightarrow O_f)$, if the impact of cation type is disregarded. In the literature, it has been observed that the relocation upon recoil from the closed cages to the open cages in zeolite X is lower (40–50%) than in zeolite Y (60–70%) [21]. They have the same structure, but zeolite Y has a higher Si/Al ratio. Zeolite A has a comparable structure, but an even lower Si/Al ratio and $P(C_i \rightarrow O_f)$ was also found to be lower. It seems that the increased charge density of the framework for a higher fraction of aluminium ions, heightens the bond strength of the cations in the closed cages.

The relatively low $P(C_i \rightarrow O_f)$ is disadvantageous for increasing the specific activity. A relatively large fraction of the produced ¹⁶⁶Ho nuclides will remain in the closed cages. Consequently, these can not be extracted after irradiation, which results in a poor yield.

4.3.4. Radiolysis

The extraction of ¹⁶⁵Ho nuclides after irradiation suggested that there was no substantial damage to the zeolite structure for an irradiation time of 3 min. The extraction was similar as without irradiation, while in the case of structural damage a release of target nuclides was expected, resulting in an increased amount of extracted ¹⁶⁵Ho. Furthermore, washing irradiated Ho(80°C, 3 h) LTA resulted in a concentration of ¹⁶⁵Ho on the order of μM or lower, which was below the detection limit of the applied measurement method with the ICP-MS. A holmium concentration in the order of μM was also found for washing more than three times before irradiation, as is shown in Figure 4.1. The effect of radiolysis was further investigated by a structural analysis with XRD and MAS-NMR of Na-LTA before and after an irradiation of 3 min.

4.3.4.1. XRD

The diffractogram of Na-LTA, measured with the X-ray powder diffractometer before and after irradiation for 3 min in BP3, is shown in Figure 4.21. The obtained spectra seemed to be similar before and after irradiation. The small discrepancies in the number of counts was caused by a slightly different measurement time. There were no new peaks or an increase in peak width observed, which indicated that the crystal structure stayed intact. However, to see a significant difference in the diffractogram, at least 1% of the structure should have changed. The irradiation time of 3 min was far too short to induce this. To investigate radiolysis, a longer irradiation time is required.

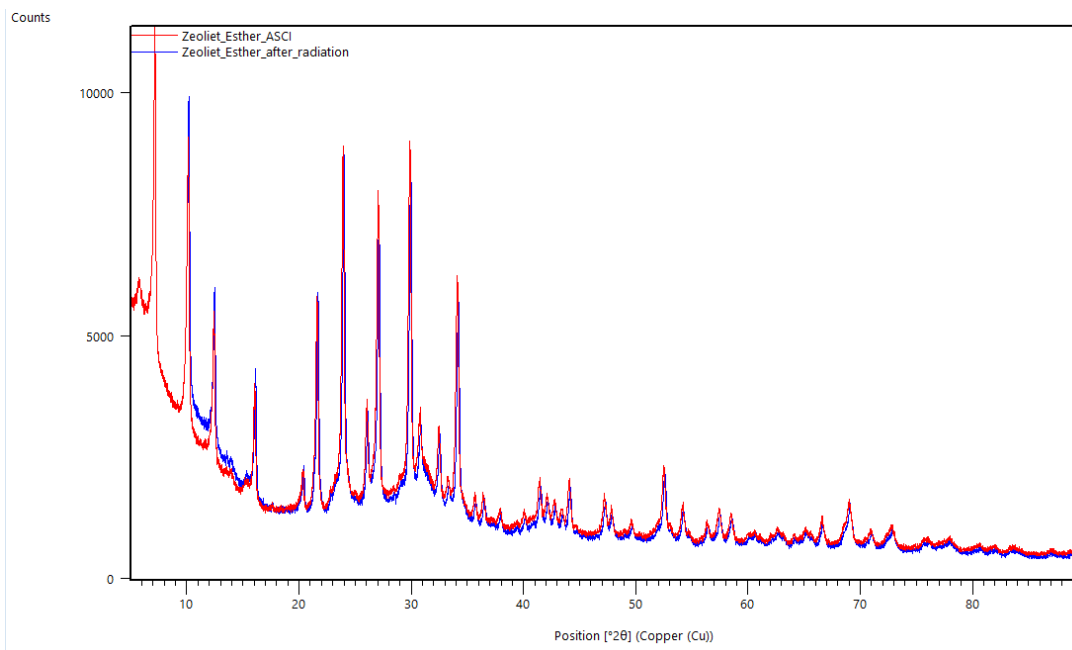


Figure 4.21: Diffractogram of Na-LTA before (–) and after (–) irradiation for 3 min, measured with XRD.

4.3.4.2. MAS-NMR

The ^{27}Al - and ^{29}Si -MAS-NMR spectra of Na-LTA before and after an irradiation for 3 min in BP3 are given in Figures 4.22 and 4.23. There were no apparent changes in the ^{27}Al -MAS-NMR spectrum before and after irradiation. For both spectra there was one peak around 60 ppm with a large intensity and a second peak with a much smaller intensity close to zero. The other peaks in the spectra are spinning sidebands, caused by the rotation of the sample. The ^{29}Si -MAS-NMR spectrum before and after irradiation also seemed to be similar. Surprisingly three peaks were observed, while in literature a single sharp resonance peak centred at -89.0 ± 1 ppm has been measured for zeolite A [51]. The position of the peak with the largest intensity at -89.5 ppm corresponded to the single peak found in literature. The multiple peaks in the spectra denoted different aluminium and silicon environments, while for the structure of zeolite A with a strict ordering of alternating Si and Al atoms, only one environment was expected. It is unclear what caused these extra peaks. Nevertheless, the spectra before and after irradiation corresponded very well: similar intensities and no new peaks. This indicated that the Al and Si environments stayed the same; no effects of radiolysis were detected.

4. Results and Discussion

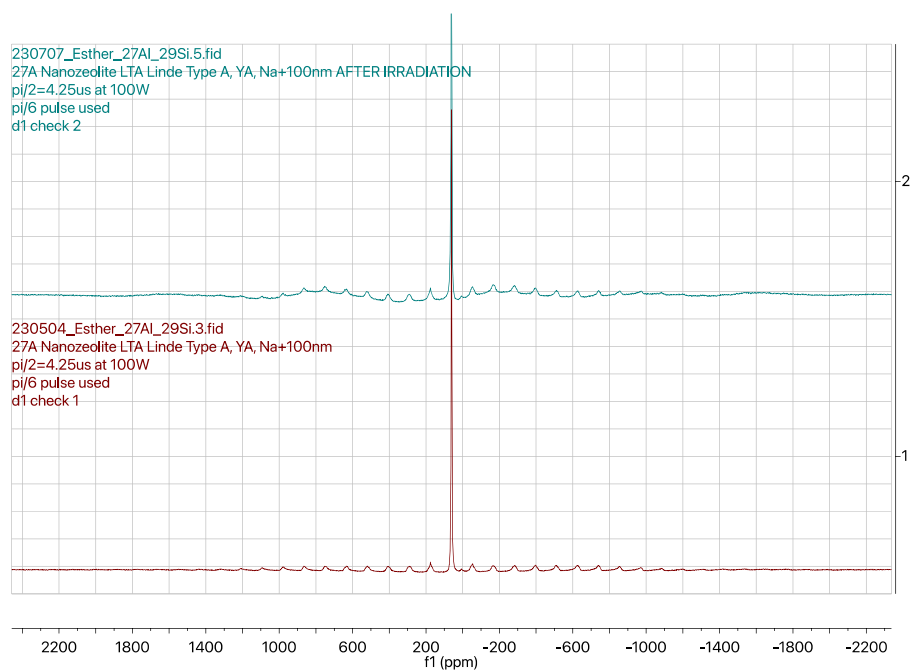


Figure 4.22: ²⁷Al-MAS-NMR spectrum of Na-LTA before and after irradiation for 3 min. The lower red graph was measured before irradiation, the upper blue graph after irradiation.

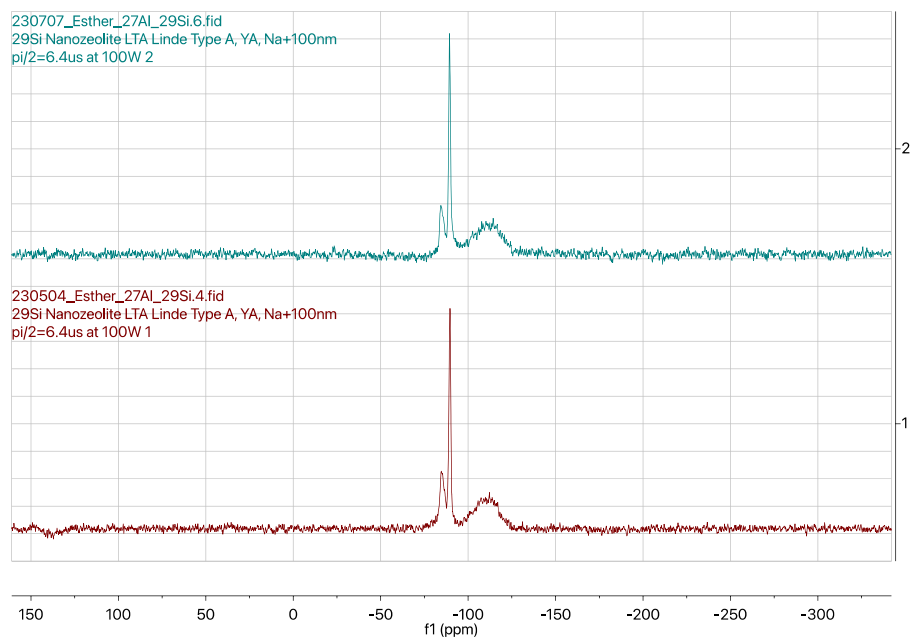


Figure 4.23: ²⁹Si-MAS-NMR spectrum of Na-LTA before and after irradiation for 3 min. The lower red graph was measured before irradiation, the upper blue graph after irradiation.

5. Conclusion

The aim of this thesis was to increase the specific activity of ^{166}Ho produced via a (n,γ) reaction from ^{165}Ho in zeolite A utilising the Szilard-Chalmers effect. In order to apply zeolite A, first suitable procedures to process zeolite A were required.

- **Loading**

A holmium wt% of $18.3\pm 0.1\%$ in zeolite A was achieved with a loading procedure at 80°C for 1 hour. Longer loading periods yielded marginal improvements, with only a slight increase (1.1 ± 0.1 wt% higher for 1 day). At 80°C noticeably more holmium was loaded than at room-temperature ($13.7\pm 0.5\%$ for 1 hour). For efficient loading, a minimum concentration of 0.1 M holmium chloride solution should be applied.

- **Calcination**

After calcination at 600°C for 6 hours, $93.3\pm 0.1\%$ of the holmium ions were locked in the closed cages. This was more effective than calcination at 300°C , for which only $75.2\pm 0.4\%$ of the holmium ions were locked in the closed cages. During calcination 9.4 ± 0.9 wt% of H_2O was removed. The rehydration afterwards was a slow process.

- **Holmium extraction**

For an extraction with 1 ml of saturated ammonium chloride solution, the extraction at 50°C was the most efficient compared to 80°C or room-temperature. Additionally, an extraction time of 0.5 hours was sufficient for a 1 ml extraction. $39.3\pm 0.7\%$ of the holmium ions were extracted from the open cages after five extractions of 1 ml for 0.5 hours at 50°C . By extracting three times with 15 ml of saturated ammonium chloride solution for 1 day each at room-temperature, a higher extraction efficiency was obtained ($55\pm 1\%$). However, this is still noticeably lower than the extraction efficiency for La^{3+} of 70% in zeolite X [21] and 98% in zeolite L [14].

In order for the Szilard-Chalmers effect to increase the specific activity, four general conditions need to be satisfied:

- ◇ **Change of chemical state of produced radionuclide upon recoil**

Compared to the holmium extraction without irradiation, the increase in the percentage of extracted ^{166}Ho for irradiated calcined zeolite A indicated that: the ^{166}Ho nuclides were able to change their chemical state upon recoil by relocating from the closed to the open cages. The probability of a ^{166}Ho nuclide, initially within an open cage, to relocate to an open cage upon recoil was $89\pm 7\%$. This corresponds to the expected probability considering the free volumes of the cages in zeolite A. The probability of a ^{166}Ho nuclide to relocate from a closed cage to an open cage upon recoil was $21\pm 4\%$, which implied that the recoil energy was often insufficient to break the bond of the holmium cations in the closed cages with the zeolite. This is disadvantageous as this results in a low yield.

- ◇ **No recombination or interchange**

When holmium loaded zeolite A was contacted again with 0.01 M holmium chloride, an extra holmium uptake was measured as well as an interchange of exterior holmium ions with the holmium ions in the open cages. However, it is expected that this will not limit the applications to increase the specific activity, since these newly added holmium ions could be extracted afterwards. The relocation to the closed cages and the interchange between the open and the closed cages were not examined.

5. Conclusion

◇ No release of target nuclides

A release of target ^{165}Ho nuclides due to radiolysis was not observed, since the extraction of ^{165}Ho nuclides from the open cages after irradiation was similar as without irradiation and no difference was observed in the diffractogram of sodium zeolite A obtained before or after irradiation. The similar diffractograms indicated that the change in structure was smaller than 1%. However, there seemed to be a relocation of ^{165}Ho ions from the closed cages to the open cages after extracting calcined zeolite, resulting in similar percentages of extracted ^{165}Ho target nuclides, with or without extraction prior to irradiation. It is unclear whether this relocation occurred before or during irradiation. The chemical stability of the holmium loaded zeolite A was not analysed.

◇ Separation of produced and target nuclides

The ^{166}Ho nuclides, which were relocated to the open cages of zeolite A upon recoil, could be extracted with a saturated ammonium chloride solution, while the ^{165}Ho target nuclides in the closed cages were not extracted. However, the incomplete extraction of holmium ions from the open cages is disadvantageous for applying zeolite A to increase the specific activity. The ^{166}Ho nuclides could not be separated from the ^{165}Ho target nuclides in the open cage due to incomplete extraction before irradiation, which reduced the obtained specific activity. After irradiating calcined zeolite, $\sim 1\%$ of the ^{165}Ho target nuclides were extracted in the first eluate and $\sim 3\%$ in total for a 1 ml extraction; and $\sim 2.5\%$ in the first eluate and $\sim 5\%$ in total for a 15 ml extraction. This is slightly higher than the 1–2% of extracted target nuclides with zeolite X [19, 21], but better than the 10–20% extracted with zeolite L [14]. Furthermore, the incomplete extraction of ^{166}Ho nuclides from the open cages reduced the yield.

A specific activity of ^{166}Ho of 1.4 ± 0.1 GBq/g resulted from irradiating holmium chloride hexahydrate for 3 minutes in the BP3 pneumatic irradiation facility of the 2.3 MW nuclear research reactor (Hoger Onderwijs reactor) of the Reactor Institute Delft with a thermal neutron flux of $4.69 \cdot 10^{12} \text{ s}^{-1} \text{ cm}^{-2}$ without applying the Szilard-Chalmers effect. With the Szilard-Chalmers effect by utilising zeolite A, an increased specific activity of ^{166}Ho was achieved. The obtained specific activity decreased with the number of extractions. For irradiating non-calcined zeolite A that had been extracted prior to irradiation, a slight increase of a factor 1.5–2.3 in the specific activity for the 1 ml extractions (maximal: 3.3 ± 0.2 GBq/g) was obtained. Similarly, a factor 1.4–1.7 for the 15 ml (maximal: 2.44 ± 0.09 GBq/g) was obtained. The extractions with 1 ml had a yield of $9.2 \pm 0.1\%$ for the first eluate and $31.5 \pm 0.3\%$ in total. The 15 ml extractions had a higher yield of $34 \pm 3\%$ for the first eluate and $53 \pm 2\%$ in total. For irradiating calcined zeolite A with or without extraction prior to irradiation, a substantial increase in specific activity of a factor 2.4–5.2 for the 1 ml extraction (maximal: 7.3 ± 0.3 GBq/g) was obtained and 1.6–3.6 for the 15 ml extraction (maximal: 5.1 ± 0.2 GBq/g). However, these had a considerably lower yield of $3.0 \pm 0.1\%$ for the first eluate and $9.8 \pm 0.1\%$ in total for the 1 ml extraction; and $9.6 \pm 0.3\%$ for the first eluate and $14.4 \pm 0.4\%$ in total for the 15 ml extraction. This obtained yield is substantially less than the yield of 50–70% for other cations in zeolite X [19, 21] and L [14].

To conclude, zeolite A has the potential to increase the specific activity of ^{166}Ho produced by a (n,γ) reaction utilising the Szilard-Chalmers effect. Considering the above mentioned requirements for increasing the specific activity with the Szilard-Chalmers effect, the way to further improve the specific activity of ^{166}Ho could be by exploring other zeolite types with characteristics that satisfy these requirements better.

6. Recommendations

In this chapter several recommendations are made for future research required to successfully implement zeolite A for specific activity enhancement, as well as some suggestions for experiments to elaborate on the findings of this thesis.

6.1. Future research required for applying zeolite A

First of all, it is very important to increase the extraction efficiency in order to successfully apply zeolite A for increasing the specific activity of ^{166}Ho . This is needed to increase the yield for extraction after irradiation. Furthermore, the extraction before irradiation has to be improved to minimise the amount of holmium in the open cages before irradiation, which is required to reduce the amount of extracted ^{165}Ho target nuclides after irradiation, since this extraction decreases the specific activity. In this thesis the same extraction procedure was applied before and after irradiation. However, it would be better to apply different extraction procedures optimised to the two cases. For instance, a short processing time is essential for the extraction after irradiation, while the extraction before irradiation is not time sensitive. The extraction efficiency could possibly be increased by the extraction with different cations. In literature the cations Ba^{2+} and Na^{+} are sometimes used for the extraction of zeolite X and L [21, 14]. Additionally, a higher ammonium concentration could be applied for extraction temperatures above 20°C , although the precipitation of the ammonium has to be taken into account for temperature decreases.

Moreover, to obtain a zeolite with only holmium ions in the closed cages and none in the open cages, the relocation of holmium ions from the closed to the open cages after the extraction of calcined samples needs to be eliminated. Campbell [19] has found that in zeolite X this relocation before irradiation can be reduced by rehydrating the zeolite between calcination and extraction. Additionally, it should be investigated whether this relocation occurs before or during irradiation. To this end, calcined extracted zeolite A samples have to be extracted again after drying and a subsequent waiting period. Also the influence of the increased temperatures during irradiation on this relocation has to be examined.

To achieve a larger percentage of holmium ions locked in the closed cages before irradiation, it would be interesting to investigate the effect of the wt% Ho. The closed cages are probably maximally filled for the relative high wt% Ho of $18.3 \pm 0.1\%$ that was utilised. For a lower wt% Ho, an even higher percentage of holmium ions might be locked, reducing the percent of extracted target nuclides after irradiation.

In order to use the extracted ^{166}Ho in further applications, a method is needed to back-extract the ^{166}Ho from the saturated ammonium chloride solution. This could possibly be done by sublimating the ammonium chloride, since this is a common procedure to separate ammonium chloride from non-volatile substances [54].

Furthermore, longer irradiation times have to be applied. It is expected this will improve the increase of specific activity. The amount of ^{166}Ho will increase, while the amount of extracted target nuclides is expected to remain constant. However, with further increasing the irradiation time, a release of ^{165}Ho nuclides is expected due to structural damage. The irradiation time of 3 min used for this thesis, was insufficient to cause measurable radiolysis effects. Radiolysis for a higher neutron fluence and gamma dose should be examined.

6. Recommendations

The data suggests that zeolite A is probably not the best choice of zeolite type, due to: the poor extraction efficiency, the low probability of relocation of ^{166}Ho nuclides from a closed cage to an open cage upon recoil and the large fraction of extracted target nuclides. Other studies suggest better characteristics for zeolite X [19, 21], although only different cations than holmium have been analysed. In future research, zeolite X or other zeolite types could be applied to increase the specific activity of ^{166}Ho .

Additionally, it would be interesting to apply zeolites for increasing the specific activity of other lanthanides as well. Since lanthanides have comparable chemical and physical characteristics, the methods applied in this thesis could also be applied for other lanthanide elements. For example, ^{153}Sm , ^{175}Yb and ^{177}Lu could be used, since they are promising candidates for cancer treatment [55].

6.2. Elaborate on current findings

In this thesis only a distinction between the open and closed was made, while literature suggests that the open cage consists of two distinct binding sites: site II and III [27]. Multiple findings in this thesis suggested that the distribution of cations over these sites varied. For example, it seemed that this was influenced by the previous as well as the current temperature, the wt% Ho and the relocation upon recoil. Furthermore, it appeared that the extraction efficiency of the sites differed. For future research, it would be interesting to apply a model which considers all three binding sites. In such a study, other cations could be used for extraction to distinguish the different sites, since in zeolite X and L other cations including Ba^{2+} have been applied for the extraction of specific sites in the open cages [21, 14].

In this thesis only a preliminary investigation of the recombination and interchange of holmium ions was conducted. More experiments are required to fully understand these processes. For example, the interchange of holmium ions between the open cages and the exterior should be quantified. This could be done by exchanging zeolite A containing a tracer of ^{166}Ho loaded in the open cages with a non-radioactive holmium chloride solution. By evaluating the activity in the supernatant, it would be feasible to determine the amount of interchanged holmium ions. To get a more realistic view of the interchange occurring during extraction, a ^{165}Ho loaded zeolite A sample should be extracted with a saturated ammonium chloride solution, instead of using milliQ, containing a small amount of tracer ^{166}Ho , with a concentration comparable to the holmium concentration in the eluates. The activity in the zeolite after extraction would indicate the extent of interchange of ^{165}Ho ions with ^{166}Ho nuclides. Moreover, the interchange between the open and closed cages has to be investigated further.

The rehydration of zeolite A after calcination needs further investigation. This could be done by determining the water content after contacting calcined zeolite A with milliQ for different periods of time. For instance, gravimetric analysis or INAA measurements of the sodium and holmium content, could be used to determine the water content. The hydration state of the zeolite before irradiation could also be of interest. Dyer et al. [18] have found that in zeolite A the probability of the relocation upon recoil depends on the extent of hydration. It would be interesting to study the irradiation of fully rehydrated or in water suspended calcined zeolite A samples, as this might increase the probability of relocation from the closed cages to the open cages upon recoil. This would increase the specific activity and the yield.

Bibliography

- [1] Structure Commission of the International Zeolite Association. Database of zeolite structures: Framework type LTA. https://europe.iza-structure.org/IZA-SC/framework_3d.php?STC=LTA, 2007. Accessed: 9-7-2023.
- [2] S Zeisler and K Weber. Szilard-Chalmers effect in holmium complexes. *Journal of radio-analytical and nuclear chemistry*, 227(1-2):105–109, 1998.
- [3] Syed M Qaim. Therapeutic radionuclides and nuclear data. *Radiochimica Acta*, 89(4-5):297–304, 2001.
- [4] Chai-Hong Yeong, Mu-hua Cheng, and Kwan-Hoong Ng. Therapeutic radionuclides in nuclear medicine: current and future prospects. *Journal of Zhejiang University. Science. B*, 15(10):845, 2014.
- [5] Hun Yee Tan, Chai Hong Yeong, Yin How Wong, Molly McKenzie, Azahari Kasbollah, Mohamad Nazri Md Shah, and Alan Christopher Perkins. Neutron-activated theranostic radionuclides for nuclear medicine. *Nuclear medicine and biology*, 90:55–68, 2020.
- [6] Nienke JM Klaassen, Mark J Arntz, Alexandra Gil Arranja, Joey Roosen, and J Frank W Nijssen. The various therapeutic applications of the medical isotope holmium-166: a narrative review. *EJNMMI radiopharmacy and chemistry*, 4(1):1–26, 2019.
- [7] Suzanne E Lapi and Michael J Welch. A historical perspective on the specific activity of radiopharmaceuticals: what have we learned in the 35 years of the ISRC? *Nuclear medicine and biology*, 39(5):601–608, 2012.
- [8] D Habs and U Köster. Production of medical radioisotopes with high specific activity in photonuclear reactions with γ -beams of high intensity and large brilliance. *Applied Physics B*, 103:501–519, 2011.
- [9] Leila Safavi-Tehrani, George E Miller, and Mikael Nilsson. Production of high specific activity radiolanthanides for medical purposes using the UC Irvine TRIGA reactor. *Journal of Radioanalytical and Nuclear Chemistry*, 303:1099–1103, 2015.
- [10] Michiel Van de Voorde, Karen Van Hecke, Thomas Cardinaels, and Koen Binnemans. Radiochemical processing of nuclear-reactor-produced radiolanthanides for medical applications. *Coordination Chemistry Reviews*, 382:103–125, 2019.
- [11] KP Zhernosekov, DV Filosofov, and Frank Rösch. The Szilard-Chalmers effect in macrocyclic ligands to increase the specific activity of reactor-produced radiolanthanides: Experiments and explanations. *Radiochimica Acta*, 100(8-9):669–674, 2012.
- [12] Tibor Braun and Henrik Rausch. Radioactive endohedral metallofullerenes formed by prompt gamma-generated nuclear recoil implosion. *Chemical physics letters*, 288(2-4):179–182, 1998.
- [13] Wout Schenk. Investigation of the processes expected in a continuous flow szilard-Chalmers system for production of high specific activity radionuclides. Master's thesis, Delft University of Technology, 2022.

BIBLIOGRAPHY

- [14] Paul Anthony Newell. *Szilard-Chalmers recoil studies in Zeolite L, offretite and erionite*. PhD thesis, Imperial College London, 1976.
- [15] LVC Rees and CJ Williams. Neutron irradiation of Linde molecular sieve 13X. *Transactions of the Faraday Society*, 61:1481–1491, 1965.
- [16] Edward FT Lee and Lovat VC Rees. Effect of calcination on location and valency of lanthanum ions in zeolite Y. *Zeolites*, 7(2):143–147, 1987.
- [17] Pin Pah Lai and Lovat VC Rees. Szilard-Chalmers cation recoil studies in zeolites X and Y. Part 3.—recoils from locked to open sites. *Journal of the Chemical Society, Faraday Transactions 1: Physical Chemistry in Condensed Phases*, 72:1827–1839, 1976.
- [18] A Dyer, Qin Guan-Lin, and LVC Rees. Szilard-Chalmers cation recoil studies in zeolite A. *Zeolites*, 3(2):108–112, 1983.
- [19] David O Campbell. Isotopic enrichment of the product of a neutron capture (n, γ) reaction in lanthanide and actinide exchanged zeolites. Technical report, Oak Ridge National Lab., Tenn.(USA), 1973.
- [20] Cristina Martínez and Joaquín Pérez-Pariente. Zeolites and ordered porous solids: fundamentals and applications. *Valencia, Spain: FEZA*, 2011.
- [21] Pin Pah Lai. *Szilard-Chalmers recoil studies in zeolites X & Y*. PhD thesis, Imperial College London, 1975.
- [22] Koutaro Honda, Masaya Itakura, Yumiko Matsuura, Ayumu Onda, Yusuke Ide, Masahiro Sadakane, and Tsuneji Sano. Role of structural similarity between starting zeolite and product zeolite in the interzeolite conversion process. *Journal of nanoscience and nanotechnology*, 13(4):3020–3026, 2013.
- [23] Marek Majdan, Agnieszka Gladysz-Plaska, Stanislaw Pikus, Dariusz Sternik, Oksana Maryuk, Emil Zieba, and Pawel Sadowski. Tetrad effect in the distribution constants of the lanthanides in their adsorption on the zeolite A. *Journal of molecular structure*, 702(1-3):95–102, 2004.
- [24] T Bo Reed and DW Breck. Crystalline zeolites. ii. Crystal structure of synthetic zeolite, type A. *Journal of the American Chemical Society*, 78(23):5972–5977, 1956.
- [25] Colin A Fyfe, John M Thomas, Jacek Klinowski, and Gian C Gobbi. Magic-angle-spinning NMR (MAS-NMR) spectroscopy and the structure of zeolites. *Angewandte Chemie International Edition in English*, 22(4):259–275, 1983.
- [26] Pin Pah Lai and Lovat VC Rees. Szilard-Chalmers cation recoil studies in zeolites X and Y. Part 1.—ion exchange in zeolites X and Y. *Journal of the Chemical Society, Faraday Transactions 1: Physical Chemistry in Condensed Phases*, 72:1809–1817, 1976.
- [27] Chintansinh D Chudasama, Jince Sebastian, and Raksh V Jasra. Pore-size engineering of zeolite A for the size/shape selective molecular separation. *Industrial & engineering chemistry research*, 44(6):1780–1786, 2005.
- [28] Amged Al Ezzi and Hongbin Ma. Equilibrium adsorption isotherm mechanism of water vapor on zeolites 3A, 4A, X, and Y. In *ASME International Mechanical Engineering Congress and Exposition*, volume 58417, page V006T08A059. American Society of Mechanical Engineers, 2017.

- [29] Ivan Petrov and Todor Michalev. Synthesis of zeolite A: a review. 51:30–35, 2012.
- [30] IAEA. Live chart of nuclides. <https://www-nds.iaea.org/relnsd/vcharthtml/VChartHTML.html#lastnuc=Ho-165>. Accessed: 23-5-2023.
- [31] Malgorzata Norek and Joop A Peters. MRI contrast agents based on dysprosium or holmium. *Progress in nuclear magnetic resonance spectroscopy*, 59(1):64–82, 2011.
- [32] Hudson Institute of Mineralogy. The mineralogy of holmium. <https://www.mindat.org/element/Holmium>. Accessed: 23-5-2023.
- [33] Andreas O Tirlir, Peter P Passler, and Bernd M Rode. The lanthanoid hydration properties beyond the ‘gadolinium break’: dysprosium (iii) and holmium (iii), an ab initio quantum mechanical molecular dynamics study. *Chemical Physics Letters*, 635:120–126, 2015.
- [34] Leila Safavi-Tehrani. *Production of High Specific Activity Radioisotopes via the Szilard-Chalmers Method, Using the UC-Irvine TRIGA® Reactor*. PhD thesis, UC Irvine, 2016.
- [35] Ali Bahrami-Samani, Reza Bagheri, Amir R Jalilian, Simindokht Shirvani-Arani, Mohammad Ghannadi-Maragheh, and Mojtaba Shamsaee. Production, quality control and pharmacokinetic studies of ¹⁶⁶Ho-EDTMP for therapeutic applications. *Scientia pharmaceutica*, 78(3):423–434, 2010.
- [36] Mirla Fiuza Diniz, Diogo Milioli Ferreira, Wanderson Geraldo de Lima, Maria Lucia Pedrosa, Marcelo Eustáquio Silva, Stanley de Almeida Araujo, Kinulpe Honorato Sampaio, Tarcisio Passos Ribeiro de Campos, and Savio Lana Siqueira. Biodegradable seeds of holmium don’t change neurological function after implant in brain of rats. *Reports of Practical Oncology & Radiotherapy*, 22(4):319–326, 2017.
- [37] Zhifang Chai, Amares Chatt, Peter Bode, Jan Kučera, Robert Greenberg, and David B Hibbert. Vocabulary of radioanalytical methods (IUPAC recommendations 2020). *Pure and Applied Chemistry*, 93(1):69–111, 2021.
- [38] FF Knapp Jr, S Mirzadeh, AL Beets, and M Du. Production of therapeutic radioisotopes in the ORNL High Flux Isotope Reactor (HFIR) for applications in nuclear medicine, oncology and interventional cardiology. *Journal of radioanalytical and nuclear chemistry*, 263:503–509, 2005.
- [39] Leo Szilard and TA Chalmers. Chemical separation of the radioactive element from its bombarded isotope in the Fermi effect. *Nature*, 134(3386):462–462, 1934.
- [40] Pin Pah Lai and Lovat VC Rees. Szilard-Chalmers cation recoil studies in zeolites X and Y. Part 2.—recoils from open to locked sites. *Journal of the Chemical Society, Faraday Transactions 1: Physical Chemistry in Condensed Phases*, 72:1818–1826, 1976.
- [41] RB Firestone and V Zerking. CD-ROM for the PGAA-IAEA database. In *Database of prompt gamma rays from slow neutron capture for elemental analysis*. 2007.
- [42] Gerhart Friedlander, Joseph W Kennedy, Edward S Macias, and Julian M Miller. *Nuclear and radiochemistry*. John Wiley & Sons, 1981.
- [43] Paul A Newell and Lovat VC Rees. Szilard-Chalmers cation recoil studies in zeolite L. *Zeolites*, 3(1):28–36, 1983.

BIBLIOGRAPHY

- [44] Nicholas M Musyoka, Leslie F Petrik, Eric Hums, Andreas Kuhnt, and Wilhelm Schwieger. Thermal stability studies of zeolites A and X synthesized from South African coal fly ash. *Research on Chemical Intermediates*, 41:575–582, 2015.
- [45] Florian Mayer, Wuyuan Zhang, Thomas Brichart, Olivier Tillement, Célia S Bonnet, Éva Tóth, Joop A Peters, and Kristina Djanashvili. Nanozeolite-LTL with Gdiii deposited in the large and Euiii in the small cavities as a magnetic resonance optical imaging probe. *Chemistry-A European Journal*, 20(12):3358–3364, 2014.
- [46] Thermo Fisher Scientific US. Trace elemental analysis (TEA) information. <https://www.thermofisher.com/nl/en/home/industrial/spectroscopy-elemental-isotope-analysis/spectroscopy-elemental-isotope-analysis-learning-center/trace-elemental-analysis-tea-information.html>. Accessed: 26-5-2023.
- [47] Perkinelmer. Trace elemental analysis (TEA) information. https://resources.perkinelmer.com/corporate/cmsresources/images/46-73247bro_wizard2gammacounter.pdf. Accessed: 26-5-2023.
- [48] Nuclear Power. High purity germanium detectors - HPGe. <https://www.nuclear-power.com/nuclear-engineering/radiation-detection/semiconductor-detectors/high-purity-germanium-detectors-hpge/>, 2022. Accessed: 27-5-2023.
- [49] Anton Paar. X-ray diffraction (XRD). <https://wiki.anton-paar.com/en/x-ray-diffraction-xrd/>, journal=Anton Paar. Accessed: 29-5-2023.
- [50] David I Hoult and Balram Bhakar. NMR signal reception: Virtual photons and coherent spontaneous emission. *Concepts in Magnetic Resonance: An Educational Journal*, 9(5):277–297, 1997.
- [51] Colin A Fyfe, John M Thomas, Jacek Klinowski, and Gian C Gobbi. Magic-angle-spinning NMR (MAS-NMR) spectroscopy and the structure of zeolites. *Angewandte Chemie International Edition in English*, 22(4):259–275, 1983.
- [52] Paul A Newell and Lovat VC Rees. Ion-exchange and cation site locations in zeolite L. *Zeolites*, 3(1):22–27, 1983.
- [53] Joop A Peters and Kristina Djanashvili. Lanthanide loaded zeolites, clays, and mesoporous silica materials as MRI probes. *European Journal of Inorganic Chemistry*, 2012(12):1961–1974, 2012.
- [54] L.S.M. Kaur. *Science for Ninth Class Part 1 Chemistry*. S. Chand Publishing, 2016.
- [55] Cathy S Cutler, C Jeffrey Smith, Gary J Ehrhardt, Tammy T Tyler, Silvia S Jurisson, and Edward Deutsch. Current and potential therapeutic uses of lanthanide radioisotopes. *Cancer biotherapy & radiopharmaceuticals*, 15(6):531–545, 2000.
- [56] Lisa A Price, Zöe Jones, Antony Nearchou, Gavin Stenning, Daniel Nye, and Asel Sartbaeva. The effect of cation exchange on the pore geometry of zeolite L. *AppliedChem*, 2(3):149–159, 2022.
- [57] Mutsuo Igarashi, Takehito Nakano, Pham Tan Thi, Yasuo Nozue, Atsushi Goto, Kenjiro Hashi, Shinobu Ohki, Tadashi Shimizu, Andraž Krajnc, Peter Jeglič, et al. NMR study of thermally activated paramagnetism in metallic low-silica X zeolite filled with sodium atoms. *Physical Review B*, 87(7):075138, 2013.

BIBLIOGRAPHY

- [58] Yunxia Yang, Nick Burke, Junfang Zhang, Stanley Huang, Seng Lim, and Yonggang Zhu. Influence of charge compensating cations on propane adsorption in X zeolites: experimental measurement and mathematical modeling. *RSC Advances*, 4(14):7279–7287, 2014.
- [59] Alexandra I Lupulescu, Manjesh Kumar, and Jeffrey D Rimer. A facile strategy to design zeolite L crystals with tunable morphology and surface architecture. *Journal of the American Chemical Society*, 135(17):6608–6617, 2013.

A. Structure of zeolite X and L

In this thesis zeolite A is often compared to zeolite X or L. In Figure 2.1 an overview of the building blocks for these zeolites is given. Figures A.1 and A.2 give a more detailed image of the structure of zeolite X and L. Zeolite X has a structure comparable to that of zeolite A, except that for zeolite X the β -cages are connected by hexagonal-prisms instead of cubes, resulting in a slightly larger open cage [21]. The structure of zeolite L is not built from β -cages, but is built from cancrinite cages connected by hexagonal prisms [56]. Consequently, zeolite L has a quite different structure than zeolite A and X.

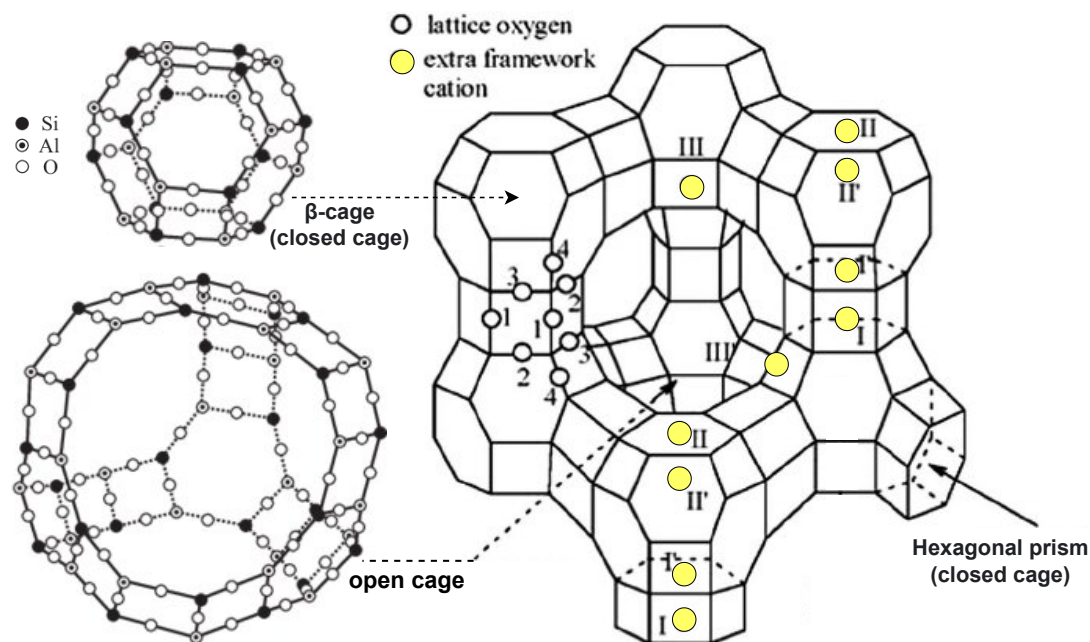


Figure A.1: Structure of zeolite X, composed of two secondary building blocks: truncated-octahedra and hexagonal prisms. The truncated-octahedron forms a β -cage, this is a closed cage. The hexagonal prism is also a closed cage. The enclosed polyhedron is an open cage. The different cations sites are indicated by the yellow circles. [57, 58]

A. Structure of zeolite X and L

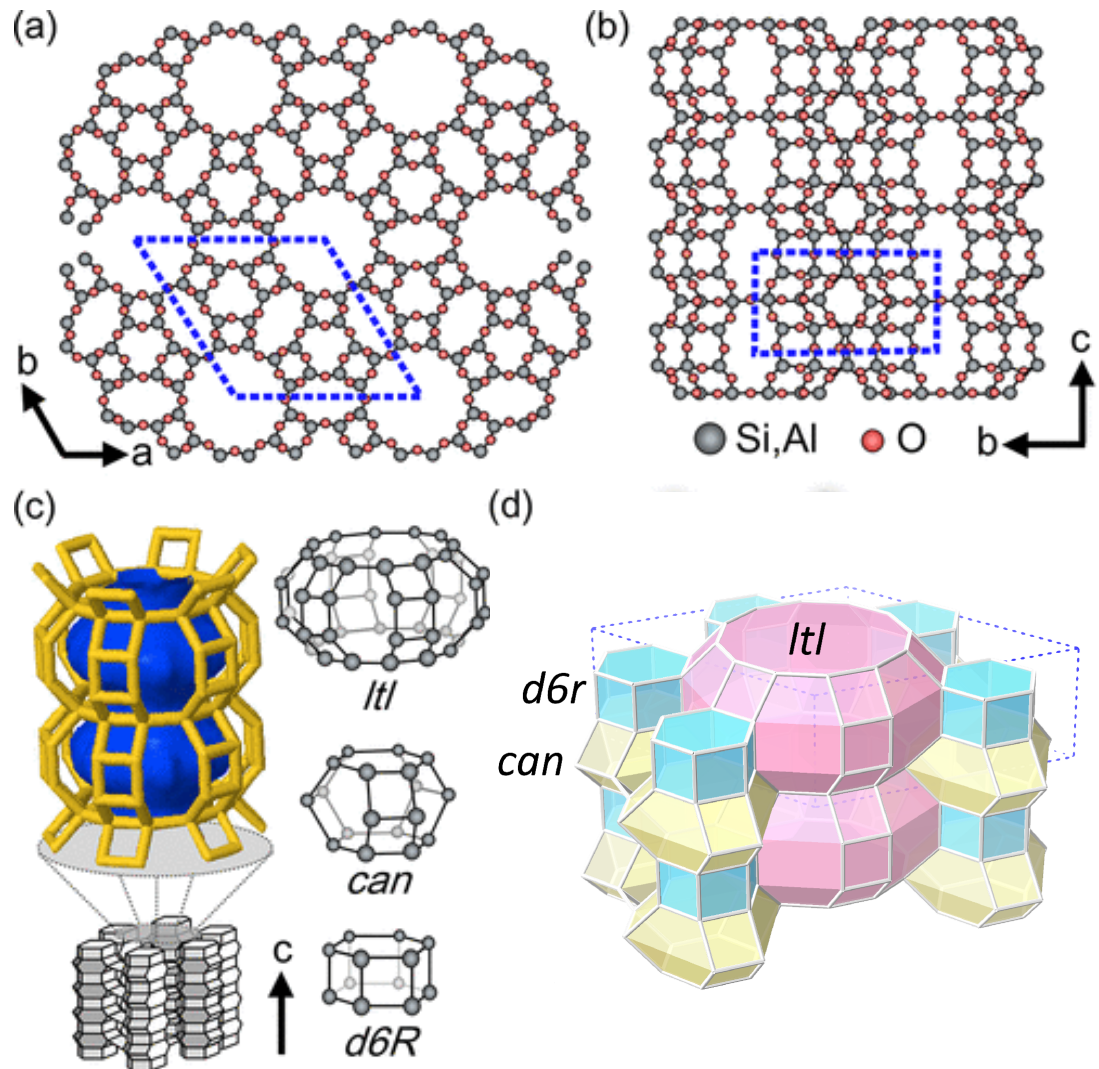


Figure A.2: Structure of zeolite L. The blue dashed line indicates a unit cell. (a) Top view (001); (b) side view (100); (c) secondary building blocks and the channel they form; (d) cages in zeolite L. [56, 59]

B. Further calculations

B.1. Water extraction in furnace

To determine the water decrease during heating in the furnace for a calcination procedure at 600°C, a corrected zeolite mass before the furnace was required. This was calculated with two methods. The average of R_{H_2O} calculated with both methods for $m_{before,corr}$ was used. For the first method, the mass added to the crucible, $m_{crucible}$ in g, was determined by the difference between the mass of the Eppendorf with zeolite after the desiccator, $m_{desiccator}$ in g, and the mass of this after the zeolite was added to the crucible. The percentage of zeolite lost in the furnace and due to transferring into and out of the crucible, %L was determined with the activities measured at the tracer study. The activity added to the crucible, $A_{crucible}$ in CPM, was the difference between the activity in the Eppendorf tube after the desiccator, $A_{desiccator}$ in CPM, and the activity left in the Eppendorf after most of the zeolite was added to the crucible. The activity of the zeolite in the Eppendorf tube after the furnace, A_{after} in CPM, was measured as well.

$$\%L = \frac{A_{crucible} - A_{after}}{A_{crucible}} \quad (B.1)$$

The corrected mass with method one, $m_{before,corr1}$ in g, was calculated with:

$$m_{before,corr1} = m_{crucible} \cdot (1 - \%L) \quad (B.2)$$

For method two, the percentage of zeolite that ends up in the Eppendorf tube after the furnace compared to the amount of zeolite after the desiccator, %T in %, was calculated with $A_{desiccator}$ and A_{after} .

$$\%T = \frac{A_{after}}{A_{desiccator}} \quad (B.3)$$

The corrected mass with method two, $m_{before,corr2}$ in g, was then calculated as:

$$m_{before,corr2} = m_{desiccator} \cdot \%T \quad (B.4)$$

B.2. Determining O_i for probability of relocation upon recoil

O_i after calcination was determined with the percentage of holmium extracted for calcined zeolite at the tracer study, $\%Ex_{calc,trac}$. For non-extracted zeolite (#3 and #7 of Table 3.4), O_i was calculated as:

$$O_{i,non-elu} = \frac{\%Ex_{calc,trac}}{P(O_f \rightarrow Ex)} \quad (B.5)$$

In case the zeolite was extracted before irradiation (#4 and #8 of Table 3.4), O_i was calculated with:

$$O_{i,elu} = \frac{O_{i,non-elu} \cdot [1 - P(O_f \rightarrow Ex)]}{1 - O_{i,non-elu} \cdot P(O_f \rightarrow Ex)} \quad (B.6)$$

B.3. Error analysis for ¹⁶⁶Ho relocation upon recoil

The error in the probability of relocation upon recoil could not be determined with the standard deviation of a triplicate experiment, since the results of different samples were combined. The error of a quantity, denoted by u with the quantity as subscript, was calculated with the partial derivatives of its formula and the error of the utilised triplicate experiments. The error of $P(O_i \rightarrow O_f)$ was calculated with Equation B.7:

$$u_{P(O_i \rightarrow O_f)} = P(O_i \rightarrow O_f) \sqrt{\left(\frac{u_{\%Ex}}{\%Ex}\right)^2 + \left(\frac{u_{P(O_f \rightarrow Ex)}}{P(O_f \rightarrow Ex)}\right)^2} \quad (\text{B.7})$$

For the calculation of the error of $P(C_i \rightarrow O_f)$, the error of O_i was required. For non-extracted zeolite the error of O_i was:

$$u_{O_{i,non-elu}} = O_{i,non-elu} \sqrt{\left(\frac{u_{\%Ex_{calc,trac}}}{\%Ex_{calc,trac}}\right)^2 + \left(\frac{u_{P(O_f \rightarrow Ex)}}{P(O_f \rightarrow Ex)}\right)^2} \quad (\text{B.8})$$

In case the zeolite was extracted before irradiation, the error of O_i was calculated with Equation B.9:

$$\left(\frac{u_{O_{i,elu}}}{O_{i,elu}}\right)^2 = \frac{1}{\left(1 - O_{i,non-elu} \cdot P(O_f \rightarrow Ex)\right)^2} \left(\frac{u_{O_{i,non-elu}}}{O_{i,non-elu}}\right)^2 + \frac{(O_{i,non-elu} - 1)^2}{\left(1 - P(O_f \rightarrow Ex)\right)^2 \left(1 - O_{i,non-elu} \cdot P(O_f \rightarrow Ex)\right)^2} \left(u_{P(O_f \rightarrow Ex)}\right)^2 \quad (\text{B.9})$$

The error of $P(C_i \rightarrow O_f)$ was calculated with Equation B.10:

$$\left(\frac{u_{P(C_i \rightarrow O_f)}}{P(C_i \rightarrow O_f)}\right)^2 = \frac{1}{\left(\frac{\%Ex}{P(O_f \rightarrow Ex)} - O_i \cdot P(O_i \rightarrow O_f)\right)^2} \cdot \left[\left(\frac{\%Ex}{P(O_f \rightarrow Ex)}\right)^2 \left(\frac{u_{\%Ex}}{\%Ex}\right)^2 + \left(\frac{\%Ex}{P(O_f \rightarrow Ex)}\right)^2 \left(\frac{u_{P(O_f \rightarrow Ex)}}{P(O_f \rightarrow Ex)}\right)^2 + \frac{\left(\frac{\%Ex}{P(O_f \rightarrow Ex)} - P(O_i \rightarrow O_f)\right)^2}{(1 - O_i)^2} (u_{O_i})^2 + O_i^2 \left(u_{P(O_i \rightarrow O_f)}\right)^2 \right] \quad (\text{B.10})$$

C.Extraction characteristics

This appendix provides the graphs and tables corresponding to the six extraction characteristics mentioned in Section 3.2.3 for non-irradiated zeolite A and in Section 3.5.2 for irradiated zeolite A. For a clear overview, some of the graphs given in Chapter 4 are repeated. For all the graphs in this appendix, each point represents a change of the ammonium chloride solution and they are connected by lines to clarify the measurement points of one experiment. For the legend the notation as described in Section 3.2, is applied to specify the zeolite sample and performed extraction procedure.

C.1. Extraction characteristics for non-irradiated zeolite

Table C.1: Decrease in wt% Ho for the extractions with a 15 ml ammonium chloride solution at room-temperature. All samples are loaded for 1 h at 80°C, resulting in an initial wt% Ho of $18.3\pm 0.1\%$.

Calcination	Extraction			Wt% Ho after extraction	Decrease of wt% Ho
	t_{ex} (d)	# of extractions	Comments		
-	1	3		9.9 ± 0.1	8.4 ± 0.2
600°C	1	3	E3 4 h	17.9 ± 0.1	0.4 ± 0.1
600°C	1	3	10 ml extraction, E3 4 h	18.0 ± 0.1	0.2 ± 0.2
600°C	3	1		17.8 ± 0.1	0.4 ± 0.2
300°C	1	2	E2 4 h	16.4 ± 0.2	1.9 ± 0.2

C. Extraction characteristics

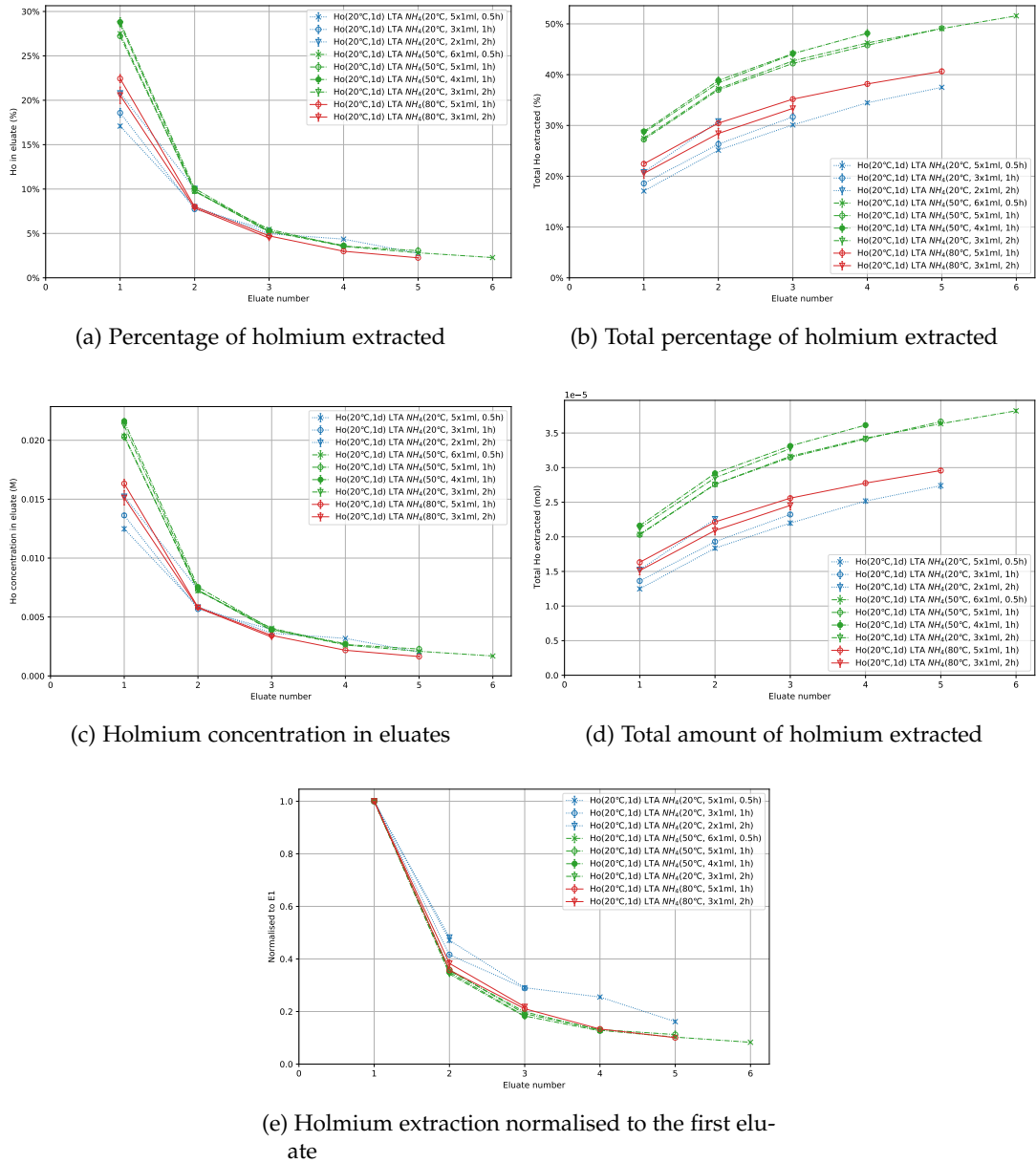
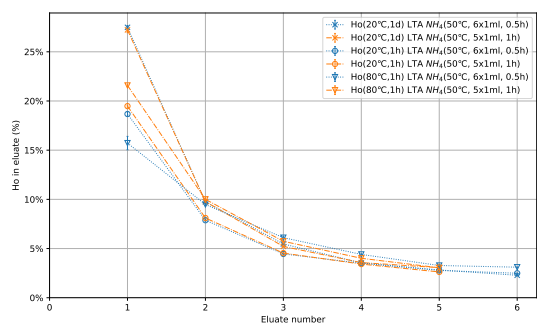
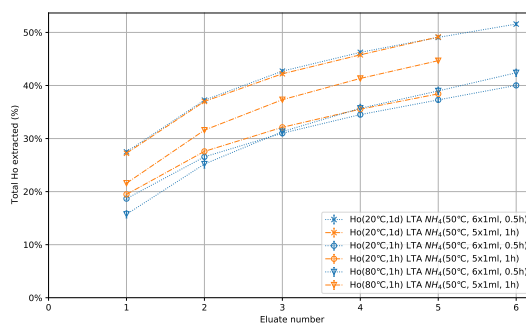


Figure C.1: Extraction characteristics for holmium extraction from the open cages with a 1 ml ammonium chloride solution for different extraction times and temperatures. All samples were loaded at 20°C for 1 d before extraction. Extraction at 20°C is given in blue with dotted lines, at 50°C in green with dash-dotted lines and at 80°C in red with solid lines. The markers indicate the applied extraction time: crosses for 0.5 h; circles for 1 h; and triangles for 2 h. The holmium was measured with the tracer study and the error is given as one standard deviation from the mean of the triplicate.

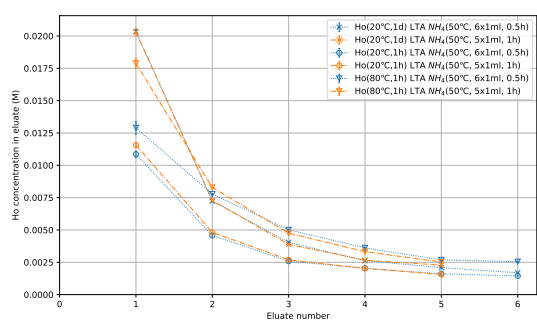
C.1. Extraction characteristics for non-irradiated zeolite



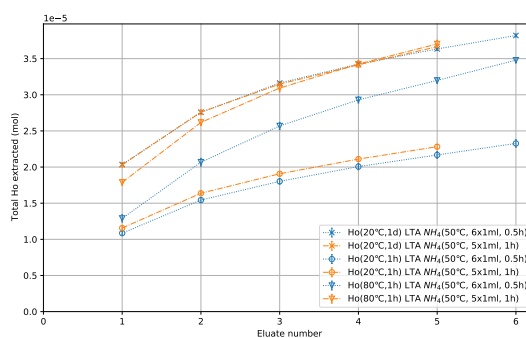
(a) Percentage of holmium extracted



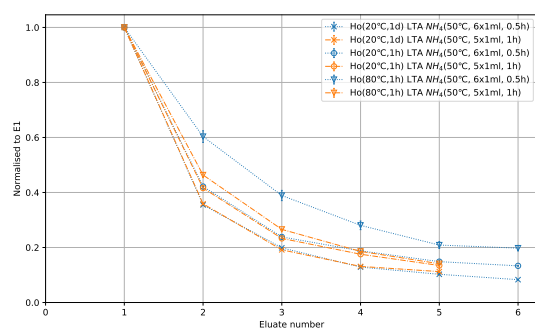
(b) Total percentage of holmium extracted



(c) Holmium concentration in eluates



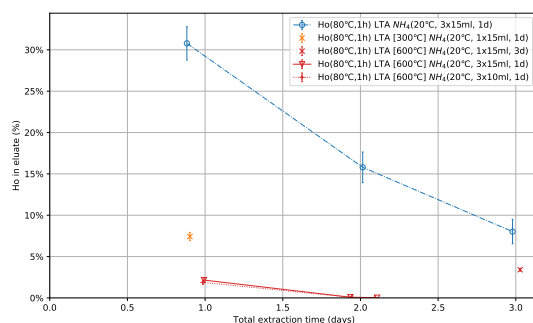
(d) Total amount of holmium extracted



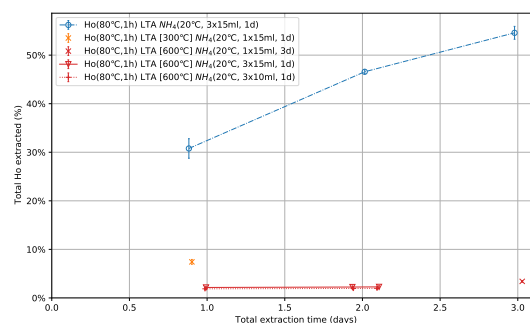
(e) Holmium extraction normalised to the first eluate

Figure C.2: Extraction characteristics for holmium extraction from the open cages with a 1 ml ammonium chloride solution for different different loading procedures. All the extractions were performed at 50°C. An extraction time of 0.5 h is denoted in blue with dotted lines and of 1 h in orange with dash-dotted lines. The markers indicate the loading procedure: crosses for 1 d at 20°C; plus signs for 1 h at 20°C; and triangles for 1 h at 80°C. The holmium was measured with the tracer study and the error is given as one standard deviation from the mean of the triplicate.

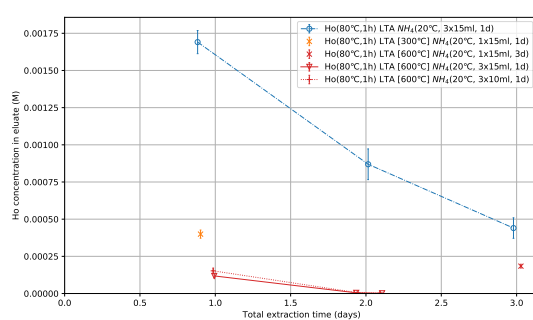
C. Extraction characteristics



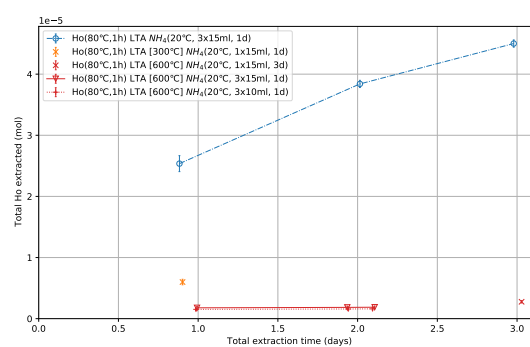
(a) Percentage of holmium extracted



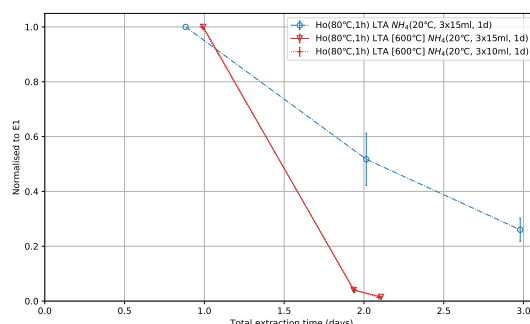
(b) Total percentage of holmium extracted



(c) Holmium concentration in eluates



(d) Total amount of holmium extracted



(e) Holmium extraction normalised to the first eluate

Figure C.3: Extraction characteristics for holmium extraction with a 15 ml ammonium chloride solution at room-temperature. Blue represents non-calcined samples, yellow was calcined at 300°C and red was calcined at 600°C. Also an extraction with 10 ml saturated ammonium chloride solution is included (+). The holmium was measured with the tracer study and the error is given as one standard deviation from the mean of the triplicate.

C.1. Extraction characteristics for non-irradiated zeolite

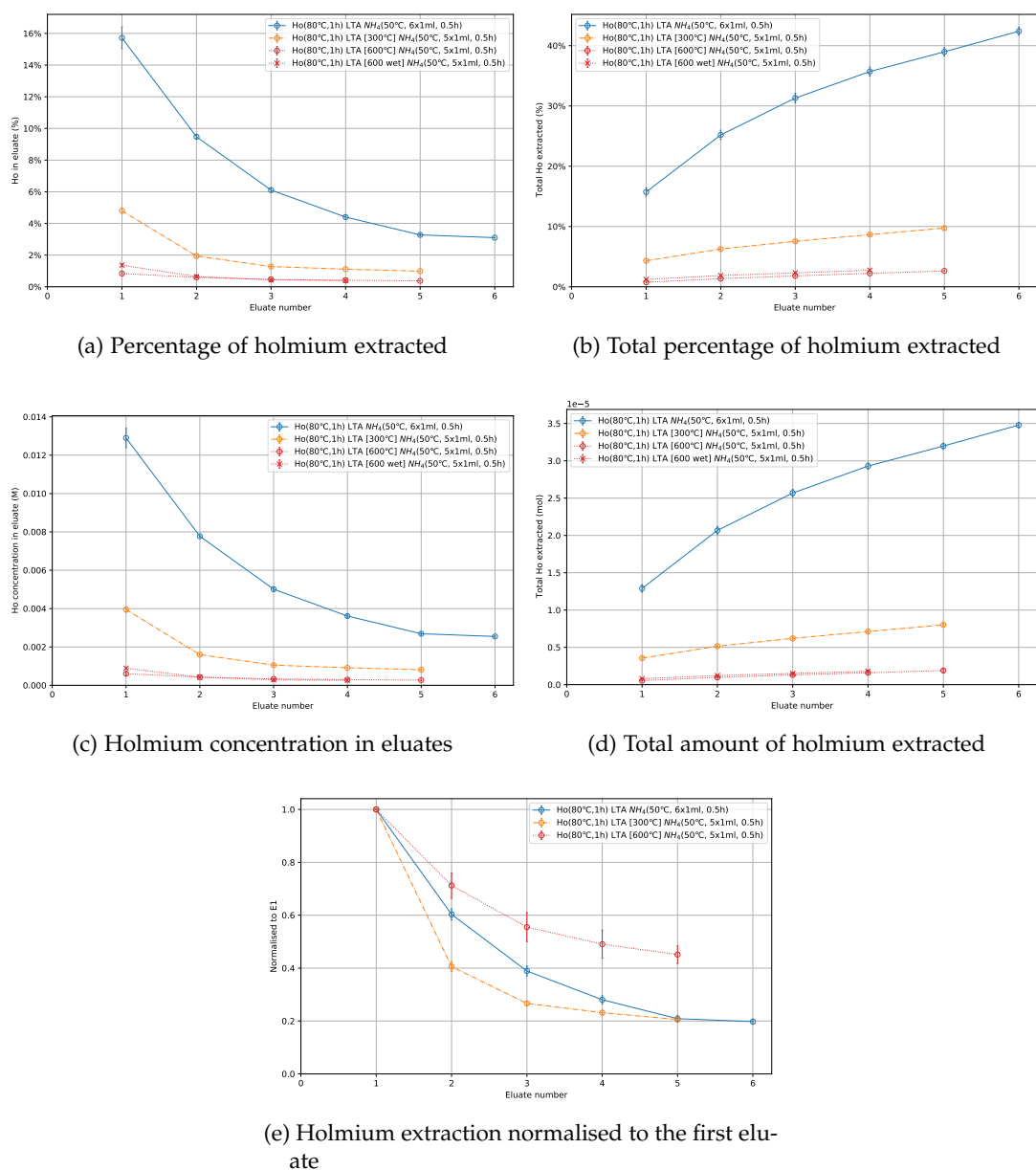


Figure C.4: Influence of calcination on the extraction characteristics for a 1 ml extraction. All samples were loaded for 1 h at 80°C and extracted with 1 ml for 0.5 h per eluate at 50°C. Calcination at 600°C is denoted in red with dotted lines, at 300°C in orange with a dash-dotted line and no calcination in blue with a solid line. The circles represent samples that were dried before calcination, while the samples denoted by crosses were put in the oven with 0.2 ml MiliQ. The percentage was measured with the tracer study, with 100% equal to the holmium in the open and closed cages of the zeolite before extraction. The error is given as one standard deviation from the mean of the triplicate.

C. Extraction characteristics

Table C.2: Decrease in wt% Ho for the 1 ml extractions.

Loading	Calcination	Initial wt% Ho	Extraction		# of extractions	Comments	Wt% Ho after extraction	Decrease of wt% Ho
			T_{ex}	t_{ex} (h)				
23.5 h at 20°C	-	16.4±0.3	20°C	0.5	5		12.0±0.1	4.4±0.3
				1	4	E4 overnight	10.4±0.1	6.0±0.3
				2	3	E3 overnight	10.5±0.2	5.9±0.3
				0.5	6		9.9±0.2	6.5±0.3
				1	5		10.2±0.1	6.2±0.3
				1	4		10.56±0.02	5.8±0.3
			50°C	2	3	E3 1.75 h	11.0±0.1	5.4±0.3
				1	5		11.3±0.3	5.1±0.4
				2	3		12.4±0.1	4.0±0.3
				0.5	6		9.2±0.2	4.5±0.5
				1	5		9.5±0.1	4.2±0.5
				0.5	6		12.5±0.1	5.7±0.1
1 h at 80°C	-	18.3±0.1	50°C	1	5		12.5±0.2	5.8±0.2
				0.5	6		12.5±0.1	5.7±0.1
				1	5		12.5±0.2	5.8±0.2
1 h at 20°C	-	18.3±0.1	50°C	0.5	5	Dehydrated after oven	20.3±0.1	-2.0±0.1
				1	4	wt% Ho = 20.6±0.6	20.0±0.1	-1.7±0.2
				0.5	5	E1 3 h, in furnace with	20.0±0.1	-1.7±0.2
				1	4	0.2 ml milliQ	20.0±0.1	-1.7±0.2
				0.5	5		18.4±0.2	-0.2±0.2
				1	4		18.4±0.2	-0.2±0.2

C.2. Extraction characteristics for irradiated zeolite

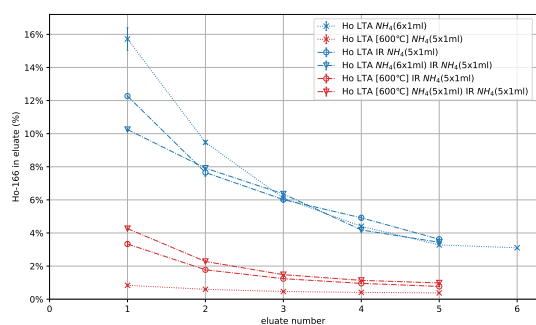
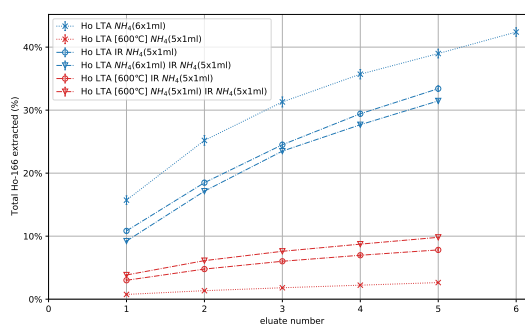
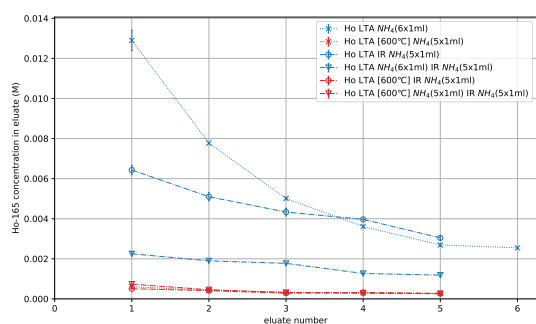
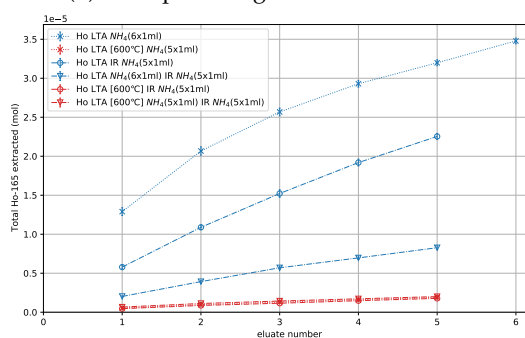
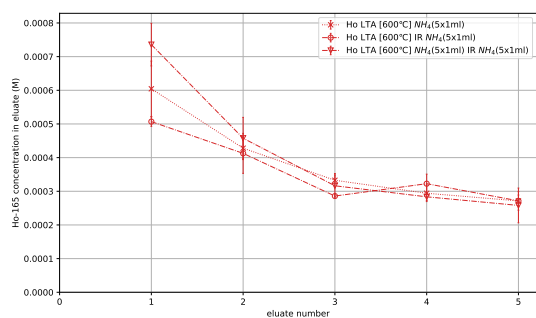
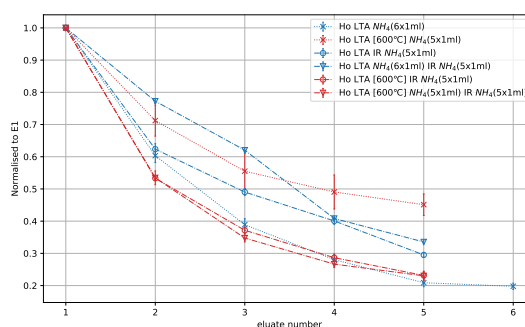
(a) Percentage of ^{166}Ho extracted(b) Total percentage of ^{166}Ho extracted(c) ^{165}Ho concentration in eluates(d) Total amount of ^{165}Ho extracted(e) ^{165}Ho concentration in eluates for calcined zeolite(f) ^{166}Ho extraction normalised to the first eluate

Figure C.5: ^{165}Ho and ^{166}Ho extraction characteristics of irradiated zeolite with a 1 ml ammonium chloride solution. (e) is a zoomed version of (c). All samples were loaded at 80°C for 1 h and all extractions were performed at 50°C with an extraction time of 0.5 h. The results from the tracer study for the extraction of holmium from non-irradiated samples are given for comparison by crosses connected by the dotted lines. Irradiated samples are represented by dash-dotted lines. Samples that were calcined before irradiation are given in red, blue represents non-calcined samples. The triangles represent samples that were extracted with ammonium chloride before irradiation, the samples denoted by circles were not extracted before irradiation. The activity of ^{166}Ho was measured with the Wallac gamma counter, the concentration of ^{165}Ho with the ICP-MS. The error is given as one standard deviation from the mean of the triplicate.

C. Extraction characteristics

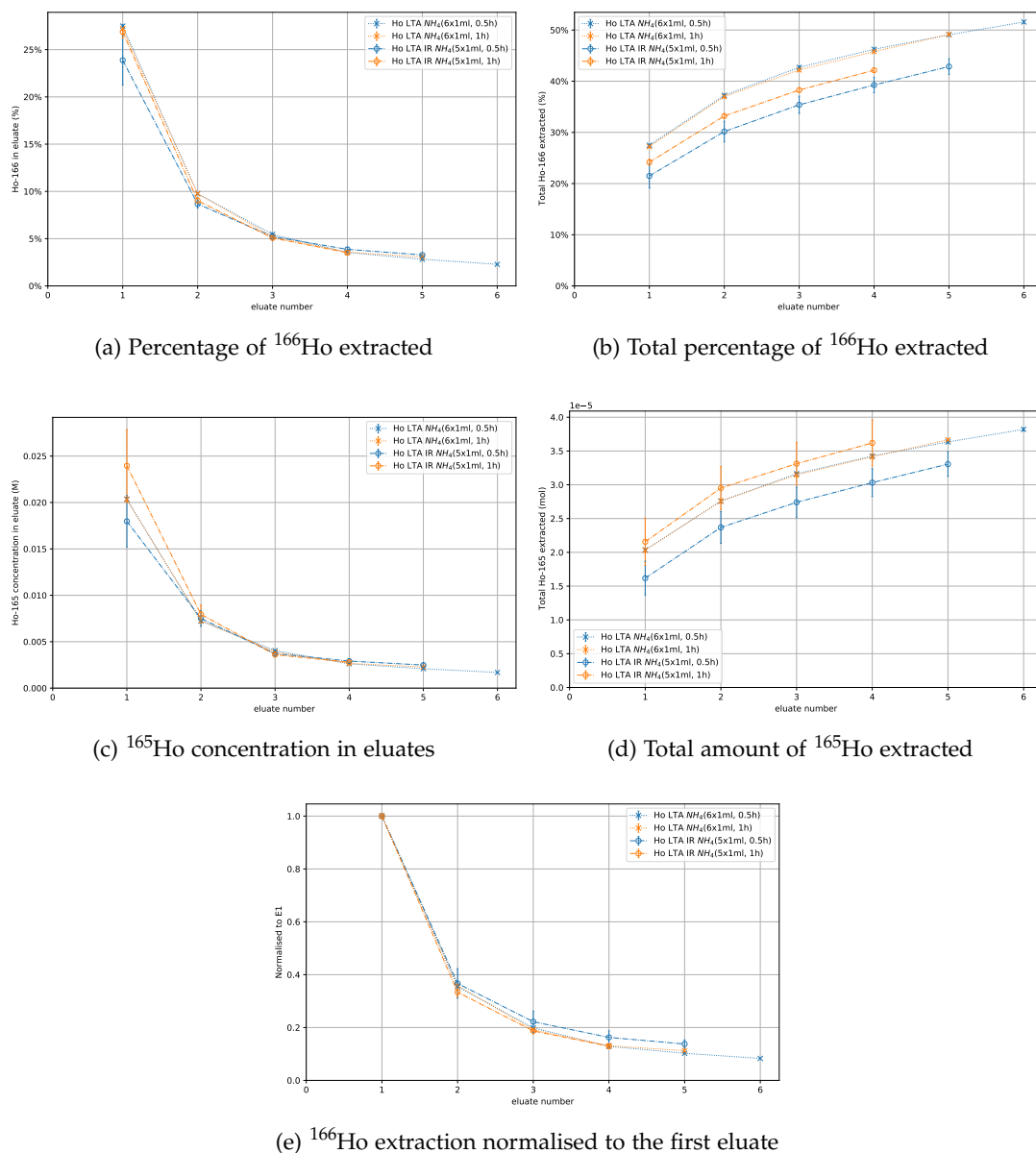
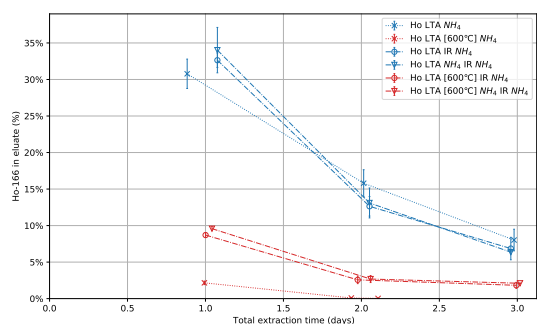
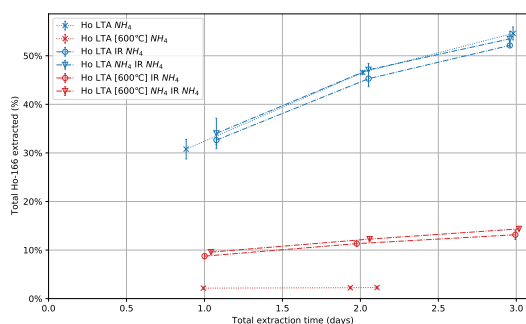


Figure C.6: ^{165}Ho and ^{166}Ho extraction characteristics of irradiated zeolite loaded at 20°C for 1 d with a 1 ml ammonium chloride solution. For (a) and (b), 100% represents the total amount of ^{166}Ho in the zeolite before extraction. A short hand notation similar as described in Section 3.2, is applied to specify the extraction procedure. All samples were loaded at 20°C for 1 d and all extractions were performed at 50°C . An extraction time of 0.5 h is represented in blue and of 1 h in orange. The results from the tracer study for the extraction of holmium from non-irradiated samples are given for comparison by crosses connected by the dotted lines. Irradiated samples are represented by circles connected by dash-dotted lines. The activity of ^{166}Ho was measured with the Wallac gamma counter, the concentration of ^{165}Ho with the ICP-MS. The error is given as one standard deviation from the mean of the triplicate.

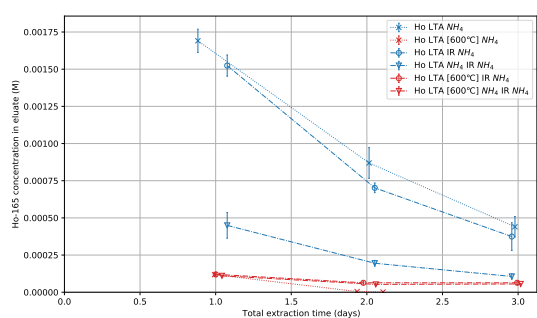
C.2. Extraction characteristics for irradiated zeolite



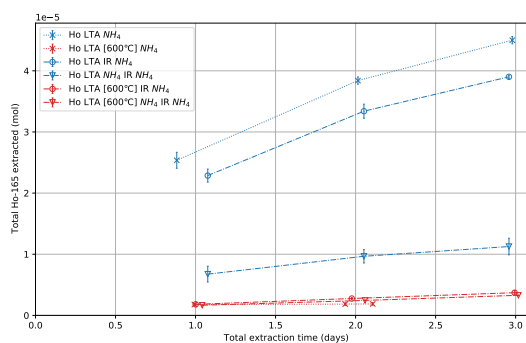
(a) Percentage of ^{166}Ho extracted



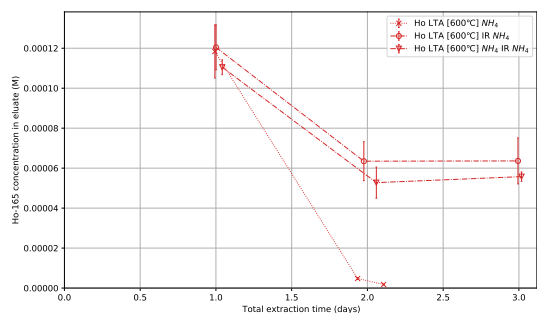
(b) Total percentage of ^{166}Ho extracted



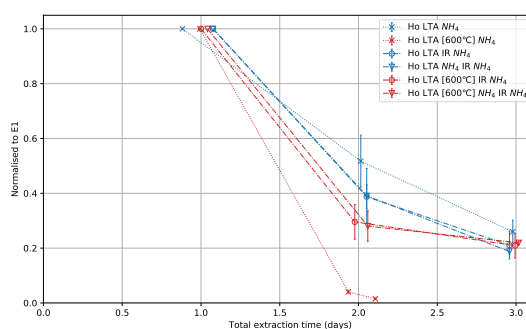
(c) ^{165}Ho concentration in eluates



(d) Total amount of ^{165}Ho extracted



(e) ^{165}Ho concentration in eluates for calcined zeolite



(f) ^{166}Ho extraction normalised to the first eluate

Figure C.7: ^{165}Ho and ^{166}Ho extraction characteristics of irradiated zeolite with a 15 ml ammonium chloride solution. In (a) and (b), 100% represents the total amount of ^{166}Ho in the zeolite before extraction. A short hand notation similar as described in Section 3.2, is applied to specify the extraction procedure. All samples were loaded at 80°C for 1 h and all extractions were performed three times with 15 ml for 1 d at room-temperature. The results from the tracer study for the extraction of holmium from non-irradiated samples are given for comparison. These are represented with crosses connected by the dotted lines. Irradiated samples are represented by dash-dotted lines. Samples that were calcined before irradiation are given in red, blue represents non-calcined samples. The triangles represent samples that were extracted with ammonium chloride before irradiation, the samples denoted by circles were not extracted before irradiation. The activity of ^{166}Ho was measured with the Wallac gamma counter, the concentration of ^{165}Ho with the ICP-MS. The error is given as one standard deviation from the mean of the triplicate.

D. Supplementary information about the applied methods

D.1. Tracer study

In this section some additional comments are made about the tracer study. During the irradiation of holmium chloride hexahydrate also ^{35}S was produced, but with a 10^3 times lower activity than that of ^{166}Ho directly after production. ^{35}S has a half-life of 87 d [30]. Consequently, this had not decayed away after waiting 1–3 days before the stock solution was used. ^{35}S only emits β^- -particles, hence this does not influence the measured gamma spectrum if bremsstrahlung is neglected.

It should be noted that for some measurements of the count-rate of a 1 ml stock solution or the count-rate after loading, a setting on the Wallac was accidentally applied that stopped the measurement after $4 \cdot 10^4$ counts. This resulted in measurement time shorter than one minute. It was expected that this did not significantly influence the results, since re-measuring some eluates with the ICP-MS gave similar concentrations as calculated with $F_{N/A}$ determined with the short measurement time.

D.2. LTA loss during experiments

Every experiment started with the same amount of Na-LTA. During the different steps, especially when the sample was transferred or when a liquid was removed, part of the zeolite sample was lost. The effect of this zeolite loss on the extraction characteristics was neglected. For the 1 ml extraction procedure with five eluates in total $0.6 \pm 0.2\%$ of the zeolite sample was lost due to removing the ammonium chloride solution by pipetting. The removed LTA was in the ammonium chloride solution, the amount of zeolite on the pipette tips was negligible. For the 15 ml extraction, the loss was a slightly higher; a bit more zeolite was lost when the liquid was decanted instead of removed by pipetting.

The transfer of a zeolite sample between vials or a crucible resulted in a noticeable zeolite loss. The transfer from an Eppendorf tube to a 15 ml tube had a zeolite loss of $0.4 \pm 0.2\%$. When a zeolite sample, which was dried for 2 d in the desiccator, was transferred from an Eppendorf tube to a crucible 2.2 ± 0.8 of the zeolite remained in the Eppendorf tube and was not used in further experiments. The subsequent transfer of the sample from the crucible to an Eppendorf tube or 15 ml tube again resulted in about one percent of zeolite loss. Consequently, the final weight for samples that were calcinated, was considerably reduced.

D.3. Pipetting

For adding a certain volume, an adjustable pipette was used with a corresponding volume range. For each volume the pipette was calibrated by pipetting ten times with milliQ. The water was weighted to determine the average and the standard deviation of the volume. The calibration was repeated for pipetting with a different hand. Furthermore, for the most applied volumes, 1 ml and 0.2 ml, an additional monthly check of a few measurements with milliQ was performed. However, variation between days or the influence of temperature changes was not accounted for.

D.4. Recommendations for similar research

It is advisable for comparable research to measure the holmium content using a tracer of ^{166}Ho measured with the Wallac gamma counter for experiments with a short processing time. For longer processing times, INAA could be used to measure holmium in solid samples and ICP-MS for solutions. It is not feasible to use the ICP-OES for measuring holmium in either zeolite samples or ammonium chloride solutions. For activity measurements, it is more favourable to use the Wallac gamma counter than the HPGe detector. However, for the Wallac a lower limit on the maximal count-rate of 10^6 CPM for the total counts should be applied, instead of for the integrated counts. Additionally, the measurement of the detector efficiency should be repeated twice more to determine the error of a triplicate. This should be done as well for the specific activity of ^{166}Ho produced without the Szilard-Chalmers effect.

The Ho wt% measured in this thesis was affected by the water content of the sample. In order to attain a more consistent measurement of the wt%, the mass of the sample could be determined after drying in an oven, in place of in a vacuum desiccator.

